December 15, 2022

Understanding Air Quality Trends in Richmond-San Pablo, California

Results from the Richmond Air Monitoring Network

PSE Bringing science to energy policy

Authors

Boris Lukanov, PhD | PSE Healthy Energy
Karan Shetty, MESM | PSE Healthy Energy
Audrey Smith, MPH | PSE Healthy Energy
Lee Ann L. Hill, MPH | PSE Healthy Energy
Rebecca Sugrue, PhD | UC Berkeley and Lawrence Berkeley National Laboratory
James Butler, MS | UC Berkeley and Lawrence Berkeley National Laboratory
Chelsea Preble, PhD | UC Berkeley and Lawrence Berkeley National Laboratory
Thomas Kirchstetter, PhD | UC Berkeley and Lawrence Berkeley National Laboratory

Acknowledgements

Funding

About PSE Healthy Energy

PSE Healthy Energy is a nonprofit research institute dedicated to supplying evidence-based scientific and technical information on the public health, environmental, and climate dimensions of energy production and use. We are the only interdisciplinary collaboration focused specifically on health and sustainability at the intersection of energy science and policy. **Visit us at psehealthyenergy.org and follow us on Twitter @PhySciEng**.

PSE

PSE Healthy Energy
1440 Broadway, Suite 750
Oakland, CA 94612
510-330-5550
info@psehealthyenergy.org
www.psehealthyenergy.org

PSE

Table of Contents

PSE

Table of Contents

PSE

Expanding Access to Hyperlocal Air Quality Data

Air pollution is a leading contributor to the global burden of disease, yet for decades, communities have lacked access to localized air quality data. Sparse state and federal networks of regulatory air monitors provide important air quality data at the regional level, but are unable to provide more granular information, such as block-by-block or neighborhood scale data.

The increased availability, quality, and affordability of low-cost air monitors in recent years has enabled communities and regulators to deploy denser networks of low-cost air monitors. The air quality data from these networks provides high spatial resolution that can be used to inform local air pollution mitigation strategies and protect public health.

The Richmond Air Monitoring Network (RAMN)

As a result of California Assembly Bill 617 (AB 617), and with support from the California Air Resources Board (CARB) through the Community Air Grants Program, PSE Healthy Energy (PSE) and the Asian Pacific Environmental Network (APEN) established the Richmond Air Monitoring Network (RAMN) in 2020. RAMN is part of California Climate Investments, a statewide program that puts billions of Cap-and-Trade dollars to work reducing greenhouse gas emissions, strengthening the economy, and improving public health and the environment—particularly in disadvantaged communities. RAMN stands out as the first high-density community air monitoring network to collect continuous measurements of three important criteria air pollutants—particulate matter ($PM_{2.5}$),[1] nitrogen dioxide (NO_2), and ground-level ozone (O_3)—along with periodic measurements of black carbon (BC),[2] all with very high spatial and temporal resolution. These four air pollutants were selected based on their known impacts to public health and the environment, and the current state of low-cost air sensor technology.

The Richmond, North Richmond, and San Pablo neighborhoods are home to many sources of air pollution, including the third largest refinery in California, a coal terminal and its accompanying rail lines, three major highways with heavy commuter traffic, and various other industrial facilities and transportation activities. The region also contains some of the most

---

[1] Specifically, particulate matter with a diameter of less than or equal to 2.5 microns.
[2] An important component of PM emitted during incomplete combustion of fossil fuels and biomass, and a major portion of diesel PM.

environmentally and socioeconomically burdened communities in California.[3] Despite the high density of local air pollution sources, only one regulatory air monitoring site in the community currently tracks three of the four air pollutants monitored by RAMN. RAMN expanded the region's access to hyperlocal air quality data and provided more granular insights into the sources and patterns of local air pollution.
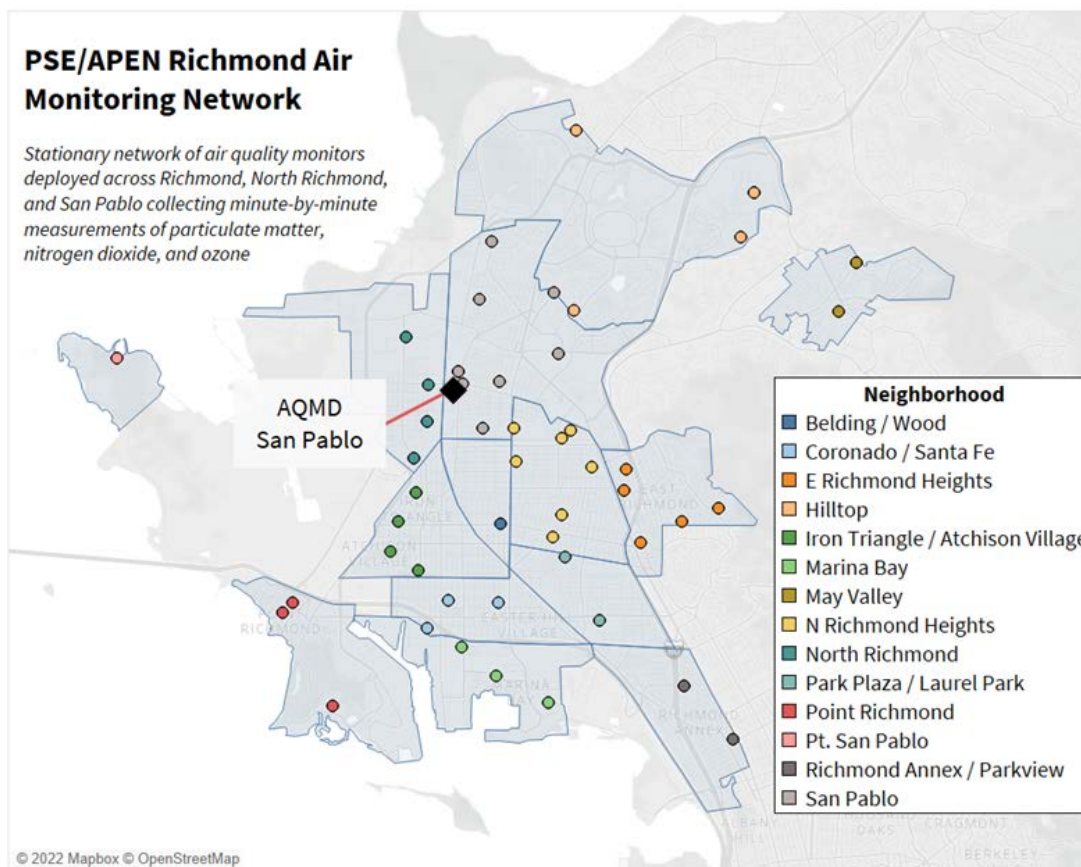
Figure ES-1. Distribution and location of the RAMN air monitors throughout 14 neighborhoods in Richmond-San Pablo. The neighborhoods were compiled by grouping City of Richmond neighborhood councils, with the goal of having more than one monitor within each neighborhood, wherever possible. Black diamond indicates the AQMD regulatory monitoring site in San Pablo.

To establish RAMN, PSE and APEN deployed 50 Aeroqual AQY1 micro air quality monitors (**Figure ES-1**) equipped with $PM_{2.5}$, NO_2, and O_3 sensors. These were placed at select locations throughout Richmond, North Richmond, and San Pablo based upon direct input from the community and various technical considerations. Monitors collected measurements each

---

[3] California Office of Environmental Health Hazard Assessment. (2021). CalEnviroScreen 4.0.

minute between January 2020 and March 2022. Additionally, PSE partnered with researchers at University of California, Berkeley and Lawrence Berkeley National Laboratory (LBNL) to add low-cost BC sensors (Aerosol Black Carbon Detectors, or ABCDs) to the 50 RAMN monitoring sites. These sensors collected BC data during one winter month and one summer month in 2021, and during one wildfire event in 2020.

Understanding Observed Variations in Air Pollution

We found that network-average concentrations of the three criteria air pollutants measured by RAMN ($PM_{2.5}$, NO_2, and O_3) generally increased and decreased in unison with concentrations measured by the Bay Area Air Quality Management District (AQMD) monitoring station located in San Pablo. This suggests that the Bay Area AQMD reference site is generally representative of the area over broader timescales. However, RAMN's more granular location-based data revealed significant variations in air pollutant concentrations across space (neighborhoods and land use areas) and greater variability over certain time periods (days of the week and hours of the day).

We can interpret data collected by RAMN by examining average air pollutant concentrations by neighborhood and comparing these levels to: (1) national ambient air quality standards, (2) regional averages measured by AQMD, and (3) other neighborhoods in the community.

Comparing Air Pollutant Concentration Levels to NAAQS

Any exposure to air pollutants may adversely impact health. When comparing absolute air pollutant concentrations by neighborhood to federal standards, we observed that:

- Average $PM_{2.5}$ concentrations measured by RAMN were generally elevated and hovered around or exceeded the federal NAAQS 3-year annual mean $PM_{2.5}$ standard of 12 μg/m³ in many Richmond-San Pablo neighborhoods.

- RAMN-wide $PM_{2.5}$ concentrations over the 27-month-long study period averaged 12.6 μg/m³.

Care must be taken when comparing RAMN data with NAAQS standards because specific data completeness and data quality requirements for NAAQS may not necessarily be met by our sensor network, including that data are averaged over a three-year period. Additionally, air quality data evaluated for NAAQS may exclude exceptional events that meet certain criteria, such as some wildfire smoke events.

PSE

RAMN observed substantially lower average NO_2 and O_3 concentrations compared to NAAQS standards. However, we note that any exposure to air pollutants can adversely impact health and adverse health effects have been observed at levels well below health-based standards.

Assessing Variations in Air Pollutant Concentrations and Comparing to AQMD

Unlike the single AQMD regulatory site tracking several criteria air pollutants Richmond-San Pablo, RAMN was able to observe spatial patterns in air pollution that revealed significant spatial variability of $PM_{2.5}$, BC, NO_2 (and even O_3) across neighborhoods and land use categories.

- Average $PM_{2.5}$ levels were highest in the south (Point Richmond, Richmond Annex), and in the north (Hilltop, May Valley), where average $PM_{2.5}$ concentrations were roughly 20 percent higher compared to the average concentrations measured by the Bay Area AQMD regulatory site in San Pablo (**Figure ES-2, top**).

- Neighborhood-average NO_2 concentrations were roughly 30 percent higher in two southern neighborhoods (Point Richmond and Marina Bay) compared to the AQMD reference monitor, as well as around 10 percent higher in several other neighborhoods close to the I-80 and I-580 freeways (Hilltop, East Richmond Heights, Park Plaza/Laurel Park, and Coronado/Santa Fe) (**Figure ES-2, middle**).

- Average O_3 concentrations were highest in northern neighborhoods (Hilltop, North Richmond, Pt. San Pablo, San Pablo, and North Richmond) located further away and downwind of major freeways and industrial zones, and lowest in southern neighborhoods (Pt. Richmond, Marina Bay, Richmond Annex/Parkview, Park Plaza/Laurel Park, Coronado/Santa Fe, and Iron Triangle/Atchison Village) (**Figure ES-2, bottom**).

- BC concentrations were up to 50 percent higher than network-average concentrations in neighborhoods near Interstate-580 [I-580] (Marina Bay, Coronado/Santa Fe, and Richmond Annex) and in neighborhoods near the Richmond Parkway and the more industrial areas to the west (Iron Triangle/Atchison Village and North Richmond).

PSE
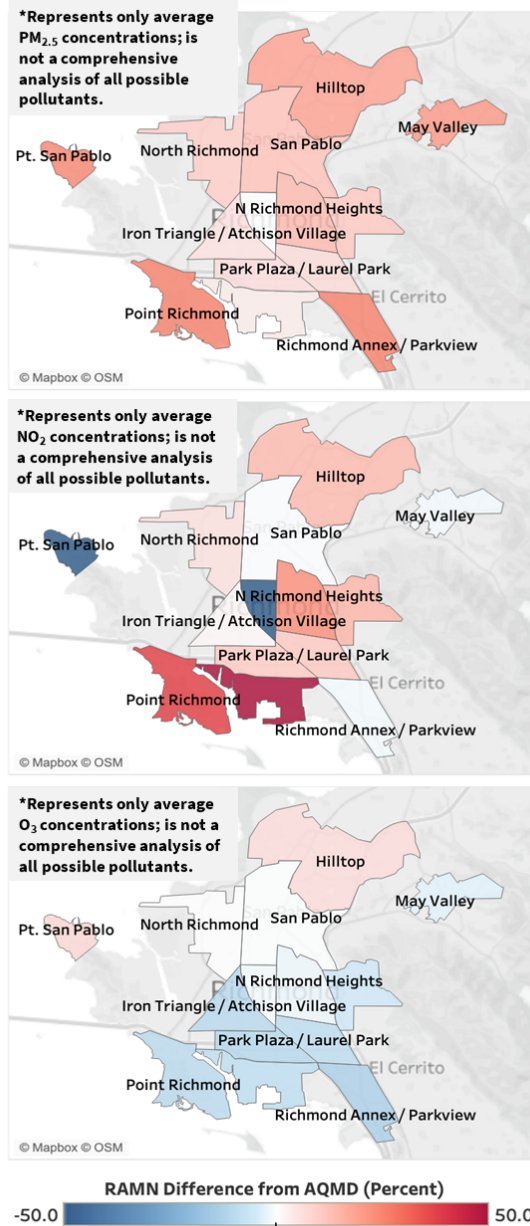
Figure ES-2. Average PM₂.₅ (top), NO₂ (middle), and O₃ (bottom) concentrations by neighborhood, shown as a percent difference from the average concentrations measured by the Bay Area AQMD regulatory site in San Pablo. Blue indicates average neighborhood concentrations observed were lower than Bay Area AQMD site while red indicates concentrations were higher.

Emission Sources Driving Air Pollution Trends

Elevated Air Pollutant Concentrations Near Freeways Points to Traffic's Impact on Air Quality

Air pollutants measured by RAMN were elevated near freeways, during commuter hours, and at times and locations associated with industrial truck and commuter traffic. Areas near the two major highways—I-80 to the east and I-580 to the south—experienced higher ambient concentrations of $PM_{2.5}$ and NO_2. Similarly, industrial areas near the Richmond Parkway to the west and I-580 to the south experienced persistently high ambient concentrations of BC, especially during the winter months and in the morning and evening commuter hours.

Further supporting a connection to traffic, RAMN observed that NO_2 concentrations were highest within a half-mile of major freeways, and dropped significantly beyond that distance. Elevated levels of $PM_{2.5}$ and NO_2 were also observed near freeways around the time of the morning and evening commute.

Heavy-Duty Trucks Likely Cause Elevated Black Carbon

BC measurements allowed for further examination of diesel combustion sources, including heavy-duty trucks. Our traffic emission estimates showed that while passenger vehicles make up the majority of annual vehicle miles traveled, light, medium, and heavy-duty trucks contribute the majority of on-road $PM_{2.5}$, PM_{10}, and NO_x emissions.

PSE
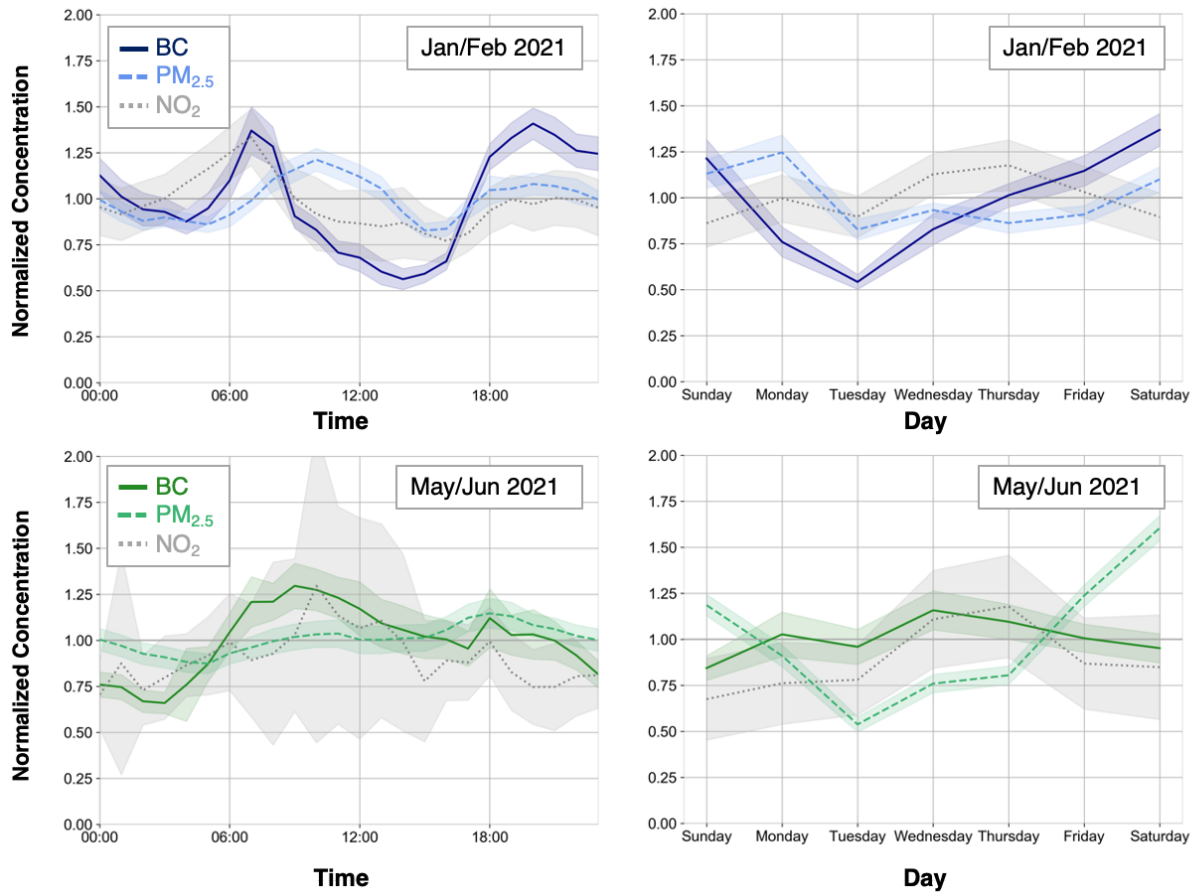
Figure ES-3. Hour-of-day (left) and day-of-the-week (right) patterns of normalized BC, PM$_{2.5}$, and NO$_2$ concentrations in the winter (top) and late spring (bottom). The lines indicate the network average across all 50 RAMN sites and the shaded areas represent the 95 percent confidence intervals.

BC concentrations varied significantly by location and season, especially when compared to PM$_{2.5}$. The wintertime early morning peak in BC concentrations is most likely due to a peak in heavy-duty diesel truck activity, enhanced by a low atmospheric boundary layer and lower wind speeds in the winter months. Peak concentrations of NO$_2$, which is the product of rapid oxidation of diesel nitric oxide (NO) emissions and present in diesel truck exhaust, also occur at the same time, further supporting this association (**Figure ES-3**).

Historically, concentrations of BC in the Bay Area have been higher on weekdays than weekends because of higher diesel truck activity during business hours. RAMN data contradicts this trend, showing lower average BC concentrations midweek. This finding suggests that the weekly activity patterns of BC emission sources, including diesel trucks, may be different than they have historically been in the Bay Area. Residential wood burning may

PSE

also be a factor here, assuming residents tend to use their fireplaces more on weekends than weekdays.

Wildfires Caused Acute Exposure Events

During the 2020 wildfire season sampling campaign, air quality in Richmond was severely impacted by wildfire smoke that was transported to the Bay Area from other regions of California (**Figure ES-4**). RAMN data showed that wildfire smoke brought air pollutant concentrations well above the regional averages and national air quality standards.
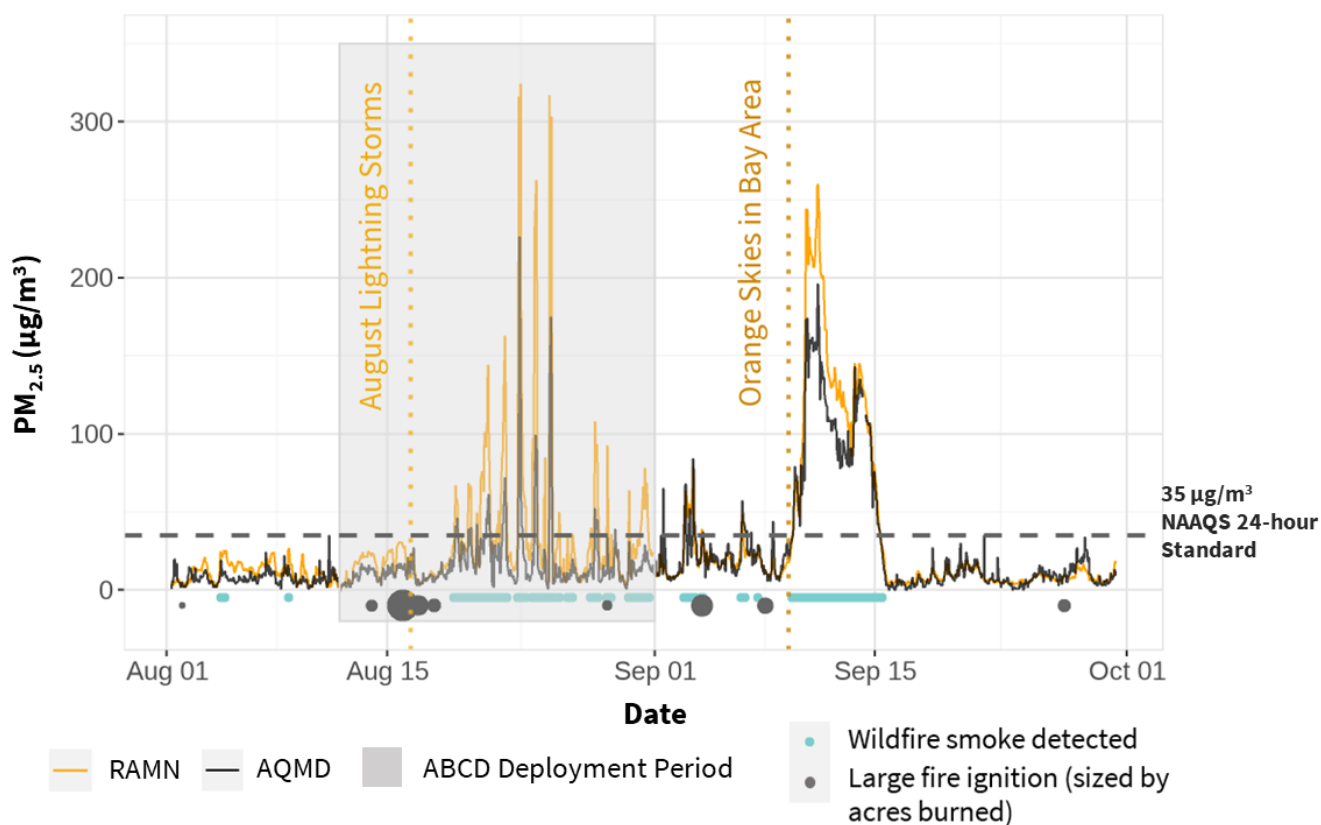
Figure ES-4. RAMN network-average and Bay Area AQMD hourly PM$_{2.5}$ concentrations during the August-September 2020 wildfire season. Also shown: reported large wildfire ignitions (black solid circles), wildfire smoke detected at ground level (blue solid circles), black carbon ABCD deployment period (gray shaded area).

Average PM$_{2.5}$ concentrations during wildfire-smoke-impacted periods were up to ten times higher than PM$_{2.5}$ concentrations when there was no smoke. While national ambient air quality standards may exclude certain exceptional events, such as some wildfires, the entire study area experienced average PM$_{2.5}$ concentrations during wildfire season that were

PSE

significantly higher than 12 µg/m^3, the primary annual national ambient air quality standard for PM$_{2.5}$ averaged over three years. During specific wildfire events, the study area also experienced average daily PM$_{2.5}$ concentrations up to five times higher than the NAAQS 24 hour limit of 35 µg/m^3, indicative of acute exposure events. BC, a short-lived climate-forcing agent and a key component of wood smoke, was also significantly elevated during wildfire events, with average peak BC concentrations roughly four times higher during smoke-impacted days than baseline conditions.

Considering Air Pollution in the Broader Community Context

In the broader context of cumulative burdens, many factors—including but not limited to air pollution—contribute to the health outcomes experienced by the community. Communities with elevated health risk factors, including higher prevalence of underlying health conditions, lack of access to healthcare, socioeconomic burdens, and poor housing conditions, face much greater risk from exposure to air pollution. In the absence of hyperlocal air quality data, CalEnviroScreen (CES)—California's geospatial tool that integrates environmental burden and socioeconomic data to identify environmental justice communities—relies upon sparse regional air quality data and emissions estimates to approximate average concentrations for certain air pollutants by census tract. RAMN was able to provide much more detailed data on PM$_{2.5}$, NO$_2$, O$_3$, and BC concentrations at the neighborhood level that could be used to inform refined exposure assessments for these air pollutants.

When comparing RAMN data to CES, we found that average air pollutant concentrations of PM$_{2.5}$, NO$_2$, and O$_3$ (with the notable exception of BC) were generally higher in neighborhoods not designated as disadvantaged communities by CalEnviroScreen. This finding underscores the importance of examining air pollution within the broader context of cumulative demographic and environmental burdens. Additional investigations on the influence of other air pollutants not measured by RAMN, such as air toxics and VOCs in particular, and the impacts of cumulative environmental, health, and socioeconomic burdens are needed to more comprehensively investigate the high prevalence of poor health outcomes experienced by the Richmond-San Pablo community.

Mitigation Strategies and Recommendations

RAMN sheds light on the hyperlocal variations of PM$_{2.5}$, NO$_2$, O$_3$, and BC concentrations throughout the Richmond-San Pablo community. RAMN data point to commuter traffic and industrial diesel-truck activities as key sources of local air pollution, suggesting that

PSE

heavy-duty vehicle electrification and other emissions reductions from traffic should be prioritized. This can be achieved through (1) requiring or providing incentives for small and large businesses to electrify truck fleets, (2) retiring old medium- and heavy-duty diesel trucks, (3) rerouting trucks away from areas experiencing cumulative environmental burdens, and (4) restricting industrial development that brings heavy traffic into dense, urban areas and environmental justice communities. Community groups would also benefit from tree planting and other urban greening efforts along traffic corridors to protect sensitive groups from vehicular air pollution.

In addition, coordinated efforts by local, regional, and state governments—with ongoing engagement with local communities and community-based organizations such as APEN—should focus on expanding local and regional electrified public transit to reduce overall vehicle travel while also improving transit options for households with limited mobility. Access to electric vehicle (EV) charging infrastructure, particularly in apartment buildings and multifamily housing residences, should be expanded to encourage EV adoption. Addressing the impacts of wildfire smoke locally (beyond forest-level interventions) may require investments in local resilience hubs and community centers where community members can find protected spaces with access to filtered air.

Current and future air monitoring efforts by the Bay Area AQMD should urgently focus on increasing community access to data on other key air pollutants not captured by RAMN. Many health-damaging air pollutants that are difficult to measure with current low-cost air sensor technology were measured by the Bay Area AQMD as part of the Richmond-San Pablo Community Air Monitoring Plan (CAMP).[4] These air pollutants include toxic air contaminants emitted from key stationary sources of air pollution in the community, which may be more correlated with health outcomes data for the study area than air pollutants measured by RAMN. These data collection efforts should be expanded and used to inform targeted actions that can help reduce exposure in the community and improve health outcomes.

In addition, the Chevron Richmond refinery community air monitoring system measures several toxic air contaminants, including ammonia, BTEX (benzene, toluene, ethylbenzene, and xylene), and BC at three locations in the community—Point Richmond, Atchison Village, and North Richmond.[5] Measurements from these sites are available to the community in real time. However, historical data from these three community air monitors are yet to be made publicly available.[6] We strongly recommend that these data are released to the public so that

---

[4] BAAQMD. (2022). Air Toxics Monitoring Study.
[5] Chevron. (2022). Chevron Richmond refinery fenceline monitoring system.
[6] Chevron. (2022. FAQs.

PSE

they can be evaluated in the context of community health outcomes and used to inform future actions and monitoring activities.

Additional information on key stationary sources in the community should also be made publicly available and used to inform future actions, monitoring activities, and evaluation of existing data, including data collected by RAMN. These additional data should include, but are not limited to:

- More detailed emissions data (e.g. by hour of day and day of week) for specific industrial activities in the area, including operational schedules of various refinery units, precise timing and duration of flaring events, fluid catalytic cracking unit (FCCU) historic hours of operation, and bulk carrier (tanker) loading and unloading schedules.

- Routing and scheduling for industry-associated heavy-duty trucking activities.

- Recent residential wood burning surveys, if available, to allow for further interpretation of anomalies in hourly, daily and seasonal BC and $PM_{2.5}$ concentration trends.

While CES air pollutant indicators (developed using sparse regional air monitoring and emissions data) can provide decent estimates of average air pollution concentrations at the census-tract level, we have shown that a distributed network of air sensors like RAMN is able to provide more granular information and measure actual ground-level concentration differences within individual census tracts. Data from RAMN and other low-cost air quality sensor networks in California can be used in combination with CES estimates to better understand hyperlocal exposure to air pollution and its role in exacerbating environmental burdens within the most impacted communities in the state.

PSE

In 2017, California adopted Assembly Bill 617 (AB 617), which sought to ensure that all Californians benefit equitably from the state's air quality and climate efforts, particularly populations living in areas most severely impacted by air pollution.[7] In response to AB 617, the California Air Resources Board (CARB) established the Community Air Grants Program to provide support for non-profit and community-based organizations to participate in the AB 617 process and to build capacity, so that they can become active partners with the government to identify, evaluate, and ultimately reduce air pollution and exposure to harmful emissions in their communities.[8]

In 2018, PSE Healthy Energy (PSE) and the Asian Pacific Environmental Network (APEN) received funding through the first round of Community Air Grants to establish the Richmond Air Monitoring Network (RAMN)—a stationary air monitoring network in Richmond, North Richmond, and San Pablo, California.[9] The area is characterized by some of the highest cumulative air pollution exposure burdens in California. As a result, Richmond-San Pablo had been selected by CARB as one of ten communities statewide targeted for focused action to improve air quality. In 2019, PSE Healthy Energy, APEN, and University of California, Berkeley (UC Berkeley) received additional funding to expand air monitoring efforts in the region by adding black carbon sensors to RAMN.[10]

The purpose of this report is to share details on our air quality monitoring efforts, key findings, and recommendations with regulators, community-based organizations, and the general public.

1.1 Importance of Air Quality: Implications for Human Health

Air pollution is a leading contributor to the global burden of disease.[11] Each year, outdoor air pollution contributes to millions of premature deaths worldwide.[12] Increasing evidence shows that long-term exposures to outdoor air pollutant concentrations at or below air quality

---

[7] Assembly Bill No 617. (2017).

[8] CARB. (2022). Community Air Grants.

[9] CARB. (2018). Community Air Grant Proposed Awardees.

[10] CARB. (2019). Community Air Grant Awardees.

[11] Murray, C. J. L., Aravkin, A. Y., Zheng, P., Abbafati, C., Abbas, K. M., Abbasi-Kangevari, M., Abd-Allah, F., Abdelalim, A., Abdollahi, M., Abdollahpour, I., Abegaz, K. H., Abolhassani, H., Aboyans, V., Abreu, L. G., Abrigo, M. R. M., Abualhasan, A., Abu-Raddad, L. J., Abushouk, A. I., Adabi, M., … Lim, S. S. (2020). Global burden of 87 risk factors in 204 countries and territories, 1990–2019: A systematic analysis for the Global Burden of Disease Study 2019. *The Lancet, 396*(10258), 1223–1249.

[12] World Health Organization (WHO). (2021). Ambient (outdoor) air pollution.

PSE

standards contribute to premature death.[13] Below we discuss the health relevance of the four key air pollutants captured by RAMN—fine particulate matter ($PM_{2.5}$), nitrogen dioxide (NO_2), ground-level ozone (O_3), and black carbon (BC). These pollutants were selected based on their known impacts on public health and the environment, as well as the quality of available low-cost sensors designed to track these pollutants. More specifically, the first three of these pollutants are classified as Criteria Air Pollutants under the Clean Air Act for their known adverse impacts on human health and the environment.[14] The U.S. Environmental Protection Agency (U.S. EPA) sets National Ambient Air Quality Standards (NAAQS) for criteria air pollutants to provide protections for public health and welfare (see **Table 1** below).[15]

1.1.1. Particulate Matter (PM)

Particulate matter (PM) is a mixture of solid particles and liquid droplets suspended in air. PM may be directly emitted (as primary PM) or may form when gaseous compounds—such as sulfur dioxide (SO_2), nitrogen oxides (NO_x), and volatile organic compounds (VOCs)—undergo chemical reactions in the atmosphere to form aerosols (secondary PM). The chemical makeup and size of PM can vary greatly.

Inhalable coarse particles with a diameter less than or equal to 10 microns (PM_{10}) may contribute to reduced visibility in air and may be inhaled and cause irritation of the upper respiratory tract. PM_{10} includes dust, pollen, and mold and can become suspended in the air from industrial activities, unpaved roadways, construction and demolition activities, and biological sources (e.g., tree pollen).[16] Fine inhalable particles, like $PM_{2.5}$—particulate matter less than or equal to 2.5 microns in diameter—can penetrate deeper into the respiratory tract and enter the bloodstream.[17] $PM_{2.5}$ may include soot, organic compounds, and metals emitted from the combustion of coal, gasoline, diesel, and wood and can stem from motor vehicles, industry, and fires.[18] Unlike coarse PM, a greater proportion of $PM_{2.5}$ includes condensed matter such as organic compounds and ammonium salts formed from atmospheric chemical reactions of gaseous pollutants. Exposure to PM is associated with premature death in people

---

[13] Dominici F, Zanobetti A, Schwartz J, Braun D, Sabath B, Wu X. (2022). Assessing Adverse Health Effects of Long-Term Exposure to Low Levels of Ambient Air Pollution: Implementation of Causal Inference Methods. Research Report 211. *Health Effects Institute.*

[14] U.S. EPA. (2021). Criteria Air Pollutants.

[15] U.S. EPA. (2022). Criteria Air Pollutants-NAAQS Table.

[16] Polidori A., Papapostolou V., Collier-Oxandale A., Hafner H., and Blakey T. (2021) Community in Action: A Comprehensive Guidebook on Air Quality Sensors.

[17] U.S. EPA. (2021). Particulate Matter (PM) Basics.

[18] Polidori A., Papapostolou V., Collier-Oxandale A., Hafner H., and Blakey T. (2021). Community in Action: A Comprehensive Guidebook on Air Quality Sensors.

PSE

with pre-existing heart and lung disease, as well as nonfatal heart attacks, irregular heartbeat, low birthweight, increased respiratory symptoms (coughing, shortness of breath), aggravated asthma, and decreased lung function.[19,20] NAAQS for PM_{10} and $PM_{2.5}$ are shown in **Table 1**.

PM concentrations tend to vary throughout the year as they are influenced by meteorology and seasonal sources such as residential fuel burning and wildfire smoke events. Locations near roadways often experience higher PM levels during morning and evening rush hours.

1.1.2 Black Carbon (BC)

Black carbon (BC) is a component of PM emitted during incomplete combustion of biomass and fossil fuels. It is commonly referred to as soot. In urban environments, local sources of BC include heavy-duty diesel trucks and other diesel engines, residential wood burning, commercial charbroilers, as well as wildfire smoke events. Prior to the wide adoption of stringent vehicle emission controls, it was much more common to see black plumes emanating from the exhaust of trucks and buses. Exposure to BC has been associated with adverse health impacts, notably respiratory and cardiovascular disease.[21] Moreover, BC is also a short-lived but potent climate pollutant.[22]

1.1.3 Nitrogen Dioxide (NO$_2$)

Nitrogen dioxide (NO_2) is an important member of nitrogen oxides (NO_x)—a group of highly reactive gases, all of which contain nitrogen and oxygen in varying amounts. Motor vehicles, power plants, and certain industrial activities that burn fuels emit NO_x primarily in the form of NO (nitrogen monoxide) but also in the form of NO_2. In the atmosphere, NO is quickly oxidized to form NO_2. NO_2 is an important air pollutant because it is a precursor to the formation of O_3 and ammonium nitrate $PM_{2.5}$.[23]

NO_2 is also a respiratory irritant that can aggravate pre-existing respiratory diseases like asthma, which may result in increased respiratory symptoms, emergency department visits,

---

[19] U.S. EPA. (2021). Health and Environmental Effects of PM.

[20] Zhu, X., Liu, Y., Chen, Y., Yao, C., Che, Z., & Cao, J. (2015). Maternal exposure to fine particulate matter ($PM_{2.5}$) and pregnancy outcomes: A meta-analysis. *Environmental Science and Pollution Research*, *22*(5), 3383–3396.

[21] World Health Organization. (2012). Health Effects of Black Carbon.

[22] Bond, T. C., Doherty, S. J., Fahey, D. W., Forster, P. M., Berntsen, T., DeAngelo, B. J., Flanner, M. G., Ghan, S., Kärcher, B., Koch, D., Kinne, S., Kondo, Y., Quinn, P. K., Sarofim, M. C., Schultz, M. G., Schulz, M., Venkataraman, C., Zhang, H., Zhang, S., … Zender, C. S. (2013). Bounding the role of black carbon in the climate system: A scientific assessment. *Journal of Geophysical Research: Atmospheres*, *118*(11), 5380–5552. https://doi.org/10.1002/jgrd.50171

[23] U.S. EPA. (2021). Basic Information about NO_2.

PSE

and hospital admissions. Long-term exposure to NO_2 may contribute to the development of asthma.[24]

The concentration of NO_2 in the air rises and falls during the day and varies seasonally, depending on combustion activity, atmospheric chemistry, and meteorology. NO_2 concentrations typically peak in the morning and evening and are higher in winter than summer. NAAQS for NO_2 are shown in **Table 1**.

1.1.4 Ozone (O_3)

Ground-level O_3 is a gaseous criteria air pollutant that forms from VOCs and nitrogen oxides (NO_X) in the presence of sunlight. Vehicle exhaust, industrial emissions, gasoline vapors, and chemical solvents, as well as natural sources, emit O_3 precursors (VOCs and/or NO_X, depending on the source). While O_3 miles above the earth's surface protects us from harmful ultraviolet radiation, ground-level O_3 is a respiratory irritant that causes airway inflammation.

Exposure to O_3 can result in substernal chest discomfort and decrements in lung function. As such, ground-level O_3 can exacerbate existing respiratory conditions, increase susceptibility to infection, and increase the frequency of asthma attacks. Adverse respiratory health effects from exposure to ground-level O_3 have been observed in healthy adults, but are more severe among sensitive subgroups, including those with pre-existing respiratory conditions.[25] NAAQS for O_3 are shown in **Table 1**.

Ambient O_3 concentrations typically peak mid-day following emissions of O_3 precursors and when sunlight intensifies, and decline throughout the evening as NO interacts with (scavenges) O_3 to form NO_2 at night.[26] Given the influence of sunlight on the transformation of NO_2 to O_3, O_3 concentrations also typically vary seasonally, with higher O_3 concentrations in summer, and lower O_3 concentrations in winter.

---

[24] Ibid.
[25] U.S. EPA. (2021). Health Effects of Ozone Pollution.
[26] Finlayson-Pitts, B. J., & Pitts Jr, J. N. (1999). *Chemistry of the upper and lower atmosphere: theory, experiments, and applications*. Elsevier. https://doi.org/10.1016/B978-0-12-257060-5.X5000-X

PSE

Table 1. U.S. EPA National Ambient Air Quality Standards for PM$_{2.5}$, PM$_{10}$, NO$_2$, and O$_3$ aimed to provide public health protection. µg/m^3 - micrograms per cubic meter; ppb - parts per billion by volume; ppm - parts per million by volume. (Source: U.S. EPA, 2022)[27]

Pollutant	Averaging Time	Level	Form
PM$_{2.5}$	1 year	12.0 µg/m^3	Annual mean, averaged over three years
	24 hours	35 µg/m^3	98th percentile, averaged over three years[a]
PM$_{10}$	24 hours	150 µg/m^3	Not to be exceeded more than once per year on average over three years[a]
NO$_2$	1 hour	100 ppb	98th percentile of 1-hour daily maximum concentrations, averaged over three years
	1 year	53 ppb[b]	Annual mean[a]
O$_3$	8 hours	0.070 ppm (70 ppb)	Annual fourth-highest daily maximum 8-hour concentration, averaged over three years[a,c]

[a]Primary and secondary standards are aimed to provide both public health protection (protecting the health of sensitive populations such as asthmatics, children, and the elderly) and public welfare protection (protection against decreased visibility and damage to animals, crops, vegetation, and buildings).

[b]The level of the annual NO$_2$ standard is 0.053 ppm. It is shown here in terms of ppb for the purposes of clearer comparison to the 1-hour standard level.

[c] Final rule signed October 1, 2015, and effective December 28, 2015. The previous (2008) O$_3$ standards are not revoked and remain in effect for designated areas. Additionally, some areas may have certain continuing implementation obligations under the prior revoked 1-hour (1979) and 8-hour (1997) O$_3$ standards.

1.2 Monitoring Air Quality

Air quality is traditionally monitored by local, state, and federal agencies using sophisticated instruments that comply with U.S. EPA Federal Reference Method (FRM) or Federal Equivalent Method (FEM) guidance for their design and operation.[28] The regulatory network of air quality monitors is deployed at the *regional* scale, resulting in a relatively sparse network of air monitors that does not cover all communities and is not designed to survey an area for local air pollution hotspots. In California, there are approximately 260 active air quality monitoring

---

[27] U.S. EPA. (2022). Criteria Air Pollutants-NAAQS Table.
[28] Code of Federal Regulations, Title 40, Chapter 53.

PSE

stations operated by federal, state and local agencies.[29] This translates to roughly one air quality monitoring site per 150,000 people.

The regulatory network of stationary air quality monitors generally measures the six criteria air pollutants (PM, NO_2, O_3, SO_2, carbon monoxide, and lead) in outdoor air and reports concentrations on an hourly basis. Certain toxic air contaminants (or air toxics) are also monitored at certain locations, although it is important to note that they are not regulated in the same way as criteria air pollutants and there are no established continuous measuring techniques that can capture the large variety of air toxics simultaneously. Air pollution measurements are typically captured at stationary air monitoring locations, although mobile air monitoring is also conducted by many state and local agencies.

1.3 Low-Cost Air Sensor Technology

With recent technological advances in sensor manufacturing and wireless communication, low-cost air sensor technology has emerged as a viable option that enables air monitoring throughout communities and can complement regulatory air monitoring. Low-cost air sensors are typically far less expensive than regulatory instruments, which allows them to be deployed in denser networks to deliver much higher spatial and temporal resolution of air pollution measurements throughout a community. In addition, residents can install them inside or outside their homes. Data from these dense networks can support the efforts of regional and state air regulators and community-based organizations to enhance understanding of air pollution at the community level.

In addition to the lower sensor cost, another advantage of low-cost air quality monitors is that they require significantly less physical space and power than is typical of reference station equipment. This allows for monitors to be installed in more locations and in closer proximity to vulnerable receptors and sensitive groups, such as near schools, day care facilities, hospitals, outside of houses where particularly vulnerable members of the community reside, in neighborhoods characterized by elevated asthma rates, in neighborhoods with high numbers of air quality complaints, etc. By identifying areas with persistently elevated levels of air pollution, actions can be taken to reduce risk and exposure for the most vulnerable populations.

---

[29] CARB. (2022). Ambient Air Monitoring - Regulatory.

PSE

Low-cost air sensors generally require less expensive maintenance (per monitor) than regulatory monitors as low-cost sensors do not require the same rigorous certification within a narrow band of tolerance that FRM and FEM air monitors do. However, this also means that accuracy, precision, and overall data quality can be affected. Sensor response can vary over time due to changes in sensitivity (sensor drift), or due to the effects of relative humidity and temperature. Sensor performance can also be affected by cross-interference with other non-target air pollutants. To maintain adequate data quality over time, it is critical to implement robust procedures for data review and develop long-term quality assurance and quality control (QA/QC) approaches that include regular re-calibration of the low-cost sensors over time. This can incur additional costs on top of the added human capital, time and effort needed to maintain a large, dense network of low-cost sensors over time.

1.4 Project Objectives

In alignment with AB 617, one goal of this project is to provide community members and local organizations in Richmond-San Pablo with high-resolution air quality monitoring data to engage and empower participation in the development of effective management plans that will reduce exposures to harmful air pollutants. This project also aims to raise public awareness about air pollution and increase community engagement in policy conversations bolstered by data and rooted in the specific places where people live, work, and play.

Broadly, the high-level objectives of this project include the following:

- **Data collection for multiple air pollutants:** We chose $PM_{2.5}$, O_3, and NO_2 because these pollutants are strongly correlated with adverse health effects and are monitored at only one regulatory site within the study area. In addition, high-quality low-cost sensors are widely available for these three pollutants. BC was also added due to the presence of local diesel-engine sources in the community. However, there is no BC monitoring at the San Pablo regulatory site.

- **High-density monitoring with data collected every minute:** Our goal was to be able to characterize local ambient concentrations and concentration gradients, detect short-lived pollution outbursts, identify local air pollution hot spots, and identify local sources of air pollution.

PSE

- **Real-time data visualization:** We visualized air quality data in real-time at the community level in a way that was publicly accessible and in collaboration with other co-existing air quality data collection efforts.[30]

- **Community engagement:** We aimed to raise community awareness, provide reliable data to address local air quality issues and encourage community participation in monitor location selection and deployment.

- **Policy engagement:** Our goal was to provide reliable, hyper-local air quality data to the community and regulators, and translate the air pollution data collected into insights that support decision making on local, regional, and statewide air quality policies.

---

[30]Aclima. (2022). Insights Richmond-San Pablo: Block by Block and Current Air Quality.

PSE

In this section, we discuss additional factors related to air quality in a community context, including an overview of local sources of air pollution, cumulative burdens experienced by the community, and existing air monitoring that predates AB 617 community air monitoring efforts. We also evaluate additional datasets relevant to air quality in Richmond San-Pablo to provide context for the patterns and trends observed by the Richmond Air Monitoring Network (RAMN). These additional datasets include an emissions inventory of key stationary sources of air pollution, estimates of vehicle activity and primary emissions from mobile sources, and wind patterns in the area. These data sources were used to inform: (1) the siting of our air monitors to ensure that high risk areas and vulnerable populations are covered by our sensor network; and (2) subsequent analyses of data collected by RAMN in relation to these known sources of air pollution and their potential impacts.

2.1 Richmond-San Pablo, California: Community Context

Richmond, North Richmond, and San Pablo (herein referred to as Richmond-San Pablo) are cities located in the San Francisco East Bay Area that are characterized by intensive industrial activities and high traffic volumes. Industrial sources of air pollution include the third largest refinery in California (Chevron U.S.A Inc.),[31] port and freight activities, a coal terminal,[32] and numerous other industrial facilities. Richmond-San Pablo is located downwind of San Francisco, which is a large source of O_3 precursors. The community is also frequently downwind of the adjacent Chevron refinery, which can be a significant source of hydrogen sulfide (H_2S), sulfur oxides, and VOC emissions from the processing units, as well as from the crude oil and other feedstock chemicals that are unloaded at the Chevron wharf complex.[33] The area is intersected by three major highways: Interstate 580 (I-580) to the south, Interstate 80 (I-80) to the east, and the Richmond Parkway to the northwest, which connects the two interstates. The approximately ten-square-mile area bounded by these major highways is home to over 100,000 people composed primarily of populations of color (Hispanic or Latino, African-American, and Asian) that live in some of the most disadvantaged communities in

---

[31]California Energy Commision (CEC). (2022). [California's Oil Refineries](#).
[32] Levin-Richmond Terminal Corporation. (2022). [Home page](#).
[33] CARB. (2022). [Facility Search Engine](#).

California as measured by CalEnviroScreen 4.0 (CES) (**Figure 1**).[34] As compared to the rest of the State, areas in Richmond-San Pablo have higher rates of disease that can be related to poor air quality, such as prevalence of asthma, heart disease, and low birth weight (**Figure 2, right**).[35] At the same time, the $PM_{2.5}$ and O_3 indicators in CES indicate area-wide levels that hover at or below the state median, suggesting a disconnect between prevalence of certain health outcomes and air pollution data for the area (**Figure 2, left**). This raises some questions about the accuracy of available and modeled $PM_{2.5}$ and O_3 data and CES methodology for these two air pollutants that we discuss later in this report.
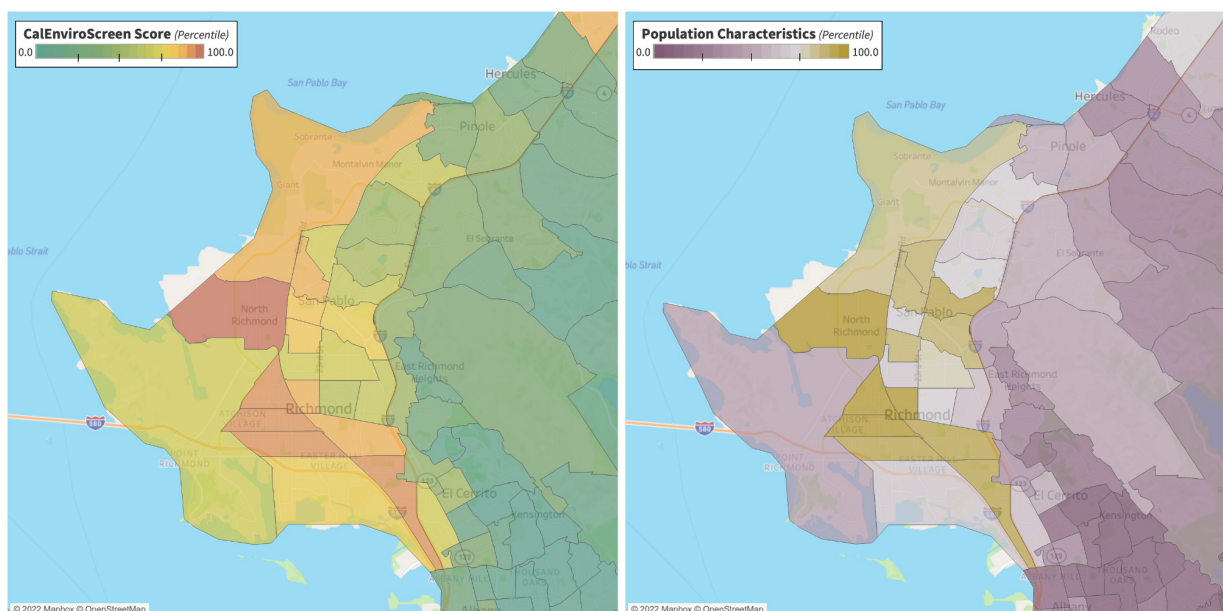
Figure 1. Map of CES 4.0 indicators by census tract in Richmond-San Pablo. Cumulative CES 4.0 score (left): Census tracts that are ranked within the top 25 percent in the combined CES score are designated as disadvantaged communities in California; colors diverge at the 75th percentile to better visualize disadvantaged communities. **Population characteristics score (right):** Represents sensitive populations and socioeconomic characteristics that can result in increased vulnerability to pollution. Population characteristics score is a component of the total CES score, shown on the left. Higher percentiles reflect census tracts with greater overall cumulative impacts and/or greater vulnerability to pollution burdens relative to other census tracts in California. Colors diverge at the 75th percentile.

---

[34] CalEnviroScreen (CES) is California's environmental justice cumulative impact methodology, which develops an EJ score for each census tract in California based on its statewide percentile values for 20 different socioeconomic, environmental, health, and demographic indicators. Disadvantaged communities in California (DACs) are communities that score in the top 25% of census tracts statewide in CalEnviroScreen 4.0.(OEHHA (Office of Environmental Health Hazard Assessment). (2021, February). Draft CalEnviroScreen 4.0.

[35] Bay Area AQMD. (2020). AB 617 Richmond-San Pablo Community Air Monitoring Plan.

PSE
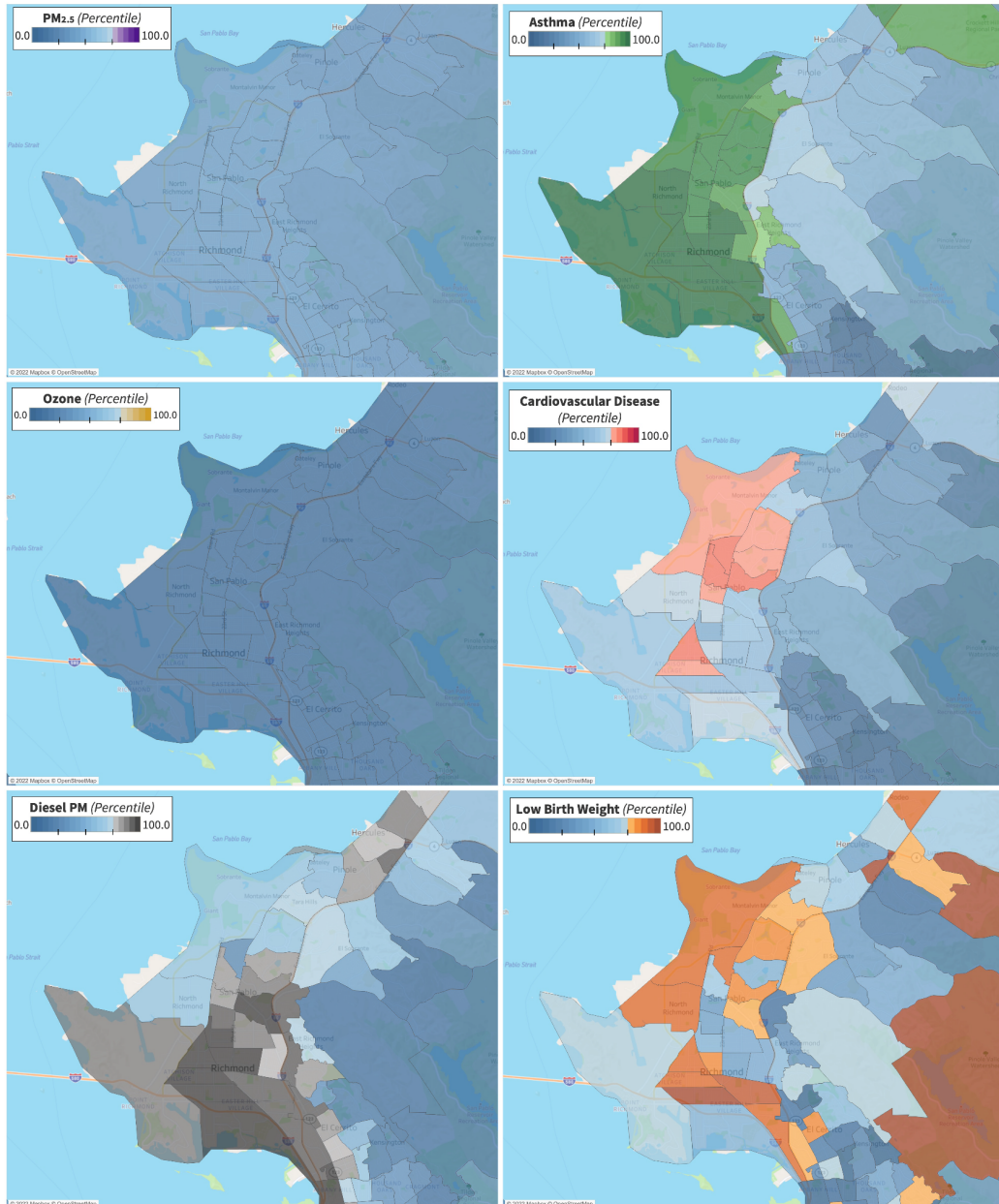
Figure 2. CES percentiles by census tract for air pollutant indicators (left) and health outcome indicators (right). Colors diverge at the 75th percentile. PM$_{2.5}$ (top left); ozone (O$_3$) (center left); diesel PM (bottom left); asthma (top right); cardiovascular disease (center right); and low birth weight (bottom right). Higher percentiles reflect census tracts with higher modeled pollutant concentrations (PM$_{2.5}$ and O$_3$) or pollutant emissions (Diesel PM) relative to other tracts in California. Higher percentiles for health outcomes reflect census tracts with higher numbers of asthma- and/or heart attack-related emergency department visits per 10,000 people, or higher percentage of low-weight births relative to other census tracts in California.

PSE

Sensitive receptor sites (schools, healthcare facilities, child care centers, senior care facilities) where populations vulnerable to air pollution may congregate are distributed throughout the community (**Figure 3, left**) whereas existing air monitors are spatially limited (**Figure 3, right**). Despite the variety of local contributors to air pollution, there is only one long-term regulatory air monitoring station in the project area that monitors for $PM_{2.5}$, NO_2, and O_3 (**Figure 3, right**). This regulatory site measures hourly O_3, NO_2, SO_2, and $PM_{2.5}$ concentrations, daily PM_{10} every 6th day, and daily VOCs every 12th day. There are two Special Purpose Monitors located close to the Chevron refinery: one in Point Richmond measuring H_2S, and one on 7th St. in Richmond measuring hourly H_2S and SO_2, and daily VOCs every 12th day.[36] In addition to these regulatory sites operated by the Bay Area Air Quality Management District (AQMD), there are three separate community air monitoring stations operated by Chevron and Sonoma Technology through an agreement with the City of Richmond.[37] These three community air monitoring sites measure $PM_{2.5}$, BC, BTEX (benzene, toluene, ethylbenzene, and xylene), and several other air toxics in real time.[38] Historical data from these sites, however, are not publicly available at present to compare with other air quality monitoring and health outcome datasets.[39]

With only one State Local Air Monitoring Station currently operated by the Bay Area AQMD in the entire Richmond-San Pablo area, sub one-hour air pollutant spikes and localized air pollution hot spots may be missed. A study conducted using Google Street View cars in Oakland revealed that air pollutant concentrations can vary sharply over very small distances (less than a quarter of a mile) and that the spatial lag for different types and sources of air pollutants can vary significantly.[40] This is especially true during times of rapidly changing weather conditions and in urban environments.[41,42] The State Local Air Monitoring Station in San Pablo is equidistant from the major traffic arteries, but is also over a mile away. As a result, pollution episodes related to heavy traffic and other mobile pollution sources may go

---

[36] Lapka, J., Fong, J., Hoag, K., & Flagg, M. (2022). Bay Area Air Quality Management District Meteorology & Measurement Division—2022 Air Monitoring Network Plan.

[37] Chevron Richmond refinery fenceline monitoring system. (2022). About.

[38] Chevron. (2022). Measurements.

[39] Chevron. (2022). Resources.

[40] Apte, J. S., Messier, K. P., Gani, S., Brauer, M., Kirchstetter, T. W., Lunden, M. M., Marshall, J. D., Portier, C. J., Vermeulen, R. C. H., & Hamburg, S. P. (2017). High-Resolution Air Pollution Mapping with Google Street View Cars: Exploiting Big Data. *Environmental Science & Technology*, *51*(12), 6999–7008. https://doi.org/10.1021/acs.est.7b00891.

[41] Karner, A. A., Eisinger, D. S., & Niemeier, D. A. (2010). Near-Roadway Air Quality: Synthesizing the Findings from Real-World Data. *Environmental Science & Technology*, *44*(14), 5334–5344. https://doi.org/10.1021/es100008x.

[42] Zhou, Y., & Levy, J. I. (2007). Factors influencing the spatial extent of mobile source air pollution impacts: A meta-analysis. *BMC Public Health*, *7*, 89. https://doi.org/10.1186/1471-2458-7-89.

PSE

undetected, and air pollution concentrations in the communities closest to the main highways and near or downwind of a variety of point source emitters remain unknown.
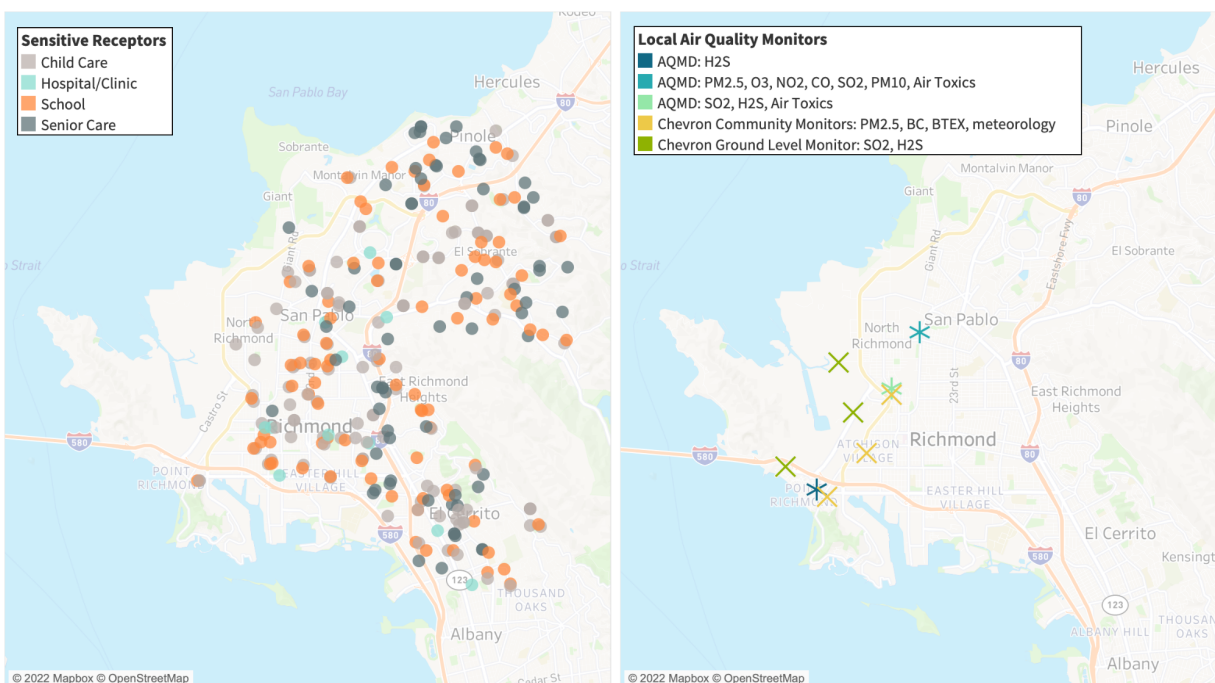
Figure 3. Sensitive receptor facilities and local air quality monitors in Richmond-San Pablo. Sensitive receptors (left): populations vulnerable to air pollution, including children, the elderly, and those with preexisting respiratory and cardiovascular conditions, congregate at childcare facilities (n=110), schools (n=88), elderly care facilities (n=68), and healthcare facilities (n=11). **Local air quality monitors (right):** Monitoring efforts that predate AB 617 stationary air quality networks include Bay Area AQMD sites (n=3, shown as " ✳ ") and monitors hosted by Chevron (n=6, shown as "X"). Color legend denotes each monitor and what they monitor for (Source: Bay Area AQMD, 2019).[43]

2.2 Stationary Sources of Air Pollution in Richmond-San Pablo

In this section, we evaluate the wide array of known stationary sources of air pollution in Richmond-San Pablo using aggregated estimated 2019 annual emissions of criteria air pollutants and air toxics from reporting (permitted) facilities in Richmond-San Pablo. Annual emissions are reported to CARB through the Criteria Pollutant and Toxics Emissions Reporting

---

[43] Bay Area AQMD. (2019). Richmond Steering Committee - Map Exercise, Sensitive Receptors.

(CTR) Program.[44,45] Using these data, we created a series of interactive data tools visualizing annual air pollutant emissions by each facility and each sector across Richmond-San Pablo.

These interactive data visualization tools are available online at https://www.psehealthyenergy.org/richmond-emissions-inventory **(Figure 4)**. This inventory only covers emissions from permitted facilities and does not include other key area-wide sources of PM, such as fugitive dust and residential wood combustion.
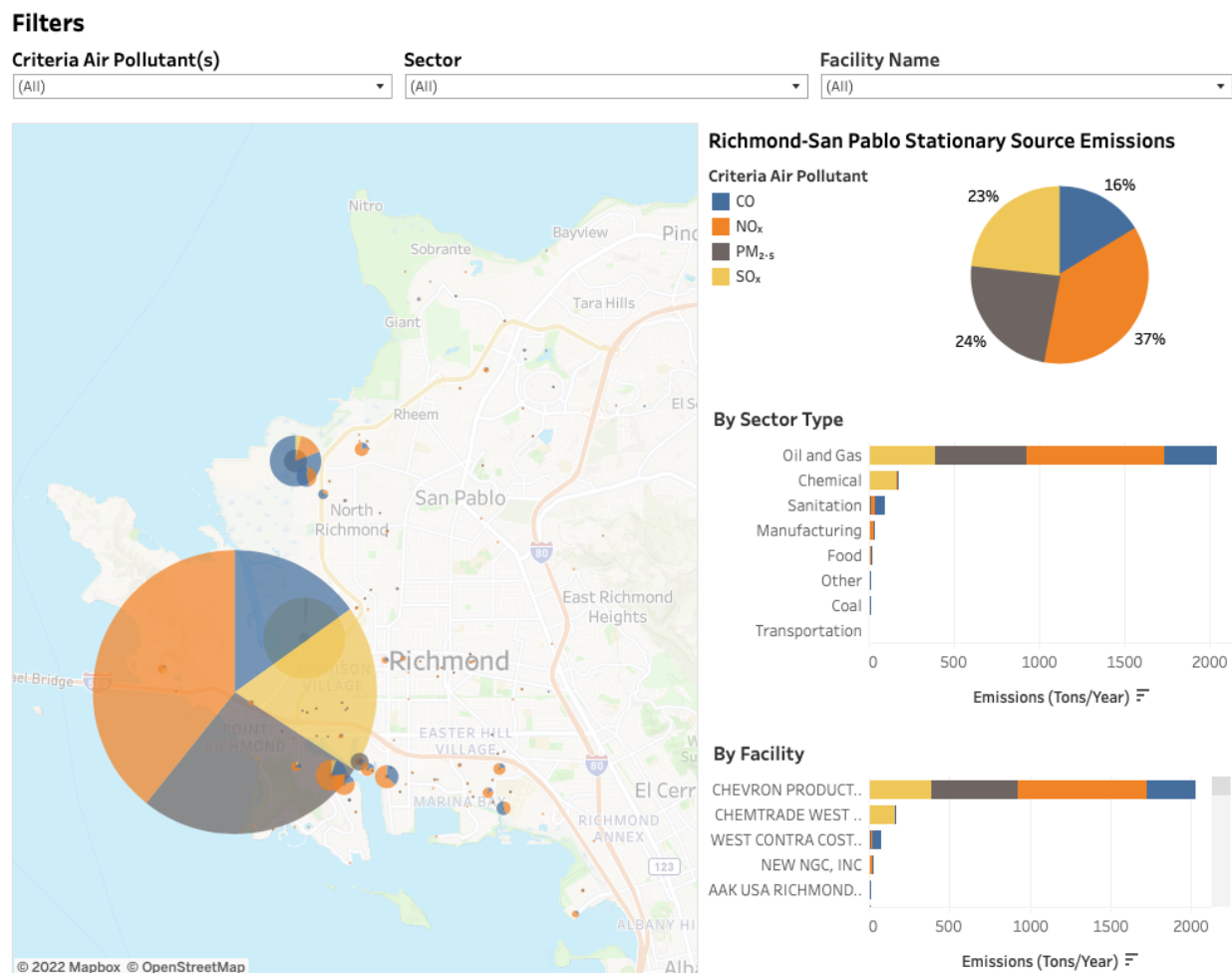
Figure 4. Stationary sources of criteria air pollutant emissions in Richmond-San Pablo. Static depiction of the interactive data visualization tool available at https://www.psehealthyenergy.org/richmond-emissions-inventory to compare emissions by facility type or by individual facility.

---

[44] CARB. (2022). Criteria Pollutant and Toxics Emissions Reporting Program.
[45] CARB. (2021). Facility Search Engine. 2019 data downloaded October 21, 2021.

Below, we discuss reported emissions inventories relevant in the context of RAMN, including primary emissions of PM, NO_X, and reactive organic gases (ROG). Reactive organic gases include VOCs that undergo chemical reactions in the atmosphere and can lead to secondary formation of O_3.

2.2.1 Facility Types

In 2019, 208 facilities in Richmond-San Pablo reported annual emissions to CARB. Broadly, the sectors of stationary source facilities in Richmond-San Pablo, listed in order of number of reporting facilities, include gas stations, manufacturing, sanitation (e.g., landfills), automotive shops, and oil and gas facilities, among others (**Figure 5, left**). Eighty-nine percent of these facilities had available geospatial information (**Figure 5, right**).
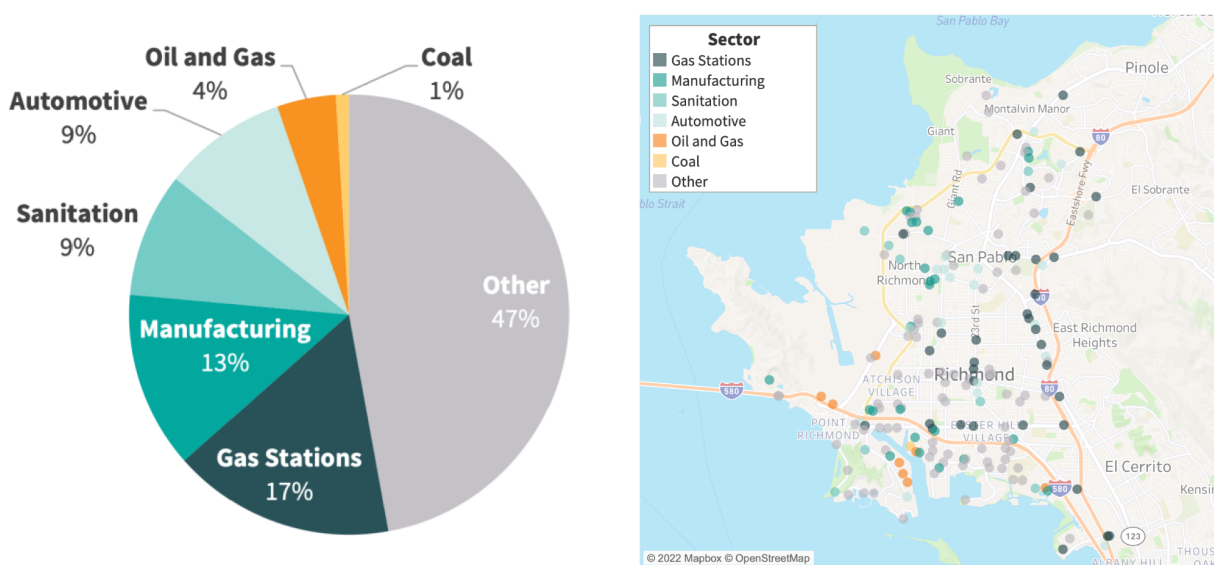
Figure 5. Stationary sources of air pollution in Richmond-San Pablo. (left) Fraction of stationary source facilities by sector; **(right)** location of stationary sources of air pollution across Richmond-San Pablo by sector. 208 permitted facilities reported annual emissions to CARB in 2019 (identified by Facility ID).

2.2.2 Stationary Source Primary Emissions of PM$_{2.5}$, NO$_X$, and ROG

Top stationary source sector emitters and top facility emitters of primary $PM_{2.5}$, NO_X, and ROG are detailed below.

- **Particulate matter ≤ 2.5 microns (PM$_{2.5}$):** The oil and gas sector, specifically the Chevron refinery, contributed approximately 95 percent of estimated primary $PM_{2.5}$ emissions from Richmond-San Pablo stationary sources in 2019 (538 tons $PM_{2.5}$),

PSE

followed by the West Contra Costa County Landfill (2.3 percent; 13 tons $PM_{2.5}$) and the Levin Coal Terminal (1.4 percent; 8 tons $PM_{2.5}$). These key stationary sources of primary $PM_{2.5}$ are located in the southwestern and northwestern regions of Richmond-San Pablo (**Figure 6, top**). Top sector emitters of total PM, PM_{10}, and $PM_{2.5}$ are shown in **Table 2**.

- **Nitrogen oxides (NO_x):** The oil and gas sector, specifically the Chevron refinery, also contributed over 90 percent of estimated primary NO_x emissions from Richmond-San Pablo stationary sources in 2019 (797 tons NO_x), followed by New NGC, Inc (2.1 percent; 18 tons NO_x) and the West Contra Costa County Landfill (1.2 percent; 10 tons NO_x). These key sources of primary NO_x are also located in the southern and northwestern regions of Richmond-San Pablo (**Figure 6**, middle).

- **Reactive organic gases (ROG):** The oil and gas sector is also the primary stationary source emitter of ROG—specifically the Chevron refinery (55.9 percent of total ROG emissions; 510 tons ROG) and the Phillips 66 terminal (15.2 percent; 138 tons). The West Contra Costa County Landfill also contributed approximately 12 percent (109 tons) of primary ROG emissions from stationary sources in Richmond-San Pablo in 2019. These ROG and O_3 precursor sources are largely overlapping with the main sources of primary $PM_{2.5}$ and NO_x and are located in the southern and northwestern regions of Richmond-San Pablo (**Figure 6, bottom**).
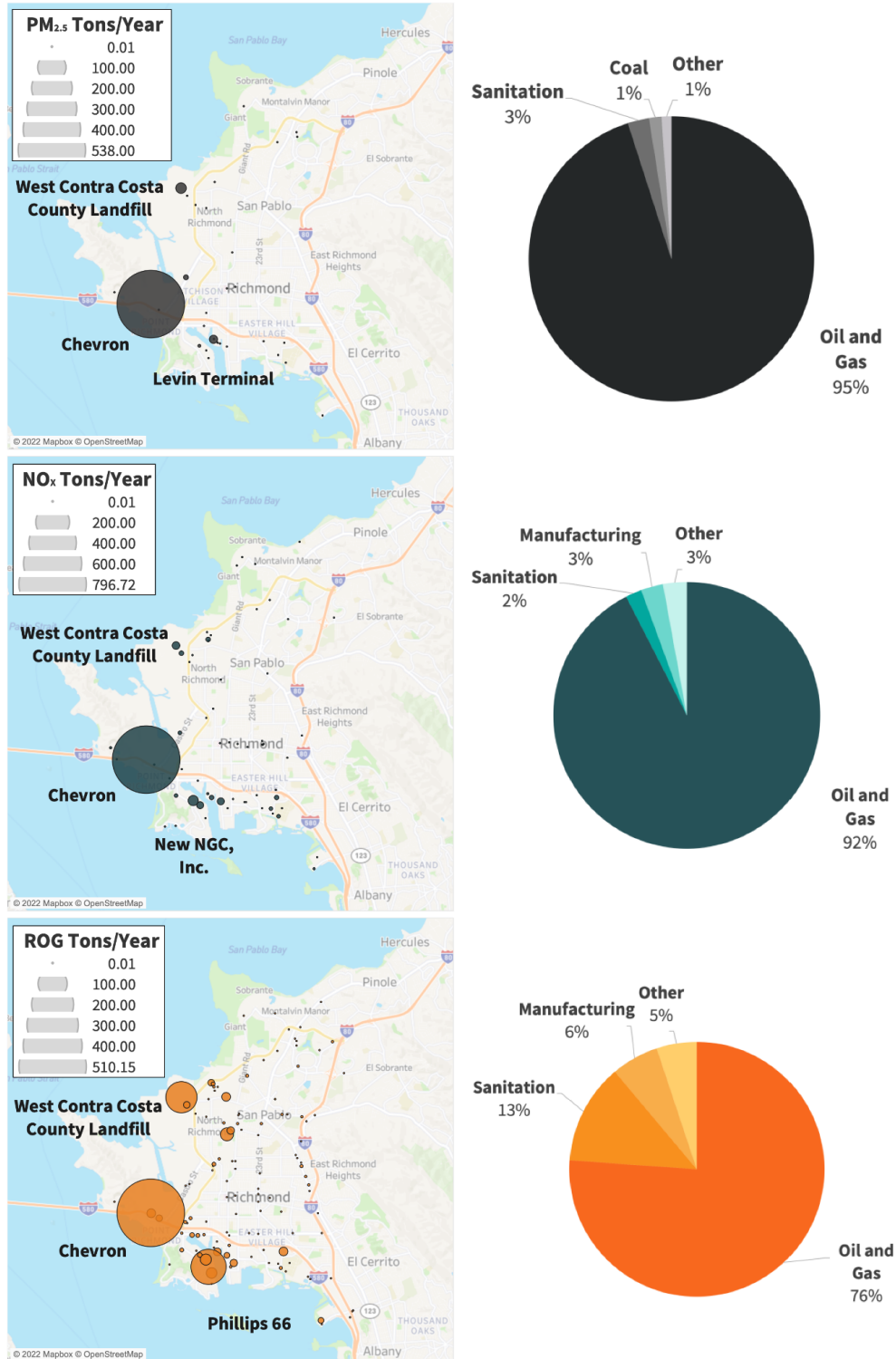
Figure 6. Proportion of Richmond-San Pablo primary stationary source emissions by sector for PM$_{2.5}$ (top), NO$_X$ (middle), and ROG (bottom). Top three emitting sectors and facilities shown for each pollutant.

Table 2. 2019 annual primary total PM, PM$_{10}$, and PM$_{2.5}$ emissions from stationary sources by sector in Richmond-San Pablo (Source: CARB, 2019).

Source Category	PM (Tons)	PM (%)	PM$_{10}$ (Tons)	PM$_{10}$ (%)	PM$_{2.5}$ (Tons)	PM$_{2.5}$ (%)
Oil and Gas	671.3	93.6	554.3	93.9	538.5	95.1
Coal	19.1	2.7	13.4	2.3	8.0	1.4
Sanitation	17.1	2.4	15.3	2.6	13.8	2.4
Manufacturing	5.0	0.7	3.4	0.6	2.2	0.4
Chemical	3.5	0.5	2.9	0.5	2.9	0.5
Transportation[1]	0.7	0.1	0.5	0.1	0.3	0.1
Food	0.6	0.1	0.6	0.1	0.6	0.1
Other[2]	0.3	0.05	0.3	0.1	0.3	0.0
Total	**717.5**	**100.0**	**590.5**	**100.0**	**566.5**	**100.0**

[1] Includes public transportation (e.g., bus, light rail) and rail freight transport, and excludes passenger cars and trucks.

[2] <2 tons of any pollutant per sector category.

PSE

2.3 On-Road Mobile Sources of Air Pollution in Richmond-San Pablo

Richmond-San Pablo's near proximity to multiple major Bay Area highways and roadways (I-580, I-80, and Richmond Parkway) means vehicular traffic likely contributes an important role in emissions for the region. Every day, tens of thousands of passenger cars and trucks commute along I-580 and I-80 alone[46], not to mention daily traffic on city roadways in Richmond-San Pablo. Internal Combustion Engine (ICE) vehicles are significant emitters of nitrogen oxides (NO_x). These vehicles also emit particulate matter from both engine exhaust as well as brake and tire wear. Below, we provide estimates of on-road mobile source emissions of NO_x and $PM_{2.5}$ in the Richmond-San Pablo region and a comparison of their magnitude compared to stationary sources.

2.3.1 Methods

Emissions estimates were calculated using emissions data by vehicle subclass from CARB's 2017 EMFAC tool, and average roadway Vehicle Miles Traveled (VMT) data calculated from Average Annual Daily Traffic and road segment length from the U.S. Department of Transportation's 2017 Highway Performance Monitoring System (HPMS). Emissions were calculated for five vehicle classes: passenger cars, light-duty (class 1-3) trucks (which includes pickup trucks and many SUV and minivan models), medium-duty (class 4-6) trucks, heavy-duty (class 7-8) trucks, and buses. For a detailed breakdown on how these emissions were calculated, see the **Appendix**.

This section focuses specifically on mobile emissions from on-road vehicles. It should be noted that there are significant mobile sources of off-road emissions in the area as well; for example, cargo ships at the Port of Richmond are an important source of diesel PM, and coal-laden trains en route to the port are sources of coal dust. In 2014, the estimated annual NO_x and PM emissions at the Port of Richmond were 73.6 and 1.6 tons, respectively, with ocean-going vessels comprising the overwhelming majority of these emissions.[47] In addition, our inventory does not include $PM_{2.5}$ and PM_{10} emissions from road dust, which can be a significant component of on-road PM emissions and in some instances may be higher than the combined $PM_{2.5}$ emissions from vehicle exhaust, brake wear, and tire wear.[48]

---

[46]Department of Transportation. (2017). CalTrans Highway Performance Monitoring System.
[47]City of Richmond. (2015). 2015 Port of Richmond Clean Air Action Plan Progress Report.
[48] Correspondence with Bay Area AQMD (2022).

PSE

2.3.2 Results: Mobile Sources

Passenger cars and light trucks consist of the majority of annual roadway vehicle miles traveled (55% and 30%, respectively) (**Table 4** below). However, passenger car emissions of $PM_{2.5}$, PM_{10}, and NO_x are much lower proportionally compared to their VMT. Light and medium truck emissions roughly correspond to their proportion of VMT. Heavy-duty trucks, which tend to be diesel-fueled, have a disproportionately large impact on roadway particulate matter and NO_x emissions—they constitute only 2.3% of roadway VMT, but contribute 27% of on-road $PM_{2.5}$ emissions, 20% of PM_{10} emissions, and 32% of on-road NO_x emissions. These trucks are of particular concern due to their disproportionate emissions and due to heavy trucking activity associated with industrial operations in the Richmond-San Pablo area.

Emissions of ROGs are roughly proportional to the VMT for each vehicle class. It should be noted that VMT proportions and pollutant emissions factors were derived from Contra Costa County traffic data from CARB,[49] and may not perfectly match the roadway VMT breakdown in the smaller area of Richmond-San Pablo. For instance, the proportion of heavy trucks in Richmond-San Pablo may be higher or lower than the fraction of trucks in Contra Costa County.

---

[49] CARB. (2017). EMission FACtor (EMFAC) tool.

Tons PM$_{2.5}$ Per Mile

0.0 — 0.5
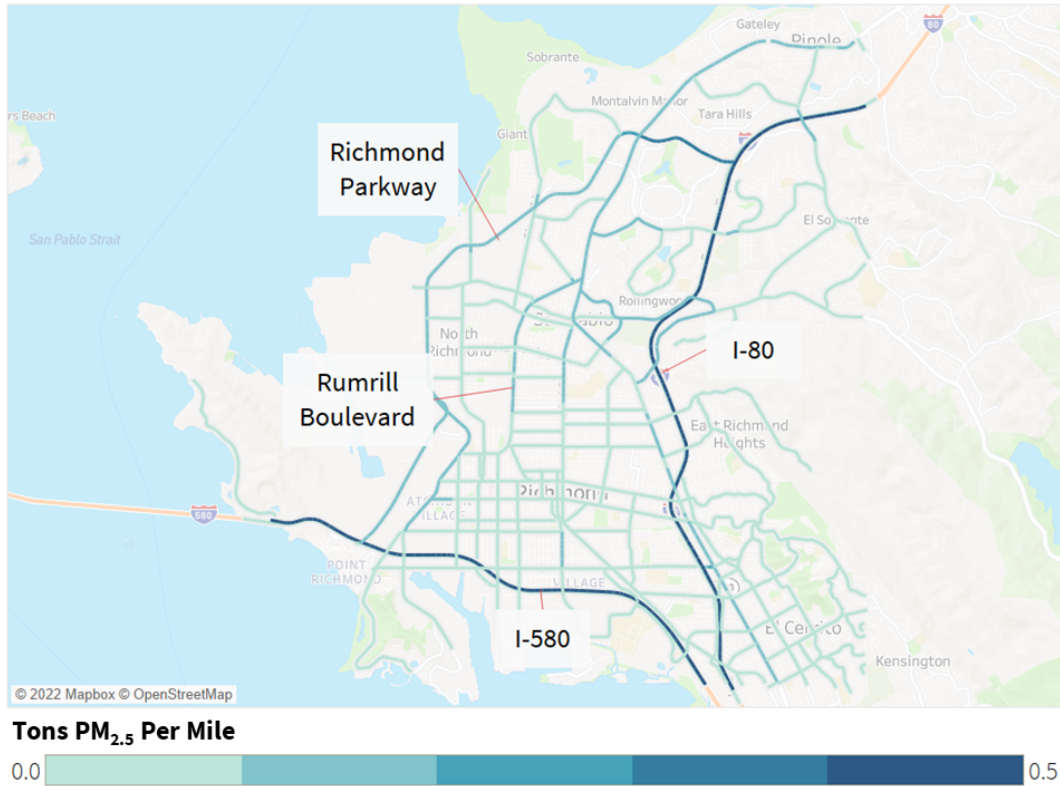
Figure 7. Map of PM$_{2.5}$ annual on-road mobile emissions per mile of road in Richmond-San Pablo. The average annual PM$_{2.5}$ emissions per mile of road segment are 0.2 tons. I-80 to the east and I-580 to the south are emissions hot spots in the region, followed by the Richmond Parkway (west) and sections of Rumrill Boulevard.

The major highways—I-80 to the east and I-580 to the south—are the main hotspots for PM$_{2.5}$ and NO$_x$ emissions, as well as the Richmond Parkway to the west and sections of Rumrill Boulevard. Driving conditions (speed, braking frequency) may affect emissions on different road segments[50] (for example, a freeway off-ramp with a tight turn may require harder braking, which would increase emissions of brake and tire wear-related PM$_{2.5}$.

Due to the lack of data on side streets, our emissions estimates are likely an underestimate. However, our results for Contra Costa county fall within 10% of CARB's mobile inventory NO$_x$ county estimate, and within 2% of CARB's PM$_{2.5}$ county estimate. NO$_x$ is the primary pollutant emitted by vehicles, followed by ROGs, both of which are precursors to secondary PM$_{2.5}$ formation.

---

[50] Shahariar , H., et al. (2022). Impact of driving style and traffic condition on emissions and fuel consumption during real world transient operation. *Fuel*. https://doi.org/10.1016/j.fuel.2022.123874
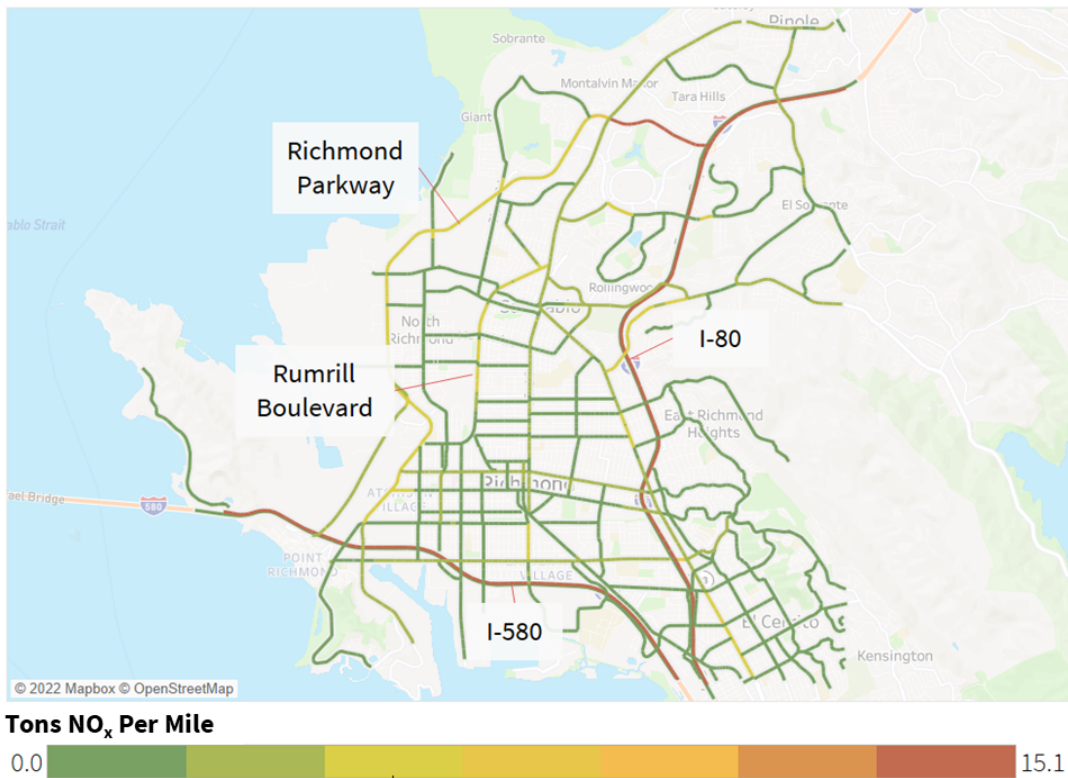
PSE

Figure 8. Map of NO$_x$ annual on-road emissions per mile of road segment in Richmond-San Pablo. The average NO$_x$ annual emissions per mile of road segment are 5.4 tons (color center). I-80 and I-580 are emissions hotspots in the region, followed by the Richmond Parkway and sections of Rumrill Boulevard.

Our methods have several limitations when estimating on-road mobile source emissions. The data used is annual and does not provide emissions at finer temporal scales that would be useful from a community standpoint to determine specific times (hours of the day or days of the week) that have particularly high emissions. As discussed above, the method also does not account for 100 percent of roadway emissions; emissions estimates do not include on-road construction equipment (tractors, etc.), or vehicles like motorcycles, motorhomes and others, for example. However, the total number of these vehicles is small and their omission likely does not alter our emissions estimates significantly.

The emissions are estimated in terms of mass units per mile and mass units per year, which is difficult to translate into ambient air concentrations without the use of an atmospheric dispersion model. Despite these limitations, our estimates still provide a general idea of the specific locations where on-road emissions are concentrated and how these compare with

PSE

estimated emissions from stationary sources. This information was used to inform our sensor site selection and subsequent analyses.

Table 3. 2017 annual estimates of primary PM$_{2.5}$, PM$_{10}$, NO$_X$, and ROG emissions from mobile sources (by vehicle class) in Richmond-San Pablo.

Vehicle Class	VMT (million miles/year)	PM$_{2.5}$ (Metric Tons)	NO$_X$ (Metric Tons)	PM$_{10}$ (Metric Tons)	ROG (Metric Tons)
Passenger Cars	733 *(55.3%)*	5.0 *(26.7%)*	124.7 *(18.8%)*	13.8 *(34.2%)*	164.9 *(48.6%)*
Light Duty Trucks	402 *(30.4%)*	5.8 *(30.8%)*	202.8 *(30.5%)*	13.5 *(33.6%)*	115.1 *(33.9%)*
Medium Duty Trucks	156 *(11.8%)*	2.6 *(13.9%)*	111.6 *(16.8%)*	4.9 *(12.2%)*	48.7 *(14.3%)*
Heavy Duty Trucks	30 *(2.3%)*	5.2 *(27.3%)*	212.7 *(32.0%)*	7.9 *(19.7%)*	9.9 *(2.9%)*
Buses	3.1 *(0.24%)*	0.26 *(1.4%)*	13.1 *(2.0%)*	0.1 *(0.2%)*	1.0 *(0.3%)*
Total	**1,324 *(100%)***	**18.9 *(100%)***	**665.0 *(100%)***	**40.3 *(100%)***	**339.4 *(100%)***
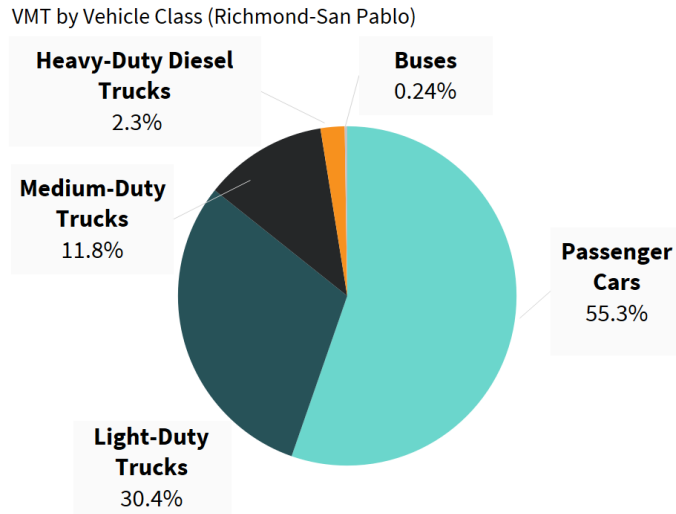
PSE

VMT by Vehicle Class (Richmond-San Pablo)

Heavy-Duty Diesel Trucks 2.3%
Buses 0.24%
Medium-Duty Trucks 11.8%
Passenger Cars 55.3%
Light-Duty Trucks 30.4%

PM2.5 Emissions by Vehicle Class (Richmond-San Pablo)

Medium-Duty Trucks 13.9%
Buses 1.4%
Passenger Cars 26.7%
Heavy-Duty Diesel Trucks 27.3%
Light-Duty Trucks 30.8%

NOx Emissions by Vehicle Class (Richmond-San Pablo)

Medium-Duty Trucks 16.8%
Buses 2.0%
Passenger Cars 18.8%
Heavy-Duty Diesel Trucks 32.0%
Light-Duty Trucks 30.5%
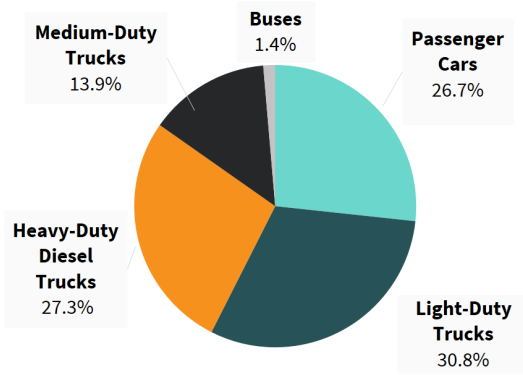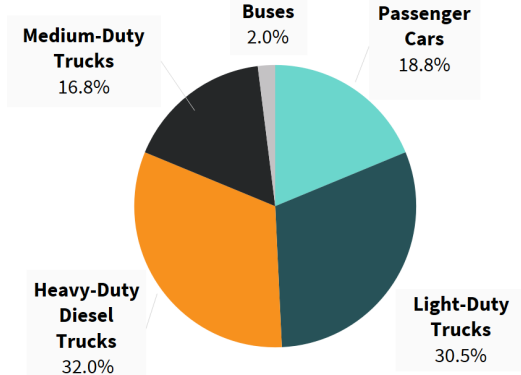
Figure 9. Percentages of VMT (miles/year), PM$_{2.5}$ (tons), and NO$_x$ (tons) contributed by each vehicle class. Passenger cars constituted the majority of roadway VMT. However, trucks contributed the most to PM$_{2.5}$ and NO$_x$ emissions. Heavy duty (Class 7-8) trucks consisted of only 2.3% of VMT but contributed 27.3% of PM$_{2.5}$ and 32.0 % of NO$_x$ emissions.

2.3.3 Comparison to Stationary Source Emissions

Generally, total estimated primary emissions of PM and NO$_x$ from on-road mobile sources in Richmond-San Pablo are slightly lower than the estimated primary emissions from stationary point sources, although, as discussed above, our on-road mobile emissions inventory is an underestimate. For PM, our estimates for stationary source emissions significantly exceed those from mobile sources—we estimate that stationary sources emitted 591 tons of PM$_{10}$ and

PSE

567 tons of $PM_{2.5}$ in 2019, while mobile sources emitted roughly 40 tons of PM_{10} and 19 tons of $PM_{2.5}$ in 2017. It should be noted again that $PM_{2.5}$ in the form of road dust from traffic was not included in these calculations, but is a significant $PM_{2.5}$ source—in 2021, they comprised nearly 34 tons of $PM_{2.5}$, or roughly double the emissions of $PM_{2.5}$ from vehicle exhaust, brake wear, and tire wear.[51] For NO_x, the two are more comparable: stationary sources emitted 876 tons of NO_x while mobile sources emitted 665 tons. Additionally, the years of our comparison differ—stationary source estimates use 2019 data while mobile source estimates use 2017 data. Finally, these estimates involve only primary air pollutants and do not take into account the formation of secondary air pollutants, which may be an important factor in Richmond-San Pablo, especially for $PM_{2.5}$. The stationary source emissions inventory only accounts for industrial sources of pollution, and does not include potential residential emission sources, like wood combustion. It should also be noted that mobile and stationary sources are not necessarily entirely separate—medium and heavy duty trucks contribute the majority of mobile emissions, and many of these trucks are likely linked to industrial activity in the area.

Our stationary and on-road mobile emissions inventories provide context regarding the scope and magnitude of air pollution and some of its sources in Richmond-San Pablo. This background information is useful in understanding historical emissions in the area, and in choosing locations for our air monitors (industrial areas, residential areas adjacent to major roadways, etc.). Real-time data from our network of air monitors can also point to sources of emissions based on our inventories, wind direction, and time of day. For instance, due to the magnitude of NO_x emissions from on-road traffic, we would expect NO_2 concentrations to be higher along neighborhoods near major freeways, and to peak during the morning and evening commute cycles.

2.4 Wind Patterns

Understanding air pollutant emission sources in Richmond-San Pablo is one of several important considerations. Another is contextualizing how air pollutants are transported across the city. Wind patterns affect the transport of pollutants, as winds can move pollutants from industrial point sources, highways, or areas outside of Richmond (i.e., San Francisco) into the city, either as primary or secondary pollutants. Emissions that occur in one neighborhood can influence ambient air pollutant concentrations in other neighborhoods downwind. Data on wind was collected from five Weather Underground stations in the region to determine prevailing seasonal wind speeds and directions. Data are recorded at five-minute intervals and were collected in 2020-2021. The five weather stations are located in

---

[51] Correspondence with Bay Area AQMD. (2022).

PSE

(1) the Hilltop neighborhood of San Pablo, (2) East San Pablo, (3) East Richmond, (4) Burg Park in Richmond, and (5) on Plunge, a swim center near Point Richmond. Of these sites, data for San Pablo Hilltop and Burg Park were only available for 2020, while data for east San Pablo were only available for 2021. Data from East Richmond and Plunge were available for both 2020 and 2021. We generated wind roses by season for each site (San Pablo Hilltop only had data for Fall and Winter) to examine wind speed, direction, and frequency throughout Richmond. Color bands indicate wind speed, the direction of each spoke indicates the direction the wind is coming from, and the length of each spoke indicates the frequency of wind readings from each direction. The longest spoke indicates the wind direction with the highest frequency (**Figures 10-11**).
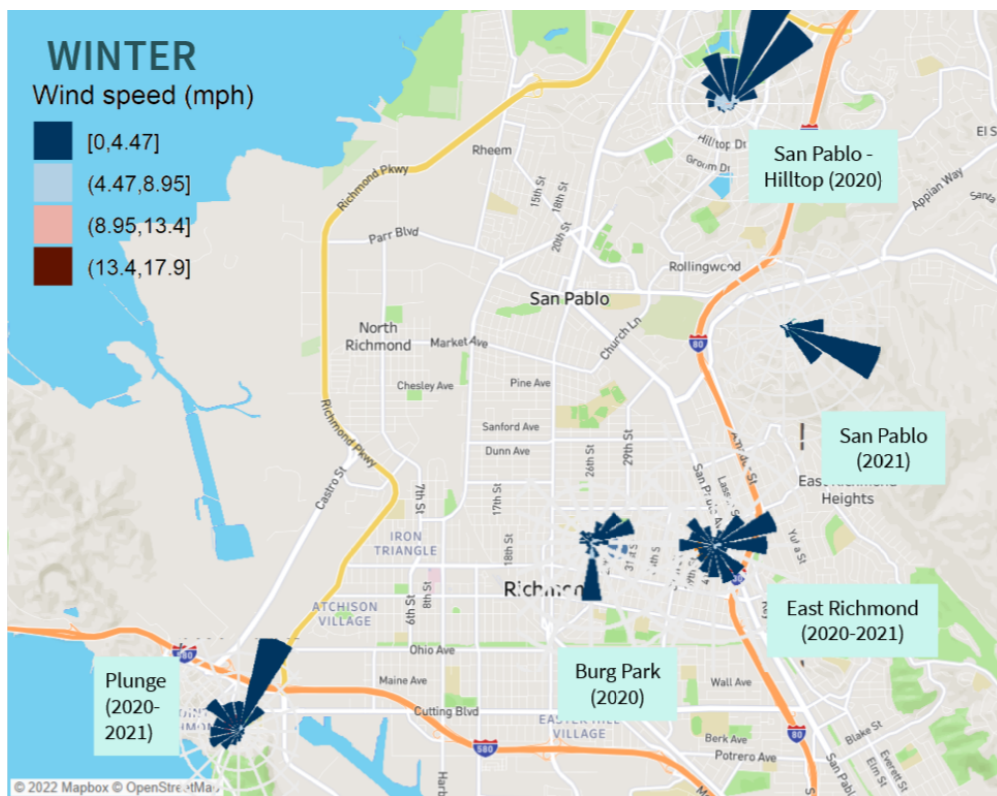
Figure 10. Wind roses across the five Weather Underground stations during the winter (December - February). The longest spokes indicate wind directions with the highest frequency.

In the winter, five-minute average wind speeds were relatively gentle across all sites (below 5 mph) (**Figure 10**). In Burg Park, the prevailing wind direction was from the south, with less frequent winds from the northeast. At the East Richmond site, winds were more variable, with prevailing winds from the northeast and the southeast. In east San Pablo, winds were more consistent—the prevailing direction was from the east. To the north in San Pablo-Hilltop,

PSE

winds primarily originated from the northeast. Similarly, on Plunge in Point Richmond, winds were also primarily blowing from the northeast. However, the station on Plunge is near the water, and may not be free from airflow and influence from nearby obstructions, so its wind readings were more variable.
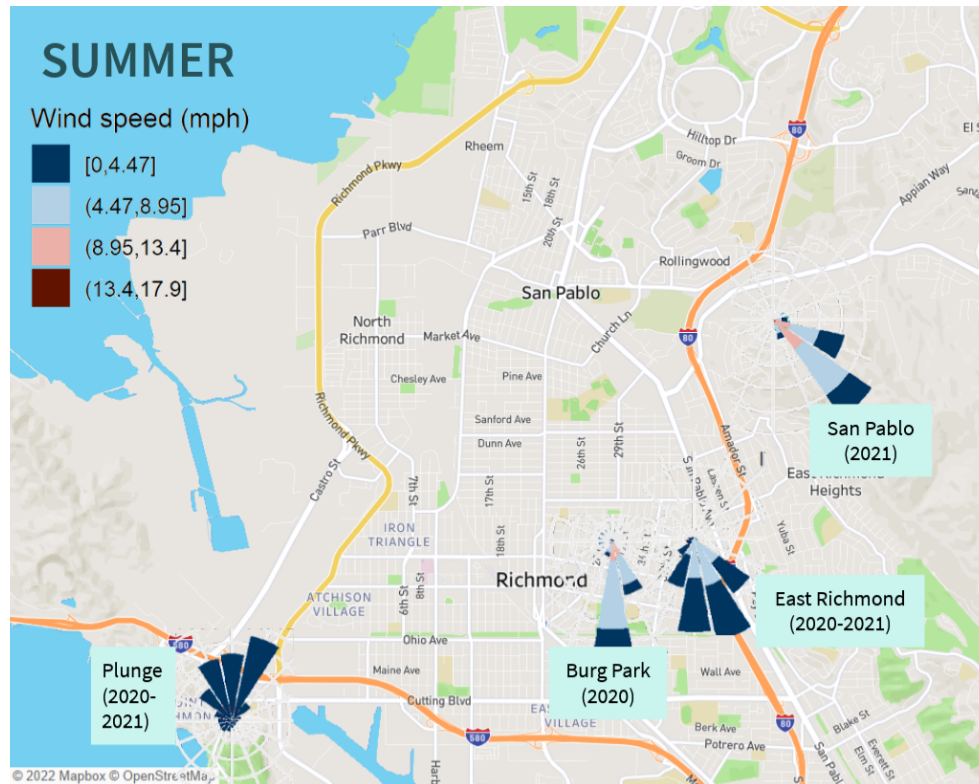
Figure 11. Wind roses across the five Weather Underground stations during the summer (June - August). The longest spokes indicate wind directions with the highest frequency.

In the summer, five minute-average wind speeds across most sites picked up, frequently between 4.5 and 9.0 mph, and sometimes reaching average speeds between 9 and 13.5 mph (**Figure 11**). Generally, wind speeds were stronger in the summer. In Burg Park, prevailing winds came from the south. In East Richmond, prevailing winds originated from the south and southeast. In East San Pablo, winds primarily came from the southeast. No data from the San Pablo Hilltop site was available during the summer. At Plunge, the wind speeds were slower, and mostly came from the north, which is unusual because other locations experience strong onshore winds in the summer.

Additionally, the Bay Area AQMD compiled hourly wind data from several wind monitors from different networks in the Richmond-San Pablo area for the period 2014-2018.[52] These wind

---

[52] Bay Area AQMD (July 2020). AB 617 Richmond-San Pablo Community Air Monitoring Plan.

PSE

data indicate that the general wind trends are southerly—prevailing winds coming from the south, southeast, and southwest.
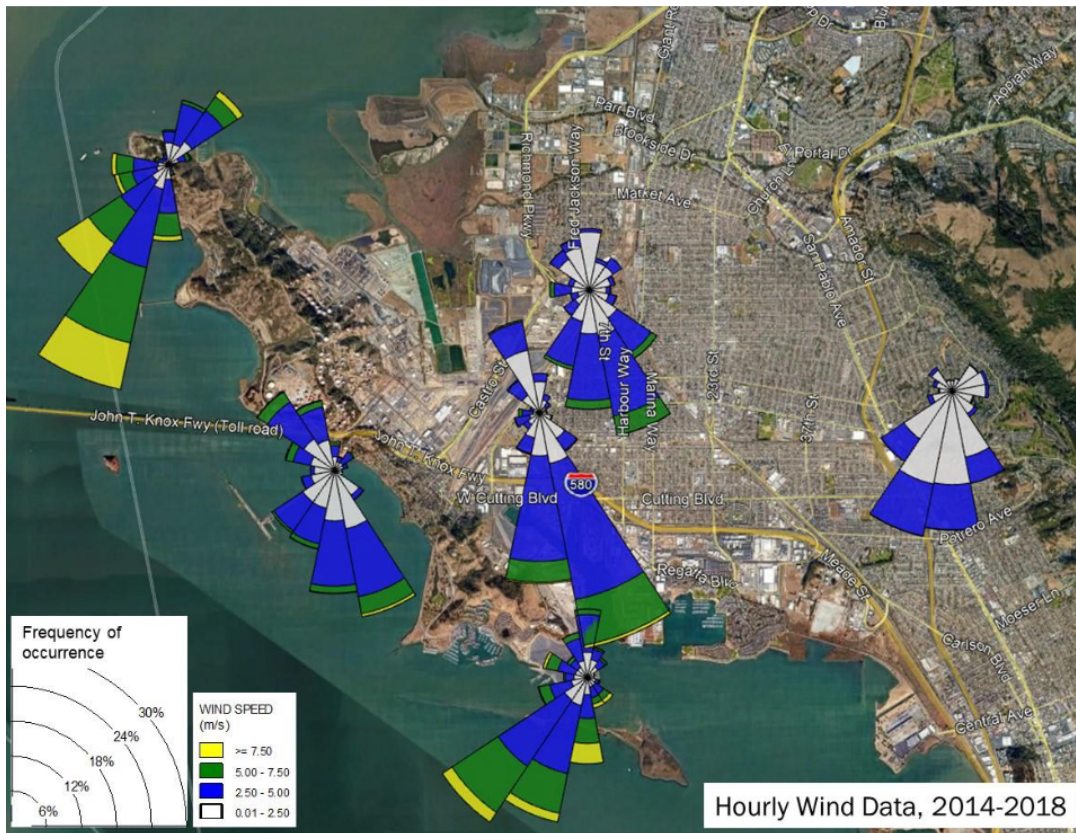
Figure 12. Wind data from Bay Area AQMD, NOAA, and Chevron wind monitors throughout Richmond as reported in the AQMD's AB-617 Community Air Monitoring Plan.[53]

Wind speed and direction will influence pollutant transport over Richmond. For example, the two major freeways, I-80 and I-580, intersect in the southeast corner of Richmond, in the Richmond Annex. South and southeast winds could therefore transport traffic pollutants into the heart of Richmond.

---

[53] Ibid.

Our overall air monitoring strategy was informed by a variety of considerations, including the project objectives, the distribution of the various emission sources, wind patterns influencing air pollutant transport, location of vulnerable populations and their proximity to emission sources, existing regulatory air quality monitoring sites, as well as feedback from the community to identify specific areas of concern.

3.1 The Richmond Air Monitoring Network

3.1.1 PM$_{2.5}$, O$_3$ and NO$_2$ Sensors

The choice of low-cost air sensor technology is critical to achieving project goals and ensuring high overall data quality and reliability. PSE considered a variety of sensor options based on the following criteria:

- Commercial availability.

- Ability to provide temporally-resolved measurements, ideally in one-minute intervals.

- Measurement of multiple criteria air pollutants—in particular, PM$_{2.5}$, O$_3$, and NO$_2$, all of which are key air pollutants in urban environments, are strongly correlated with adverse health effects, are emitted (or caused, in the case of O$_3$) by both stationary and mobile emission sources within the study area, and are not extensively monitored by the Bay Area AQMD across the Richmond-San Pablo community.

- Sensor quality, accuracy, precision, and reliability.

- Data communication via 4G cellular networks to facilitate real-time, continuous data visualization.

- Diagnostic and technical support from the manufacturer.

- Cost of less than $3,000 per air monitor, including hardware, software, and shipping costs, to fit our budget constraints.

Many commercially available low-cost air sensors have been evaluated for accuracy, precision, and reliability under various meteorological conditions and pollutant concentrations. One of the most reputable testing facilities is located at California's South Coast Air Quality Management District (SCAQMD). The Air Quality Performance Evaluation

Center (AQ-SPEC) program[54] evaluates commercially available low-cost sensors under both controlled lab environments and ambient conditions. We compared a number of reports conducted by AQ-SPEC for both PM and gaseous low-cost air sensors. Eventually, we selected the Aeroqual AQY 1 micro air quality monitor,[55] which, at the beginning of our study, was the only low-cost instrument to fit all of our selection criteria: (1) it was designed to measure key target urban air pollutants of interest—$PM_{2.5}$, O_3, and NO_2—as well as temperature and relative humidity, all in one-minute intervals; (2) received high scores from the AQ-SPEC testing program and showed strong correlation with FEM instruments;[56] (3) communicated wirelessly via WiFi and 4G cellular and stored data on the device as well as the Aeroqual Cloud to ensure against data loss; and (4) its cost fit our budget constraints. The Aeroqual AQY 1 was also the instrument of choice for SCAQMD's supplementary 100 low-cost sensor network in the Los Angeles basin as part of their AB 617 efforts,[57] which gave us additional confidence in these devices.
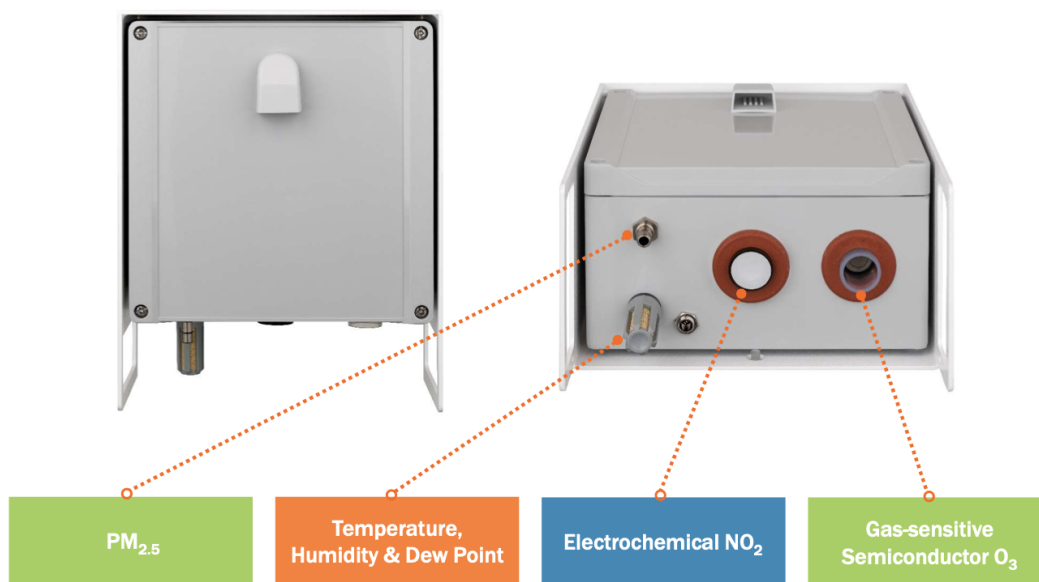
Figure 13. The Aeroqual AQY 1 Micro Air Quality Monitor. Image courtesy of Aeroqual, Inc.

The PM sensors used by Aeroqual in their AQY 1 air samplers are the SDS-011 optical particle counters (Nova Fitness Co. Ltd, China), which use a well-known light scattering method to count and size aerosol particles and convert these data to PM mass concentrations. These sensors are well-characterized in the scientific literature and have comparable performance

[54] SCAQMD. (2022). AQ-SPEC.
[55] Aeroqual. (2017). AQY, the smart air quality monitor, now available.
[56] SCAQMD. (2020). AQ-SPEC Field Evaluation Aeroqual AQY 1 (v1.0).
[57] Aeroqual. (2018). Postcard from L.A. – the highs and lows of building a 100 air quality sensor network in Los Angeles.

PSE

to the well-regarded PMS7003 particle sensor (Beijing Plantower Co. Ltd, China) used in the popular PurpleAir PA-II air monitors.[58] The SDS-011 sensor shows strong correlation with FEM instruments, good linearity of response, high accuracy, low drift, low inter-sensor variability, and has a well-characterized dependence on relative humidity (RH) and temperature.[59]

The O_3 sensor used in the Aeroqual AQY 1 units is a proprietary gas-sensitive semiconducting (GSS) tungsten oxide (WO_3) sensor manufactured by Aeroqual, Inc.[60] The sensor has consistently shown excellent correlation with FEM instruments, excellent accuracy, low inter-device variability, and has a well-characterized dependence on temperature and air flow, which is internally corrected within the device on a continuous basis.[61]

The AQY 1 measures NO_2 using an electrochemical sensor manufactured by Membrapor. The sensor is in effect an "odd oxygen" O_x sensor (sensitive to both O_3 and NO_2), whose response has also been characterized in detail.[62] Aeroqual uses their patented selective O_3 sensor to correct for O_3 interference on the electrochemical O_x sensor and thus deliver a real NO_2 measurement. The algorithm is embedded in the device and occurs in real time. Of the three sensors, the electrochemical O_x sensor was the one most prone to drift (i.e., measurement bias) and least accurate over the 2+ years of RAMN deployment in Richmond-San Pablo.

PSE procured 50 Aeroqual AQY 1 air quality monitors between May and July 2019. Each unit is roughly the size of a shoe box (4.8 inches long by 6.7 inches wide by 8.5 inches high), requires access to a power outlet, and transmits data to Aeroqual's cloud-based platform via WiFi or 4G cellular network.

3.1.2 Monitor Site Selection and Volunteer Host Recruitment

To determine optimal locations for monitor deployment, we used the following considerations:

- Locations of existing regulatory and community air monitors;

---

[58] Badura, M., Batog, P., Drzeniecka-Osiadacz, A., & Modzel, P. (2018). Evaluation of low-cost sensors for ambient $PM_{2.5}$ monitoring. *Journal of Sensors*, *2018*. DOI: 10.1155/2018/5096540

[59] Liu, H. Y., Schneider, P., Haugen, R., & Vogt, M. (2019). Performance assessment of a low-cost $PM_{2.5}$ sensor for a near four-month period in Oslo, Norway. *Atmosphere*, *10* (2), 41. https://doi.org/10.3390/atmos10020041

[60] Williams, D. E., Henshaw, G. S., Wells, D. B., Ding, G., Wagner, J., Wright, B. E., ... & Salmond, J. A. (2009). Development of low-cost ozone measurement instruments suitable for use in an air quality monitoring network. *Chem. New Zealand*, *73*, 27-33. DOI: 10.1088/0957-0233/24/6/065803

[61] Ibid.

[62] Weissert, L. F., Alberti, K., Miskell, G., Pattinson, W., Salmond, J. A., Henshaw, G., & Williams, D. E. (2019). Low-cost sensors and microscale land use regression: Data fusion to resolve air quality variations with high spatial and temporal resolution. *Atmospheric environment*, *213*, 285-295. DOI: 10.1016/j.atmosenv.2019.06.019

PSE

- Locations of stationary sources of air pollution, major roadways, and sensitive receptor sites (e.g., schools, day care centers, elderly care facilities, hospitals);

- Locations of monitors for other AB 617 community air monitoring projects (e.g., Groundwork Richmond and Ramboll);

- Location of Environmental Justice (EJ) communities;and

- Community feedback on emission sources of interest and areas of perceived poor air quality in Richmond-San Pablo.

Soliciting community input on the location of monitors was a key priority. In January 2019, PSE introduced the project to APEN members at the APEN Richmond office. The presentation was followed by a discussion about perceived air pollution hot spots and priority areas for air monitoring. APEN members indicated specific potential monitoring locations on a physical map (**Figure 14**). In addition to the in-person outreach, PSE created an online "Sensor Location Suggestion Form" shared via community email listservs to solicit additional input on desired monitor locations and gather information on volunteers interested in hosting air monitors at their homes. Once initial monitor locations were chosen and residential volunteers were selected, we coordinated with the West Contra Costa Unified School District (WCCUSD) to identify priority school locations that would help address spatial gaps in our planned air monitoring network.

Figure 14. January 2019 APEN Leader's Meeting Exercise. APEN Members indicated areas where they were interested in seeing additional air quality monitoring on a physical map.

PSE

3.1.3 Technical Advisory Committee

PSE convened a technical advisory committee of public health and air quality experts to provide ongoing technical expertise and oversight for the Richmond Air Monitoring Network. The technical advisory committee included: John Balmes, MD (UC Berkeley, UCSF, Physician Member of CARB); Katharine Hammond, PhD (UC Berkeley); Thomas Kirchstetter, PhD (UC Berkeley, Lawrence Berkeley National Laboratory); Rachel Morello-Frosch, PhD (UC Berkeley); and Ajay Pillarisetti, PhD (UC Berkeley). Committee members met periodically throughout the duration of the project and provided valuable oversight to support the scientific integrity of the air monitoring project.

3.1.4 Initial Calibration

Collocation of monitors at the Bay Area AQMD regulatory monitoring site in San Pablo was not possible at the beginning of our study. Instead, we collocated two batches of AQY 1 air monitors near reference instrumentation at CARB's Monitoring and Laboratory Division (MLD) facility in Sacramento, California, between July 2019 and January 2020. 24 AQY 1 monitors were deployed at CARB's MLD site between July and November 2019, and 26 monitors were deployed between November 2019 and January 2020.

The long initial field collocation study was important to understand overall sensor drift and inter-device variability and to correct for individual sensor bias. Our initial field calibration in Sacramento revealed some O_3 sensor drift over time that further emphasized the need for a long-term continuous calibration process throughout the duration of our community deployment in Richmond-San Pablo. Two monitors from the first collocation round in Sacramento were subsequently left for several additional months at the MLD site in Sacramento to continue monitoring for sensor drift.

3.1.5 Sensor Deployment in Richmond-San Pablo

We deployed 50 Aeroqual AQY 1 micro air quality monitors equipped with $PM_{2.5}$, NO_2, and O_3 sensors throughout Richmond-San Pablo between December 2019 and August 2020. Monitor deployment in Spring and Summer 2020 was significantly delayed due to shelter-in-place orders related to the COVID-19 pandemic. The AQYs were typically installed at a height of approximately 2 meters (m) and at locations where airflow was as unobstructed as possible (**Figure 15**). Placements at this height were not possible at 10 of the school sites and at the AQMD regulatory station, where the Aeroqual sensors were placed on rooftops. In total, 31 monitors were deployed at residences, 15 at educational facilities (WCCUSD schools and Contra Costa College), four at local businesses, one at a fire station, and two monitors were collocated at the Bay Area AQMD San Pablo regulatory monitoring site **(Figure 16)**.

PSE

**Figure 15. Examples of Aeroqual AQY 1 micro air quality monitor deployment in Richmond-San Pablo.**
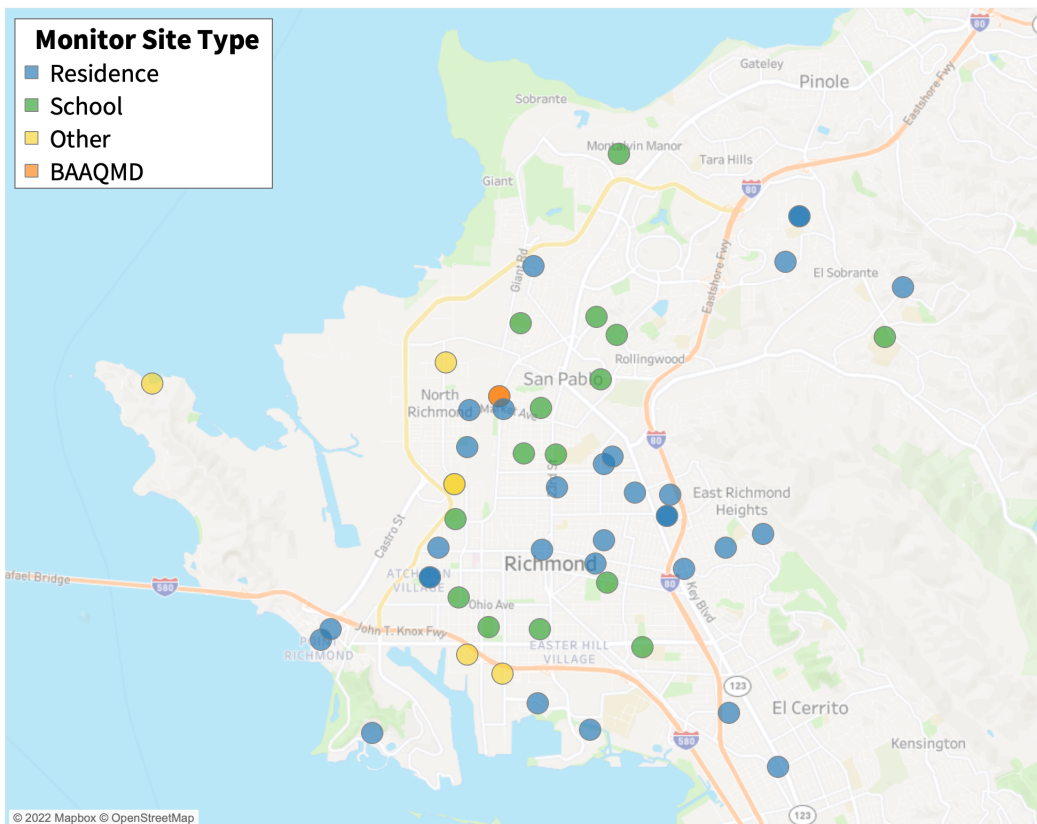
Figure 16. Aeroqual AQY 1 micro air quality monitors deployment locations throughout Richmond-San Pablo by site type (residence, school, Bay Area AQMD, other).

Our network of air monitors was spread across 14 neighborhoods and three land use categories (residential, commercial, and industrial) in the Richmond-San Pablo Area. These non-official neighborhoods were designated by grouping City of Richmond Neighborhood Councils into larger areas, with the goal of having more than one air monitor within each neighborhood. Land use categories were assigned using City of Richmond zoning data as well as satellite imagery for the sites in the San Pablo area.
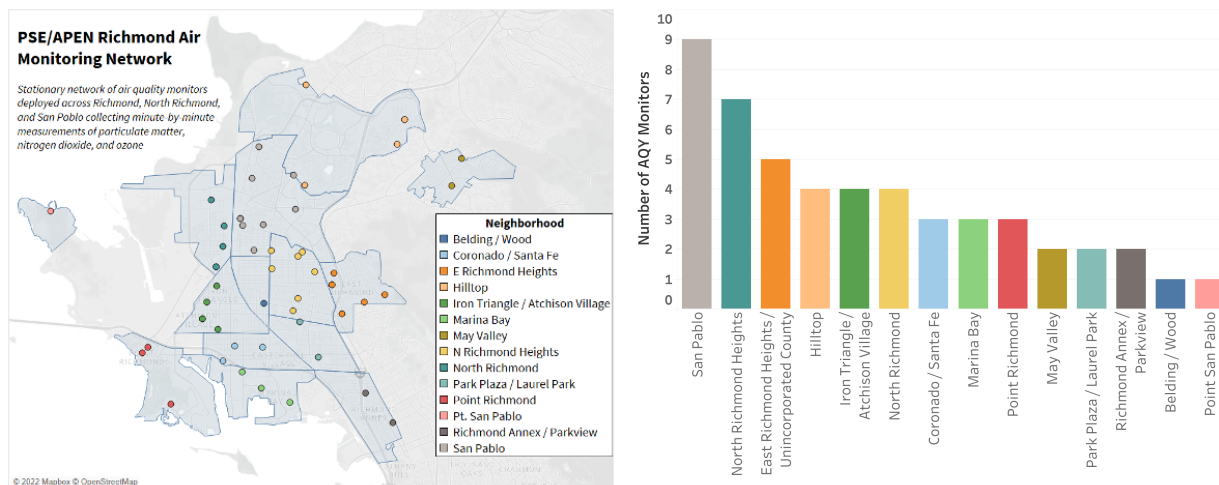
Figure 17. Distribution and location of monitors throughout the 14 neighborhoods of Richmond-San Pablo.

The 50 air monitors were not evenly distributed across neighborhoods. Two neighborhoods (San Pablo and North Richmond Heights), had upwards of six monitors, while two other neighborhoods (Belding/Wood and Point San Pablo), had only one monitor each. 32 monitors were in areas zoned as Residential, 15 monitors were in areas zoned as Commercial, and seven in areas zoned as Industrial.

3.1.6 Data Processing and Quality Assurance

As discussed above, low-cost air sensors show great promise for empowering community-driven air monitoring efforts and significantly increasing the number of places and times air quality measurements are taken. However, they still require a robust data quality assurance plan. We observed various data quality issues typically found with air monitoring networks, including sensor drift, sensor failure, sensitivity to environmental conditions (e.g., dust, humidity), and data incompleteness. We used a multi-step quality assurance protocol to address these issues. This process is summarized in **Figure 18**, and described in more detail in the **Appendix**. All code used throughout this process was written in a mix of Python and R.

Moment matching calibration
* Uses mean and variance to develop gain and offset based on proxy site
* Applied to raw data to obtain calibrated values

Data filtration
* Remove negative values
* Remove readings from flatlined sensors
* Remove readings from sensors with over-elevated values for >24 straight hours
* Remove consistently over-elevated sensors

```
Aeroqual Cloud → 5, 10, or 60-minute data → Corrected data → Corrected data with anomaly flags → Corrected, filtered data with anomaly flags → Final Dataset
```

Downloader scripts
* Backfills missing values in last eight weeks
* Combines new data and old
* Averages one-minute data to 10 or 60 minute

Anomaly Detection
* Decomposes data to detect network-wide $PM_{2.5}$ anomalies
* If anomaly detected and $BC/PM_{2.5}$ ratio below 5%, flag as wildfire

Growth factors
* If wildfire detected, multiply calibrated $PM_{2.5}$ by growth factor based on relative humidity

Figure 18. Overview of our data processing and quality assurance protocol.

3.1.7 Black Carbon Sensors and Site Selection

In addition to the Aeroqual AQY 1 air monitors, the Richmond Air Monitoring Network included seasonal deployment of low-cost BC sensors at the 50 RAMN monitoring sites established across Richmond-San Pablo. At each location, an Aerosol Black Carbon Detector (ABCD) was collocated with the Aeroqual AQY 1 units. The ABCD is a filter-based absorption photometer that was custom-built at the UC Berkeley and Lawrence Berkeley National Lab (LBNL), and performs comparably to the commercially-available aethalometer used in some Bay Area AQMD monitoring stations (**Figure 19**).[63] These sensors have a built-in algorithm to limit measurement bias associated with changes in temperature and relative humidity, and are housed in a waterproof enclosure equipped with solar panels and rechargeable batteries. BC and other instrument parameters are recorded at 1-Hz on a microSD card.

---

[63] Caubel, J. J.; Cados, T. E.; Kirchstetter, T. W. A New Black Carbon Sensor for Dense Air Quality Monitoring Networks. Sensors (Switzerland) 2018, 18 (3), 1–18, DOI:10.3390/s18030738.

PSE
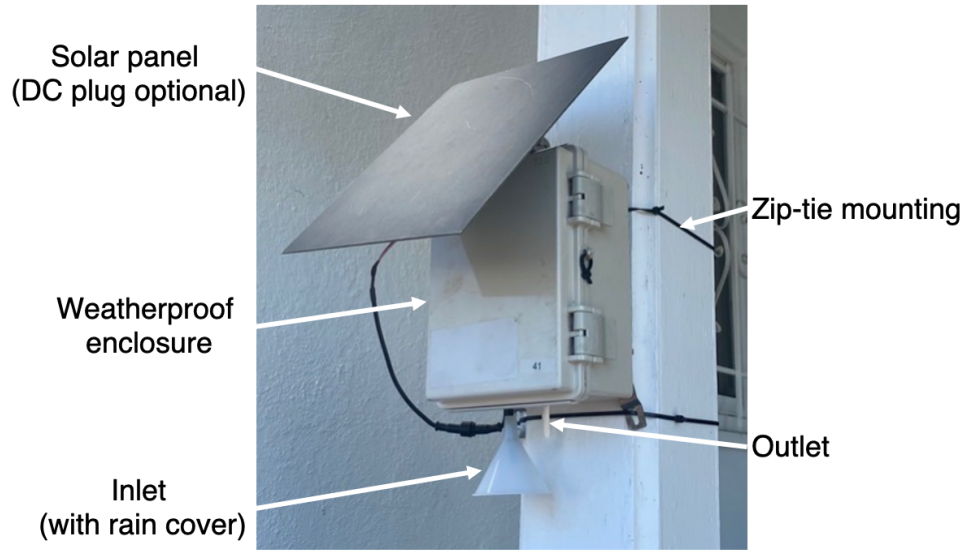
Figure 19. The Aerosol Black Carbon Detector (ABCD) pictured here is a filter-based, absorption photometer developed by LBNL and UC Berkeley.[64]

The BC sensors were deployed in three separate periods: (1) a 24-site, three-week deployment from August 12–September 1, 2020, during which time the region was heavily impacted by wildfire smoke; and two, 50-site, four-week deployments in (2) the winter period of January 14–February 10, 2021, and (3) the late spring period of May 19–June 21, 2021 (**Figure 20**). ABCDs were typically placed at the front of a home, business, or school, facing the nearest road, at a height of approximately 2 m, and within 1–2 m of the Aeroqual sensors (**Figure 21**). Such close collocation was not possible at 18 of the sites, where the Aeroqual sensors were placed on rooftops or behind locked gates. In these instances, the ABCD was placed within 100 m of the Aeroqual sensor.

---

[64] Caubel, J. J.; Cados, T. E.; Kirchstetter, T. W. A New Black Carbon Sensor for Dense Air Quality Monitoring Networks. Sensors (Switzerland) 2018, 18 (3), 1–18, DOI:10.3390/s18030738.

PSE
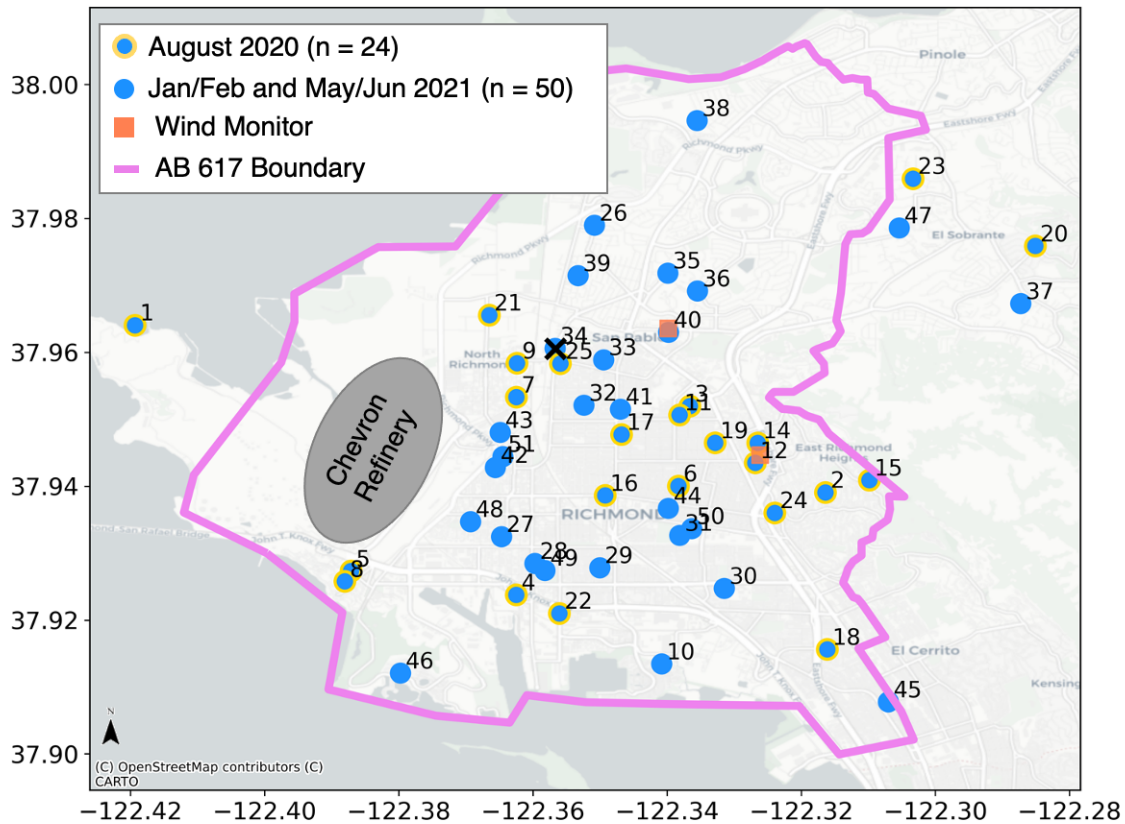
Figure 20. Richmond Air Monitoring Network locations where ABCDs and Aeroqual sensors were collocated. The subset of 24 sites included in the August 2020 deployment are highlighted with a yellow outline. The AB 617 boundary—the community boundary used for the development of a Community Air Monitoring Plan or Community Emissions Reduction Program—is outlined in pink, and wind monitors in the study area are indicated by orange squares. The Chevron Refinery is located on the west side as indicated by the gray oval. The Bay Area Air Quality Management District (AQMD) monitoring station is marked with a black "X".

Figure 21. Examples of ABCD installations in Richmond.

3.1.8 ABCD Data Quality Assurance and Control

Prior to field deployment, the temperature and humidity bias compensation of each ABCD unit was verified by sampling particle-free outdoor air using an in-line HEPA filter for 48–72 hours. Only sensors that reported hourly averaged concentrations of ±0.05 µg m^{-3} were used in this study. In addition, each unit was tested for battery life, stable and accurate air flow measurement, and correct timestamp prior to deployment in the field.

In the field, the performance of each ABCD was checked and data was manually downloaded weekly from the on-board SD cards. Maintenance was carried out on an as-needed basis if indicated from an in-field quality control screen of the downloaded data. PM$_{2.5}$ data from the Aeroqual sensors was managed by PSE and was adjusted with a proprietary correction, as described above. Additional details are provided in the **Appendix**.

PSE

3.2 Community Engagement and Public Outreach Activities

3.2.1 Online Resources

In addition to the engagement activities around monitor siting and volunteer recruitment described above, in Spring 2019 we launched a landing webpage for our project.[65] Throughout the project duration, we provided periodic updates[66] on our website and published several blogs on the benefits of low-cost sensor technologies,[67] air quality observations during COVID-19 shelter-in-place orders,[68] and neighborhood trends in air pollution in Richmond-San Pablo.[69] In Fall 2020 and in partnership with Aclima, Inc., we launched a publicly accessible online data visualization tool that showed real-time and historic air quality data collected by the Richmond Air monitoring Network.[70]

3.2.2 Community Engagement

In 2019, PSE staff (Boris Lukanov and Lee Ann Hill) were appointed to the Richmond-San Pablo Area Community Air Monitoring Plan Steering Committee to assist with developing an air monitoring plan for Richmond-San Pablo.[71] Engagement in the Steering Committee included a technical presentation of preliminary results from our sensor network, assistance with forming a technical advisory group to assist the Steering Committee with decision making, and participating in various community events, including the 2019 Path to Clean Air in Richmond and San Pablo Community Summit. Since the Community Air Monitoring Plan Steering Committee concluded its efforts, PSE continued to provide quarterly updates on monitoring progress to the community through Bay Area AQMD.[72,73,74,75] PSE also presented updates and preliminary findings to APEN members periodically throughout the project. In December 2020, PSE hosted a public webinar in partnership with Aclima to introduce and walk through the online real-time air-quality data visualization tool. PSE also participated in

[65] PSE Healthy Energy. (2022). Richmond Air Monitoring Network.

[66] PSE Healthy Energy. (2022). Richmond Air Monitoring Network: Recent News and Updates.

[67] Hill, L. and Lukanov, B. (2019). Meeting of the Minds. The Power of Data from Urban Air Quality Monitoring Networks.

[68] PSE Healthy Energy. (2020). Richmond, CA Air Monitors Show Cleaner Air During Bay Area COVID-19 Lockdown, With a Catch.

[69] PSE Healthy Energy. (2021). Richmond Air Monitoring Network Insights: Using hyperlocal data to evaluate neighborhood trends in air pollution.

[70] PSE Healthy Energy and Aclima, Inc. Real-Time Air Quality Data.

[71] Bay Area AQMD. (2022). Richmond-North Richmond-San Pablo Area - Community Health Protection Program.

[72] Bay Area AQMD. (2020). Quarterly Update on AB 617 Richmond-San Pablo Air Monitoring Projects-December 2020.

[73] Bay Area AQMD. (2021). AB 617 Richmond-San Pablo Air Monitoring Projects Quarterly Update, January-March 2021.

[74] Bay Area AQMD. (2021). AB 617 Update on Air Monitoring Projects in Richmond-North Richmond-San Pablo for April-June 2021.

[75] Bay Area AQMD. (2021). Update on Air Monitoring Projects in Richmond-North Richmond-San Pablo for July-September 2021.

the "Past, Present and Future of AB 617: Envisioning a Way Forward, Together" convening in September 2021 as part of a roundtable discussion on Innovations in Community Steering Committees, alongside the Bay Area AQMD and community-based organizations in the Bay Area. LBNL also published a blog with a companion video overview highlighting the additional air quality monitoring efforts focused on black carbon.[76]

---

[76] LBNL. (2021). Empowering a Neighborhood to Breathe Easy.

PSE

Concentrations of $PM_{2.5}$, O_3, NO_2, and BC can vary spatially (across different neighborhoods, land use areas, elevations, and terrain types) and temporally (across seasons, months, days of the week, or times of the day). These variations can be due to a variety of factors, including proximity to emission sources, local meteorology, atmospheric chemistry, traffic patterns, weekly and daily schedule of industrial activities, wildfire smoke events, etc. Below we look at the spatiotemporal variability of air pollution in the Richmond-San Pablo community and compare these trends with data from the Bay Area AQMD regulatory site in San Pablo, CES 4.0, and other data sources.

4.1 Spatiotemporal Trends in Air Pollution

In this section, we first present area-wide air pollution trends observed by RAMN over the entire study period (January 2020 - March 2022). We then discuss spatiotemporal trends in ambient $PM_{2.5}$, NO_2, and O_3 concentrations measured by neighborhood and land-use type (commercial, industrial, residential) and averaged by season, month, day of the week, and hour of the day. We also compare RAMN-observed values with concentrations measured by the Bay Area AQMD regulatory site located in San Pablo across various temporal scales and geographic contexts.

### 4.1.1 Network-Wide Trends During Full Study Period

4.1.1.1 Particulate Matter ($PM_{2.5}$)

Network-wide average daily $PM_{2.5}$ concentrations measured by RAMN during the 27 month-long deployment period (January 2020 – March 2022) are shown in **Figure 22**. Area-wide $PM_{2.5}$ concentrations measured by RAMN averaged 12.6 (95% confidence interval [CI] 12.4-12.8) micrograms per cubic meter ($\mu g/m^3$). This value is slightly higher than the NAAQS $PM_{2.5}$ annual mean limit of 12 $\mu g/m^3$ aimed to protect public health. However, care must be taken in drawing a direct comparison between the two values for a few reasons. First, there are very specific data completeness and data quality requirements for NAAQS that are not necessarily met by our sensor network, including that data are averaged over a three-year period. Additionally, air quality data evaluated for NAAQS may exclude events that meet certain criteria to qualify them as exceptional events, such as some wildfire smoke events.[77]

---

[77] U.S. EPA. (2022). Treatment of Air Quality Data Influenced by Exceptional Events.

When wildfire smoke events, which accounted for roughly three percent of our data (or 3.5 weeks out of a 27-month study period), were excluded from the data analysis, the network-wide mean $PM_{2.5}$ concentration measured by RAMN decreased by about 20 percent to 10.1 (95% CI 10.0-10.3) $\mu g/m^3$.
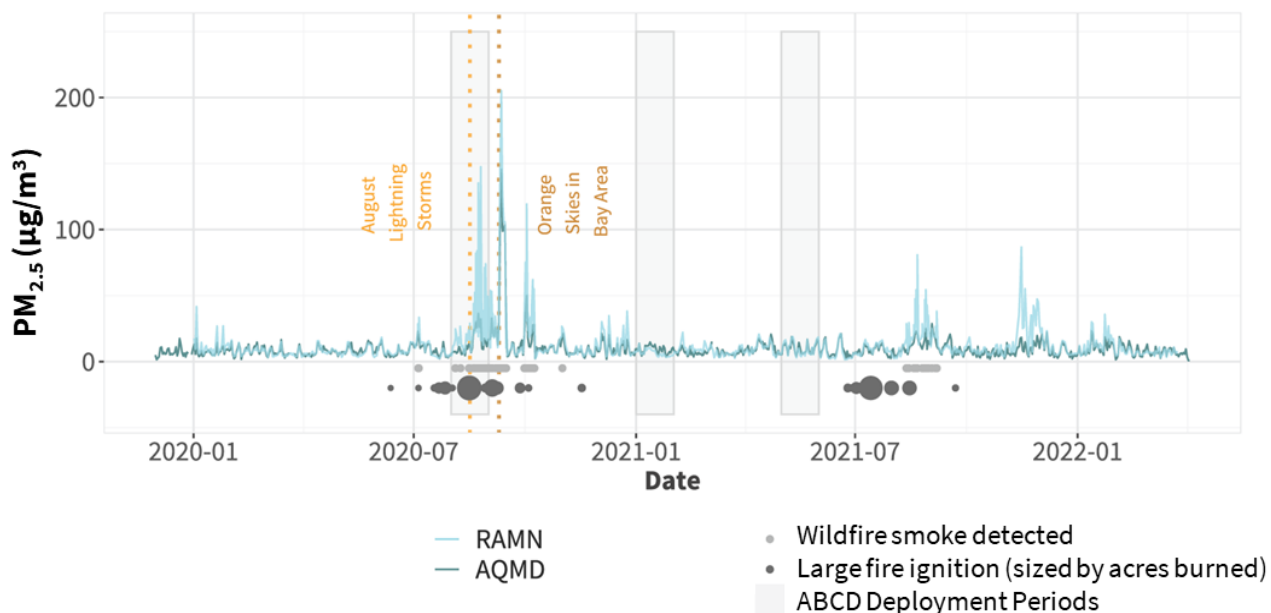

Figure 22. Time series of network-average daily PM$_{2.5}$ concentrations measured during the full study period. Wildfire smoke events are shown in gray solid circles. Known wildfire events are indicated by black solid circles, with size corresponding to the total acres burned. ABCD deployment periods are shaded in light gray.

The mean $PM_{2.5}$ concentration measured by the AQMD reference monitor during the study period was 10.1 $\mu g/m^3$. This value is lower than the 12.6 $\mu g/m^3$ average concentration measured by RAMN but still notably within 20 percent of the NAAQS 3-year annual mean limit of 12 $\mu g/m^3$. We should note that chronic exposure to $PM_{2.5}$ concentrations lower than the NAAQS have also been associated with adverse health effects. As evident from **Figure 22**, network-wide daily average concentrations measured by RAMN and the AQMD site generally increase and decrease in unison, though the average network-wide RAMN $PM_{2.5}$ concentration sometimes significantly exceeds the average $PM_{2.5}$ concentration measured at the AQMD station, especially during wildfire events. . When wildfire smoke events were excluded from the AQMD dataset, the AQMD mean value decreased by about 10 percent to 9.1 $\mu g/m^3$.

Some of the systematic differences between RAMN and the AQMD reference monitor could be due to differences in sensor technology, monitoring methods, or calibration procedures (and how these different methods respond to changes in things like PM composition). To check for

PSE

potential systematic differences due to monitoring methodology, we plotted hourly $PM_{2.5}$ data from the two AQY sensors collocated at the AQMD site versus hourly $PM_{2.5}$ data reported by the reference beta attenuation monitor (BAM) at the AQMD site in San Pablo (**Figure 23**). The scatter plots shown are for the full study period. Hourly data from both collocated sensors are well correlated with AQMD measurements ($R^2 \geq 0.85$; $0.93 \leq$ slope ≤ 1.07 of 1; zero offset < 1 $\mu g/m^3$; mean absolute error (MAE) ≤ 3.1 $\mu g/m^3$).[78] This alignment gives us additional confidence in the quality of the RAMN $PM_{2.5}$ data, although systematic errors due to calibration methods or low-cost-sensor response to PM composition are still possible.
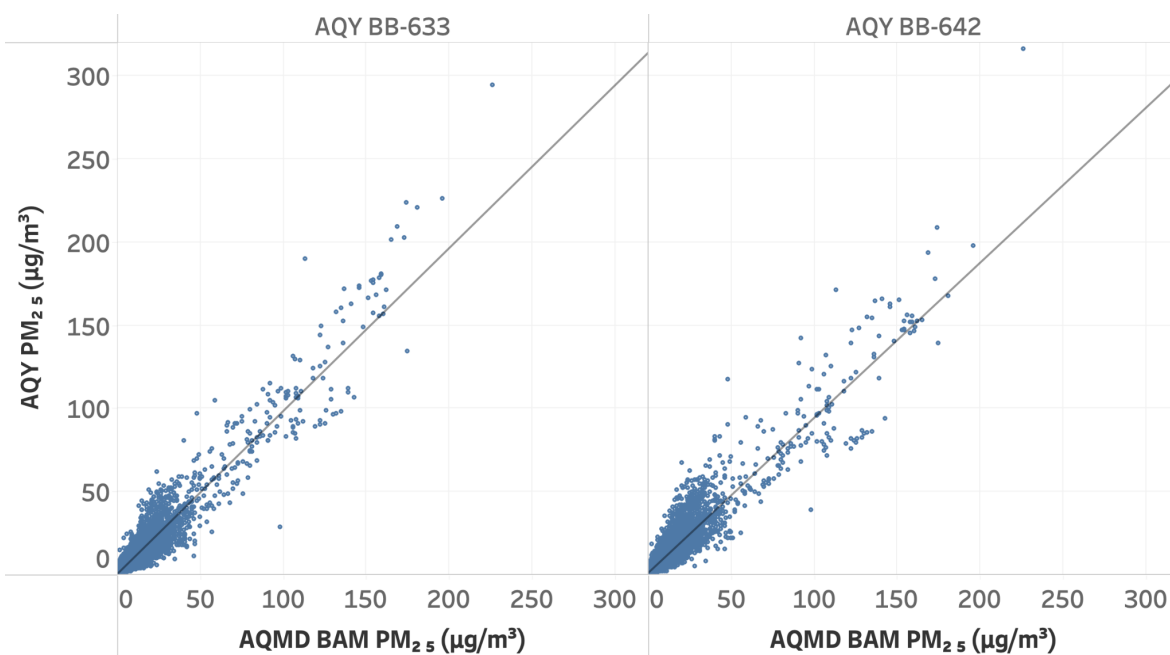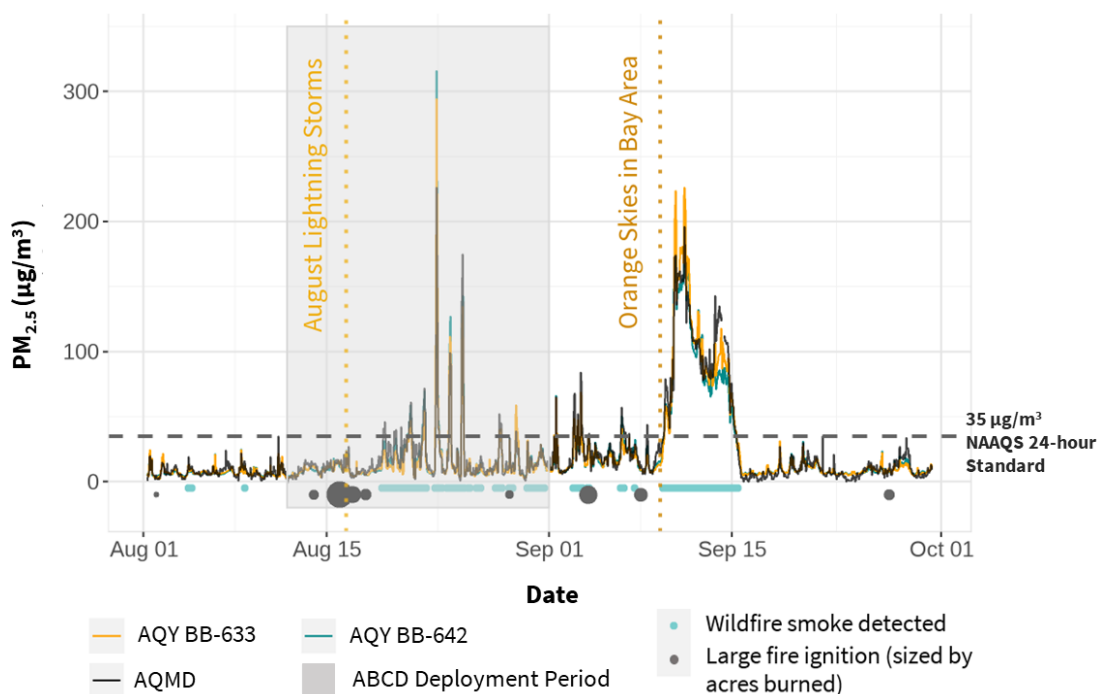

FIgure 23. Hourly PM$_{2.5}$ concentrations measured by the AQMD reference beta attenuation monitor (BAM) and two Aeroqual AQY's collocated at the San Pablo AQMD regulatory site during the full study period. Linear fit statistics: **AQY BB-633 (a)**: $R^2 = 0.89$; slope = 0.98; zero offset = 0.27 $\mu g/m^3$; mean absolute error (MAE) = 3.0 $\mu g/m^3$; room-mean-square error (RMSE) = 4.0 $\mu g/m^3$. **AQY BB-642 (b)**: $R^2 = 0.85$; slope = 0.93; zero offset = 0.91 $\mu g/m^3$; mean absolute error (MAE) = 3.1 $\mu g/m^3$; room-mean-square error (RMSE) = 4.6 $\mu g/m^3$.

Both the AQMD reference monitor and RAMN sensors collocated at the AQMD site were significantly impacted by wildfire smoke events in 2020 (**Figure 24**). Major wildfire events that impacted the Bay Area are indicated by solid black circles below the graphs, while network-wide hourly anomalies attributed to wildfire smoke at ground level are shown as gray (**Figure 22)** or light green (**Figure 24**) dots. The two sensors collocated at the AQMD site

---

[78] A value of R^2 closer to one indicates stronger correlation with the comparison variable.

PSE

measured similar concentrations to the AQMD site after applying the network-wide wildfire smoke correction to the sensor data (**Figure 24**). The wider RAMN network generally measured higher $PM_{2.5}$ concentrations than AQMD during wildfire smoke events in August and September, and this was true for both 2020 and 2021, even after applying the network-wide wildfire smoke correction to the sensor data (**Figure 22**). As noted above, this ended up elevating the mean annual $PM_{2.5}$ concentrations to a larger degree for RAMN than for the AQMD site in San Pablo when wildfire smoke events were included in the data analysis. In addition to wildfire events, RAMN also detected network-wide $PM_{2.5}$ anomalies during the colder months of the year (November, December, and January).

Figure 24. Average hourly PM$_{2.5}$ concentrations from the AQMD monitor (black) and the co-located RAMN monitors BB-633 and BB-642 (orange, blue) during the August - September 2020 wildfire season. Periods when large fire ignitions occurred (dark solid circles) and when wildfire smoke was detected by our R AnomalyDetection algorithm (blue solid circles) are shown. Gray box indicates the period when the ABCD network was also active.

The ABCD deployment periods are also shown in **Figures 22** and **24** as areas shaded in light gray. We note that the ABCD wildfire deployment period in August 2020 overlapped with all of the August wildfire smoke events but did not include the large wildfire smoke event in September 2020 (dubbed "Orange Skies" in the Bay Area). PM and BC concentrations

observed during wildfire smoke events are discussed below in detail (see Section 4.5.2. *'Impact of Wildfire Smoke'*).

4.1.1.2 Ozone (O₃)

RAMN average daily O_3 concentrations tracked well those measured at the AQMD regulatory site (**Figure 25**), both in terms of the temporal variations and absolute concentrations, suggesting that the AQMD reference monitor is well-representative of the average O_3 concentrations across the Richmond-San Pablo community. This result is not surprising given that O_3 concentrations tend to be more uniform across broader regions compared to $PM_{2.5}$ and NO_2. Despite this fact, we still observed spatial variability of O_3 concentrations across neighborhoods and site locations that could not be captured by the AQMD site alone, as discussed below.
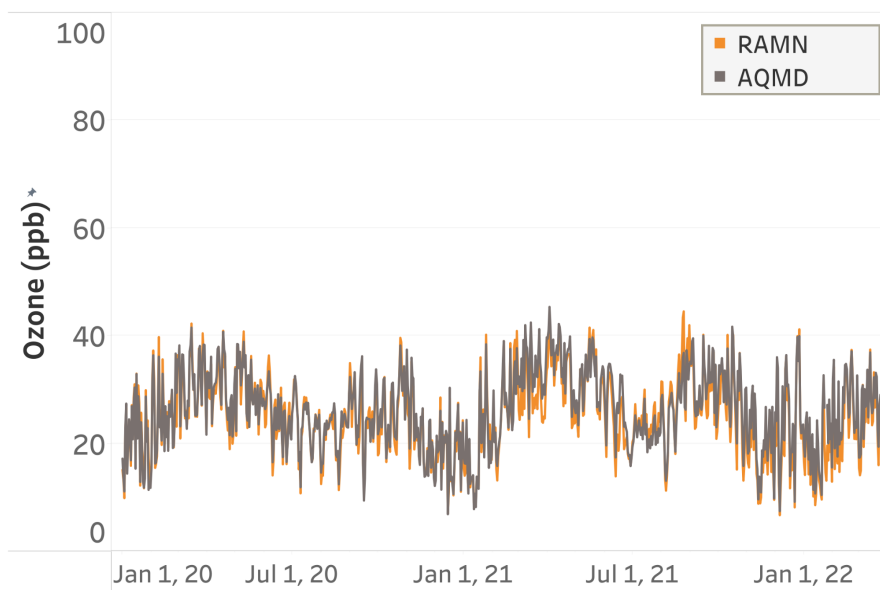
Figure 25. Time series of RAMN network-average and AQMD daily O₃ concentrations during the full study period.

The average area-wide O_3 concentration measured by RAMN during the study period was 25.4 (95% CI 25.1-25.7) parts per billion (ppb), which is almost identical to the AQMD average of 25.8 ppb within the level of uncertainty. The NAAQS standard for O_3 is 70 ppb (see **Table 1**), although, again, a direct comparison should be done with care—the NAAQS standard is calculated for the fourth-highest annual daily maximum 8-hour concentration, averaged over three years, and is therefore provided here only as a reference point. The highest 8-hour network-wide average concentration measured by RAMN was 63.3 ppb.

Figure 25 also reveals the clear seasonality expected in O_3 concentrations. The highest O_3 concentrations were observed in the spring and fall of 2020 and 2021, while the lowest concentrations were measured during the winter months. A dip in O_3 concentrations occurs in the summer months as well.

4.1.1.3 Nitrogen Dioxide (NO₂)

The time series for NO_2 is shown in **Figure 26**. The RAMN network-wide average NO_2 concentration measured over the deployment period was 8.3 (95% CI 7.9-8.6) ppb, while the AQMD site average was 7.2 ppb. These values are relatively close to one another and are well below the NAAQS annual NO_2 limit of 53 ppb (see **Table 1**).
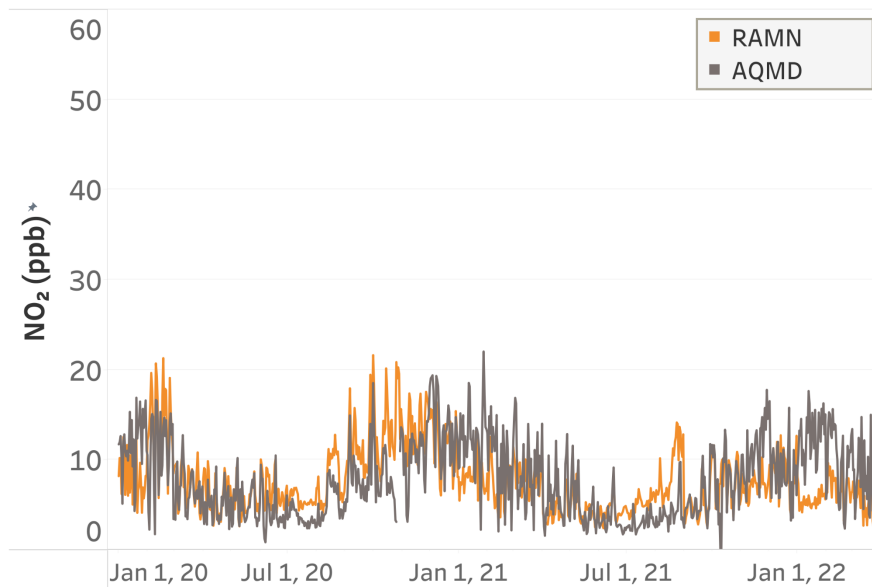

Figure 26. Time series of RAMN network-average and AQMD daily NO₂ concentrations during the full study period.

Network-wide average daily NO_2 concentrations measured by RAMN were slightly higher than AQMD during the summer months, and lower than AQMD during the 2022 winter months, suggesting potentially different patterns of NO_2 emissions and formation in various parts of the study area compared to the AQMD site location. Some of these differences may also be attributable to network calibration and data completeness issues, which impacted the NO_2 sensors significantly more than the $PM_{2.5}$ and O_3 sensors of the Aeroqual AQY 1 units.

PSE

4.1.2 Neighborhood and Land Use Spatiotemporal Trends

Concentrations of $PM_{2.5}$, O_3, and NO_2 vary spatially across different neighborhoods, land uses, terrain types and elevations. Below we assess the time periods when pollutant concentrations were high and the neighborhoods that were most impacted during those times. Pollutant concentrations were averaged both by neighborhood and by land use category, as well as by the time period being assessed (month of year, day of week, hour of day). For $PM_{2.5}$, neighborhood averages were compared to either the U.S. EPA NAAQS 3-year annual $PM_{2.5}$ mean of 12 µg/m^3 or to the Bay Area AQMD reference monitor in San Pablo by subtracting the reference monitor's average concentrations from the neighborhood-average concentrations for the given time period, resulting in the difference between each neighborhood average and the regulatory site average. Network anomalies linked to wildfires were excluded from the PM analysis below unless indicated otherwise.

4.1.2.1 Spatial Trends Over the Full Study Period

RAMN's spatially granular data revealed substantial variations in average air pollutant concentrations across neighborhoods and land use areas over the full study period. Neighborhood-average $PM_{2.5}$ concentrations measured by RAMN (excluding wildfire events) were generally higher than concentrations measured at the regulatory site, especially in neighborhoods in the south (Point Richmond, Richmond Annex) and in the north (Hilltop, May Valley) where average $PM_{2.5}$ concentrations were roughly 20 percent higher compared to the average concentrations measured by the Bay Area AQMD regulatory site in San Pablo (**Figure 27, top**).

PS≡
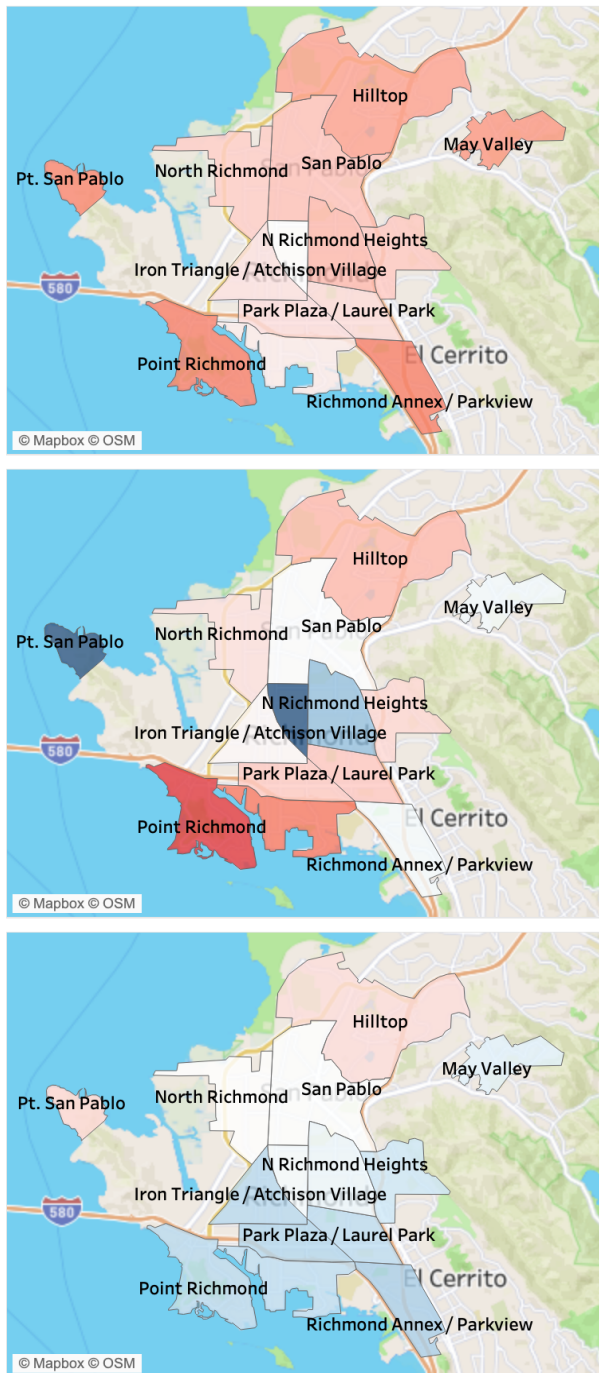
Figure 27. Average PM$_{2.5}$ (top), NO$_2$ (middle), and O$_3$ (bottom) concentrations by neighborhood, shown as a percent difference from the average concentrations measured by the Bay Area AQMD regulatory site in San Pablo. Blue indicates average neighborhood concentrations observed were lower than Bay Area AQMD site while red indicates concentrations were higher. Wildfire smoke events are excluded from the PM data.

Neighborhood-average NO$_2$ concentrations were roughly 30 percent higher in two southern neighborhoods (Point Richmond and Marina Bay) compared to the AQMD reference monitor, as well as around 10 percent higher in several other neighborhoods close to the I-80 and I-580 freeways (Hilltop, East Richmond Heights, Park Plaza/Laurel Park, and Coronado/Santa Fe) (**Figure 27, middle**). Neighborhood-average O$_3$ concentrations, a more regional pollutant, generally tracked better with concentrations recorded by the Bay Area AQMD regulatory site (**Figure 27, bottom**). However, RAMN also reported spatial variability in O$_3$ concentrations across neighborhoods and site locations—average O$_3$ concentrations were highest in northern neighborhoods (Hilltop, North Richmond, Point San Pablo, San Pablo, North Richmond), which are located further away and downwind of major freeways, and lowest in southern neighborhoods (Point Richmond, Marina Bay, Richmond Annex/Parkview, Park Plaza/Laurel Park, Coronado/Santa Fe, and Iron Triangle/Atchison Village).

PSE

4.1.2.2 Monthly/Seasonal Spatiotemporal Trends

Figure 28 (left) shows average $PM_{2.5}$, NO_2, and O_3 concentrations by month of the year as measured by RAMN and the AQMD reference monitor in San Pablo (wildfire smoke events are included here). Average monthly $PM_{2.5}$ concentrations (**top left**) were by far the highest during the wildfire season months (August-September) when RAMN measured average $PM_{2.5}$ concentrations that substantially exceeded the 12 $\mu g/m^3$ NAAQS 3-year annual mean limit in every land use category. The RAMN network average was up to two times higher than the AQMD regulatory site during those months even after applying our network-wide wildfire smoke correction. The difference is especially pronounced during the month of August, suggesting there may be other factors at play, including meteorology, wind speed/direction, and potential differences in $PM_{2.5}$ composition between wildfire smoke events in August versus September when the Bay Area skies were orange. The difference from AQMD during wildfire season months was more pronounced in southern neighborhoods (Point Richmond, Marina Bay, Richmond Annex/Parkview)—see Section 4.2 *'Wildfire Smoke Impacts on Air Quality'* and **Figure 34** below.

RAMN also measured elevated $PM_{2.5}$ concentrations compared to the AQMD regulatory site during the colder months of November and December, which were outside of wildfire season (our wildfire smoke detection algorithm did not identify wildfire smoke events during those two months). In November-December, northern neighborhoods such as San Pablo, Hilltop and May Valley were impacted by significantly higher neighborhood-average $PM_{2.5}$ concentrations compared to the AQMD reference monitor (**Figure 28, top right**). The same was true for Point Richmond and Point San Pablo. Several of these neighborhoods (primarily in the north and center of Richmond) had RAMN $PM_{2.5}$ average concentrations up to 50% higher than the AQMD average during those two months.

RAMN air monitors measured higher average NO_2 concentrations than AQMD in the fall months (across all land use categories)—this was prevalent throughout most of Richmond's neighborhoods but particularly in neighborhoods adjacent to major freeways, like Marina Bay and East Richmond (**Figure 28, middle**). NO_2 concentrations were lowest in the summer and highest in the winter. This seasonality can be related to both meteorology and atmospheric chemistry related to the formation of O_3 and secondary PM. Residential areas were the land use category most impacted by higher NO_2 concentrations overall.

O_3 concentrations tracked well with the AQMD station across all three land use categories and during all months of the year. In the spring months, when O_3 concentrations were the highest (around 35 ppb), RAMN monitors measured slightly lower average O_3 concentrations than the

PSE

AQMD station across most neighborhoods, particularly in neighborhoods in the south (**Figure 28, bottom**).
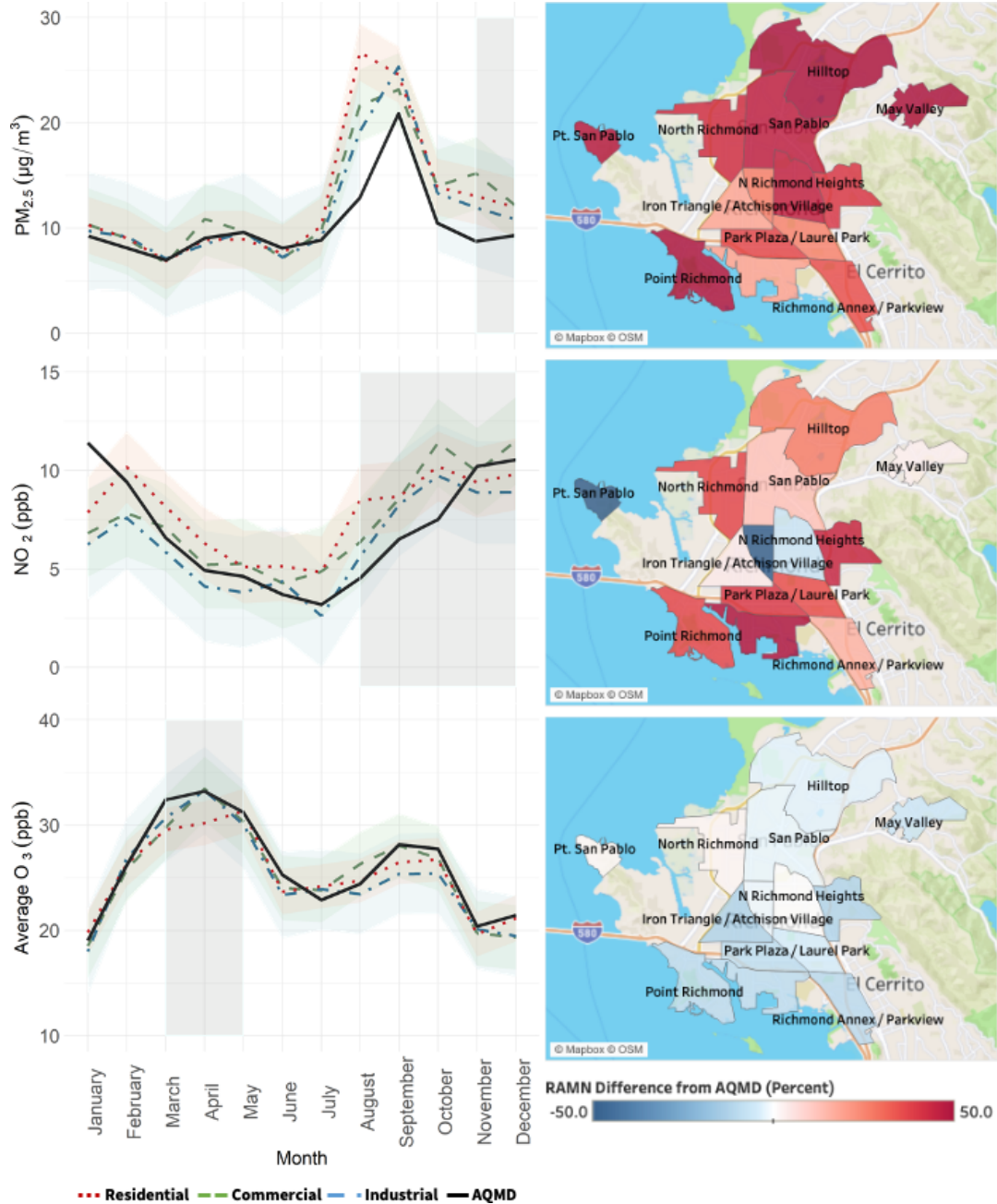

Figure 28. Average monthly PM$_{2.5}$ (top left), NO$_2$ (center left), and O$_3$ (bottom left) concentrations by land use category, paired with maps highlighting neighborhood percent differences from AQMD for each pollutant. Highlighted time periods on the left are

mapped on the right. Red-colored neighborhoods indicate RAMN pollutant concentrations higher than AQMD; blue-colored neighborhoods indicate pollutant concentrations lower than AQMD. Shaded curves on the left indicate the 95% confidence intervals. Wildfire smoke events are included in the PM data.

4.1.2.3 Weekday vs Weekend Spatiotemporal Trends

Weekend vs. weekday differences were observed for all three air pollutants. On average, both RAMN and the AQMD reference monitor measured higher average $PM_{2.5}$ concentrations on weekends compared to weekdays (**Figure 29, top**). We note, however, that RAMN-measured weekday average $PM_{2.5}$ concentrations were substantially higher than those measured at the AQMD regulatory site during weekdays, suggesting that our sensor network may be more impacted by area-wide mid-week commuter traffic and industrial activities than the AQMD reference monitor. RAMN-measured average weekday $PM_{2.5}$ concentrations exceeded the AQMD measurements in almost all neighborhoods—most notably in the Richmond Annex, Point Richmond and Point San Pablo, but also in San Pablo, Hilltop and May Valley to the north (**Figure 30, left**). In contrast, weekend differences between RAMN- and AQMD-measured average $PM_{2.5}$ concentrations were substantially smaller, with some neighborhoods (Belding/Wood and Park Plaza/Laurel Park) showing lower RAMN values than the AQMD site (**Figure 30, right**).

PSE
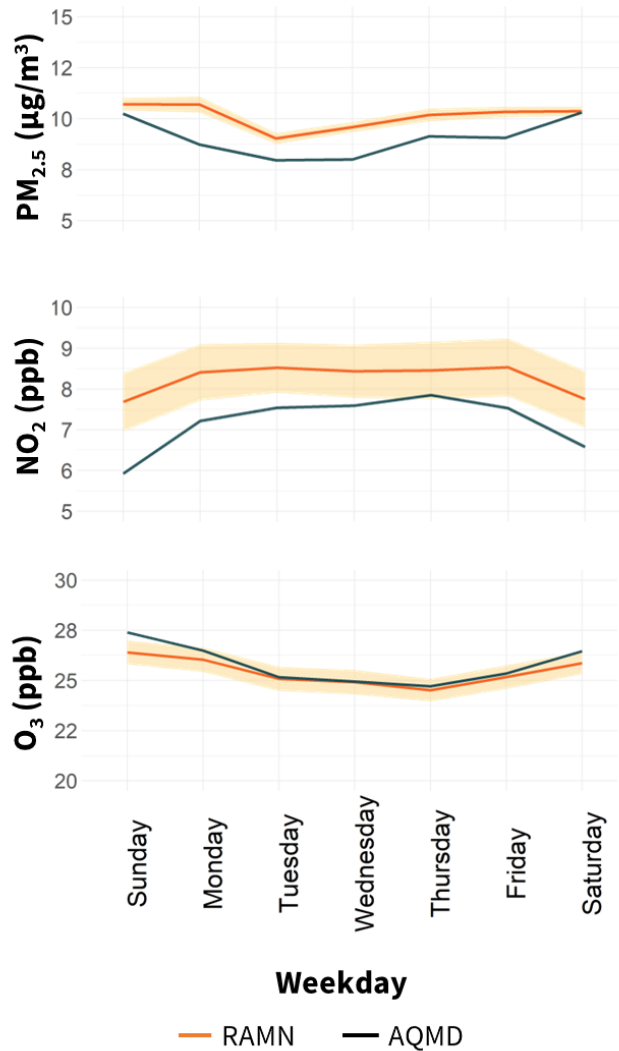
Figure 29. Average concentrations by day of the week. RAMN and AQMD-measured concentrations by day of the week: $PM_{2.5}$ (top), O_3 (middle), NO_2 (bottom). The solid orange line represents the network-average across all 50 sites and the shaded area around it represents the 95% confidence interval.

Average O_3 concentrations measured by RAMN and AQMD were also slightly higher on weekends compared to weekdays (**Figure 29, bottom**). In contrast, the opposite trend was observed for NO_2 (**Figure 29, middle**), which could be attributed to lower traffic volumes on weekends.

The fact that NO_2 concentrations are consistently higher for RAMN compared to AQMD suggests that RAMN may be more impacted by area-wide traffic compared to the AQMD

PSE

regulatory site, although some of these differences may also be due to differences in the sensors and monitoring methods. Differences between RAMN and AQMD NO_2 measurements are especially pronounced on weekends.

One reason for the higher O_3 concentrations on weekends—despite the lower average concentrations of its main precursor, NO_2—is that emissions of other O_3 precursors (such as volatile organic compounds) may still remain high, and O_3 formation tends to be highest at certain ratios of VOC to NO_x in the atmosphere. This phenomenon is known as the "weekend effect".[79,80]
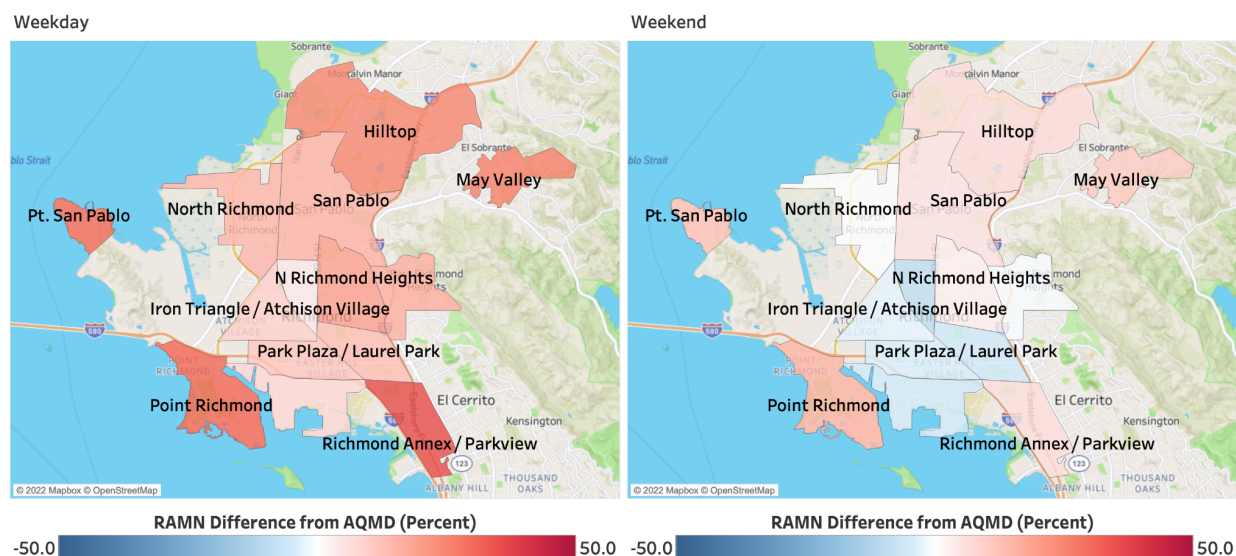
Figure 30. **Weekday (left) vs weekend (right) average PM$_{2.5}$ concentration differences between RAMN and AQMD San Pablo, by neighborhood.** Weekdays generally had higher average PM$_{2.5}$ differences from AQMD than weekdays.

4.1.2.4 Hour of Day Spatiotemporal Trends

Pollutant concentrations can vary depending on the time of day due to a variety of factors, including commuter traffic, hourly wind patterns, the daily schedules of industrial operations, etc. We see the most substantial differences between RAMN and AQMD when we look at average pollutant concentrations by hour of day. RAMN-measured PM$_{2.5}$ levels in

[79] Cleveland, W. S., Graedel, T. E., Kleiner, B., & Warner, J. L. (1974). Sunday and workday variations in photochemical air pollutants in New Jersey and New York. *Science*, *186*(4168), 1037-1038. DOI: 10.1126/science.186.4168.1037

[80] Fujita, E. M., Stockwell, W. R., Campbell, D. E., Keislar, R. E., & Lawson, D. R. (2003). Evolution of the magnitude and spatial extent of the weekend ozone effect in California's South Coast Air Basin, 1981–2000. *Journal of the Air & Waste Management Association*, *53*(7), 802-815. DOI: 10.1080/10473289.2003.10466225

PSE

Richmond-San Pablo generally peaked twice a day: in the morning (between 6:00 and 11:00 AM), and again in the evening (between 4:00 PM and 10:00 PM) (**Figure 31, top left**). These two peaks are likely associated with morning and evening commuter traffic.

In contrast, the AQMD regulatory site reported one early morning peak and significantly lower average $PM_{2.5}$ concentrations at night compared to RAMN. The two AQYs collocated at the regulatory site also reported the same pattern. This again suggests that RAMN may be more impacted by area-wide traffic emissions and that the AQMD regulatory site may not be as representative of the study area in terms of the $PM_{2.5}$ diurnal variability. On average, RAMN air monitors in industrial zones showed better alignment with the AQMD reference monitor, which is also located in an industrial area. The evening peak in $PM_{2.5}$ concentrations detected by RAMN was primarily registered by sensors located in commercial and residential zones.
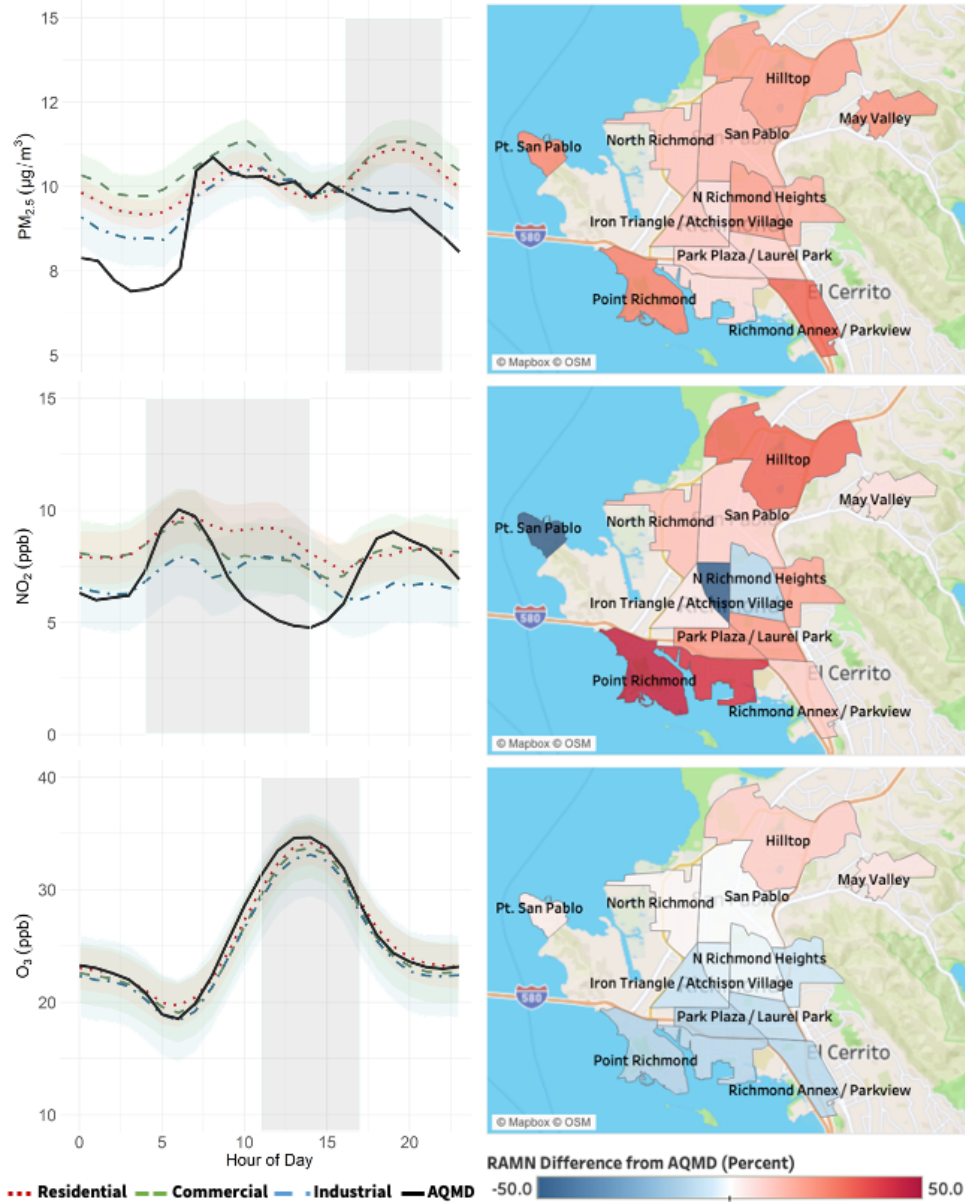
Figure 31. (a) Average hourly PM₂.₅ concentrations by land use (top left) and neighborhood PM₂.₅ average difference (µg/m³) from the AQMD reference monitor for highlighted hours (4:00 PM - 10:00 PM) (top right). Wildfire smoke events are excluded. (b) Average hourly NO₂ concentrations by land use (middle left) and neighborhood differences from the AQMD San Pablo station for highlighted hours (4:00 AM - 2:00 PM) (middle right). (c) Average hourly O₃ concentrations by land use (bottom left) and neighborhood differences from the AQMD San Pablo station (ppb) for highlighted hours (11:00 AM - 5:00 PM) (bottom right). The shaded curves on the left represent the 95% confidence intervals.

PSE

The spatial variability of $PM_{2.5}$ concentrations during the evening $PM_{2.5}$ peak between 4:00 PM and 10:00 PM, indicated by the shaded area on the plot, is mapped on the right (**Figure 31, top right**). During this evening peak, monitors in all 14 neighborhoods measured higher average $PM_{2.5}$ concentrations than the San Pablo reference monitor. RAMN air monitors in Point Richmond in the southwest and the Richmond Annex in the southeast in particular measured the largest differences from the AQMD reference site, exceeding it by about 30 percent.

Sensors in all three land use categories measured the well-characterized diurnal pattern of O_3 formation during daylight hours and were in very close agreement with the AQMD data (**Figure 31, bottom left**). The seemingly close agreement, however, conceals the noticeable spatial variability revealed by the map on the right, which shows that certain neighborhoods in the area had higher average O_3 concentrations than others **(Figure 31, bottom right)**. Neighborhoods in the north, including Point San Pablo, North Richmond, Hilltop, and May Valley, had average O_3 concentrations exceeding the San Pablo regulatory average by up to 10 percent during the shaded hours. Neighborhoods that fell below the regulatory average were in the south, including Point Richmond, Marina Bay, and the Richmond Annex.

Average NO_2 concentrations also fluctuated throughout the day, as shown in **Figure 31 (middle)**. There is an initial peak in the early morning, around 6:00 AM, mostly detected by sensors in commercial and residential areas. A second, smaller peak, is noticeable later in the morning, around 11:00 AM. Another peak appears in the evening, around 6:00 PM. The morning and evening peaks are significantly more pronounced at the AQMD site, suggesting that the AQMD location may be more affected by localized traffic potentially related to industrial activities during those hours. The spatial variability of NO_2 concentrations during the shaded time period from 4:00 AM to 2:00 PM is shown on the map to the right. During those hours, neighborhoods such as Marina Bay and Point Richmond to the south, and Hilltop to the north stand out as experiencing the highest average hourly NO_2 concentrations compared to the regulatory site. RAMN-measured average NO_2 concentrations in neighborhoods adjacent to major highways, like I-80 to the east and I-580 to the south, were also higher compared to the AQMD site.

PSE
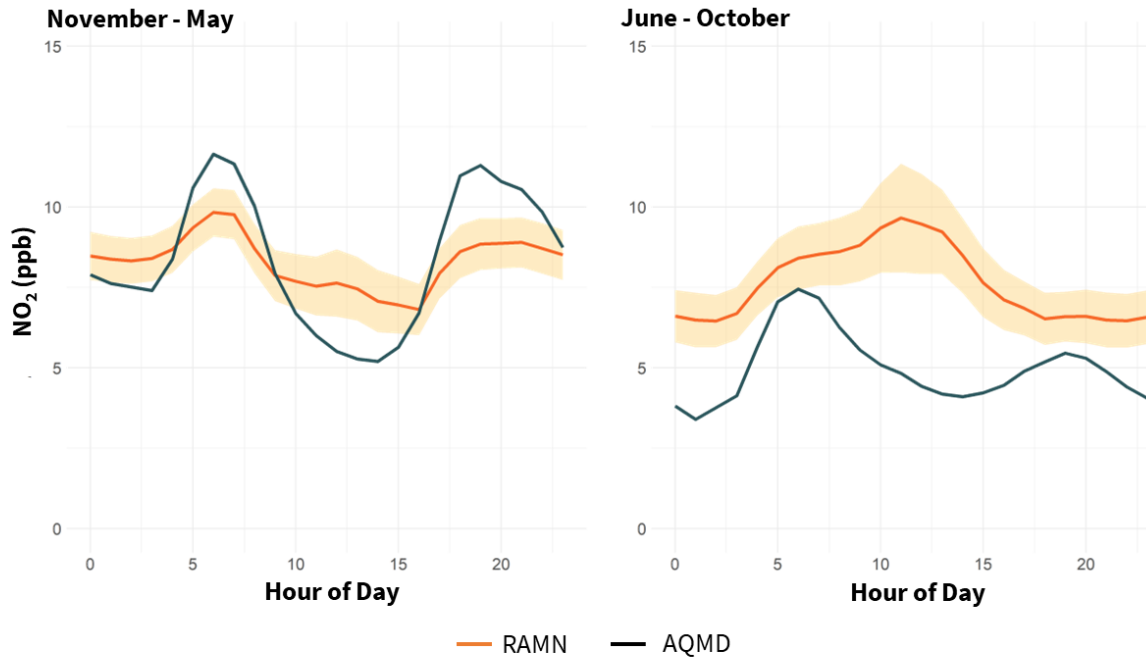
Figure 32. Average NO$_2$ concentrations by hour of the day and season. RAMN network-average and AQMD concentrations; solid orange line represents the network-average across all 50 sites and the shaded area around it represents the 95% confidence interval.

Differences between AQMD and RAMN were even more pronounced when we examined the diurnal concentrations of NO$_2$ at different times of the year (**Figure 32)**. During the winter and spring months (**Figure 32, left**), we noticed two diurnal (morning and evening) peaks for RAMN and AQMD that could likely be attributed to traffic emissions. The peaks were more pronounced for the AQMD site, which is located very close to Rumrill Boulevard and industrial sites, and may be affected by more localized heavy-duty-vehicle emissions during those hours. At night and in the middle of the day, RAMN registered higher average concentrations of NO$_2$. During the summer and fall months (**Figure 32, right**), the AQMD reference monitor still registered two (though much smaller) diurnal peaks and also measured significantly lower average NO$_2$ concentrations compared to the winter and spring months. In contrast, RAMN measured higher average NO$_2$ concentrations (more similar to the winter and spring months) and registered only one NO$_2$ peak in the middle of the day.

## 4.2 Wildfire Smoke Impacts on Air Quality: August - September 2020

Thus far, our spatiotemporal analysis has generally excluded wildfire smoke events to better understand land use and neighborhood spatial trends in PM$_{2.5}$ concentrations without the added influence of wildfire smoke. **Figure 33** illustrates the impact that wildfire smoke events

PSE

had on the neighborhood-average $PM_{2.5}$ concentrations during the full study period. The inclusion of wildfire smoke (**Figure 33, left**) increased neighborhood-average $PM_{2.5}$ values throughout most of Richmond (except in the central neighborhoods) to levels above the NAAQS 3-year annual mean $PM_{2.5}$ limit of 12 µg/m³ compared neighborhood-average $PM_{2.5}$ concentrations with wildfire smoke excluded (**Figure 33, right**).
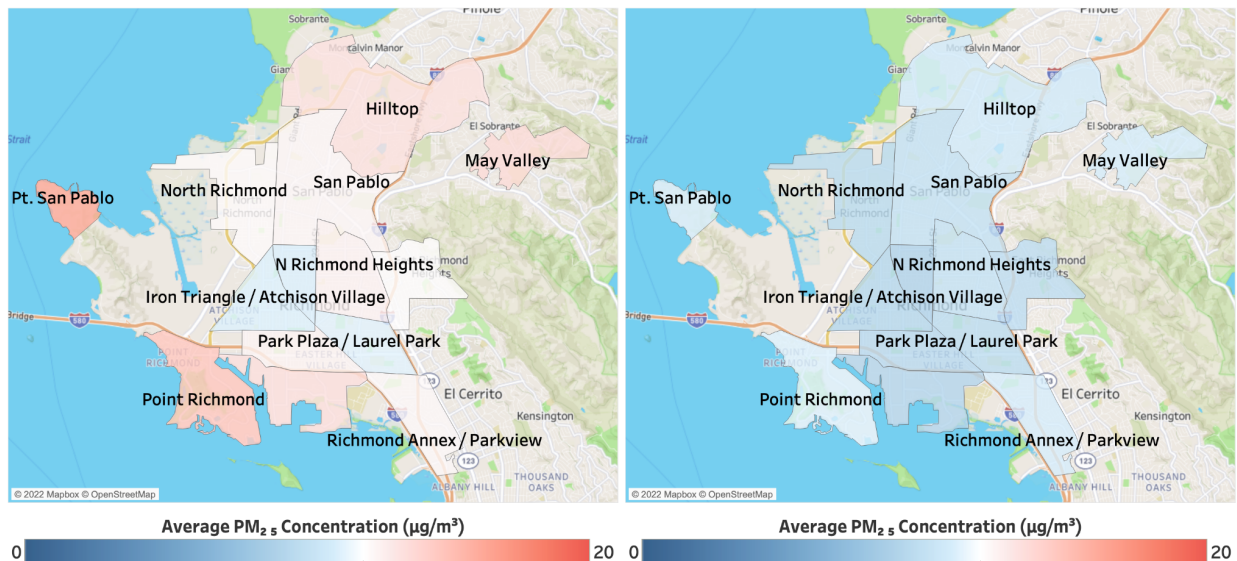
Figure 33. Average neighborhood $PM_{2.5}$ absolute concentrations during the full study period (January, 2020 - March, 2022) with wildfire smoke events included (left) and excluded (right). The color transition point is set to the NAAQS 3-year annual mean standard of 12 µg/m³.

In **Figure 34**, we also examine spatial trends exclusively during the period with most impactful wildfire smoke events (August 1st - October 1st, 2020) to assess both the severity of $PM_{2.5}$ during wildfire events and to identify the neighborhoods that experienced the highest impacts from wildfire smoke.

PSE
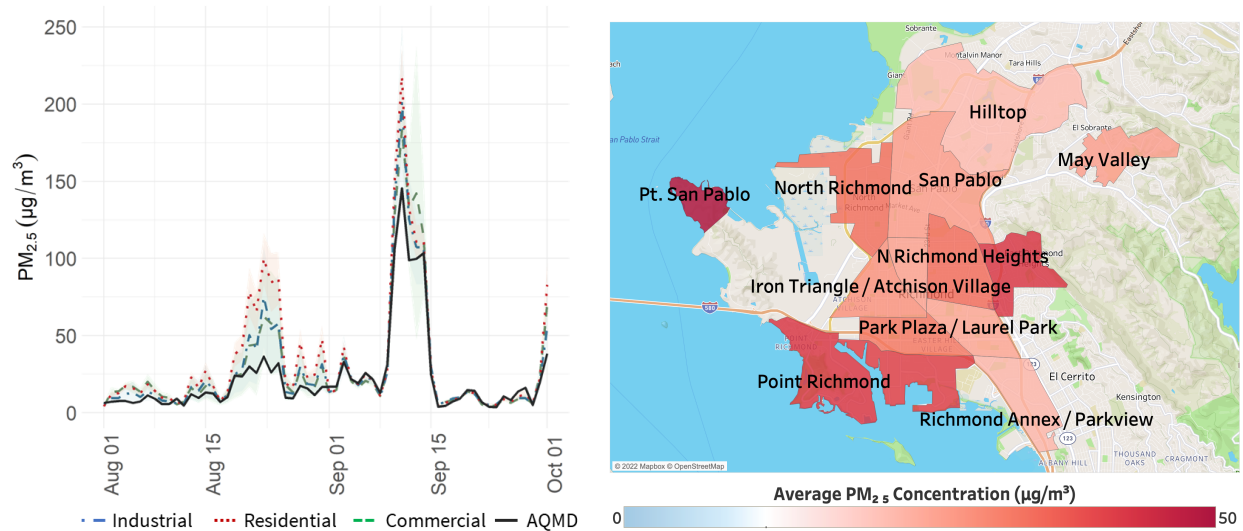
Figure 34. **Average daily PM$_{2.5}$ concentrations during the 2020 wildfire season.** Daily average PM$_{2.5}$ concentrations during the period August 1-October 1, 2020, by land use (left). Neighborhood-average PM$_{2.5}$ concentrations for the same period (right). The shaded areas on the left represent the 95% confidence intervals. The color transition point is set to the NAAQS 3-year annual mean standard of 12 µg/m^3.

During these two wildfire-season months, PM$_{2.5}$ concentrations exceeded the NAAQS 35 µg/m^3 24-hour standard on multiple occasions (on 15 days out of 62 total) across all of Richmond-San Pablo. In some areas, daily concentrations approached 200 µg/m^3 on certain occasions. Residential areas were impacted more during these wildfire smoke events, and the most impacted neighborhoods were Point San Pablo, Point Richmond, Marina Bay, East Richmond Heights and north Richmond (**Figure 34, right**). We should note, however, that every wildfire event is different and the resulting air quality impacts may vary every time (both spatially and in magnitude) due to meteorology, elevation, topography, fire behavior, etc. The spikes in PM$_{2.5}$ were identified by both RAMN and the AQMD reference monitor. However, the magnitude of the spikes was still greater in the RAMN monitor readings even after applying the network-wide wildfire correction discussed in the **Appendix** (see '*Aeroqual AQY Data Processing and Quality Assurance*' in the **Appendix**.

4.3 Proximity to Freeways

We also assessed how concentrations of NO$_2$, O$_3$ and PM$_{2.5}$ (excluding wildfire events) varied with monitor proximity to the nearest major freeways and roadways as defined by the Highway Performance Monitoring System's functional classification.[81] Distances to the nearest

---

[81] Department of Transportation. (2018). Highway Performance Management System - HPMS Field Manual.

PSE

freeway were calculated using Euclidean distance and were binned in three distance intervals of 0-0.5, 0.5-1.0, and 1.0-2.0 miles to the nearest freeway (**Figure 35**). It is important to note that these calculations do not take into account factors that are directly relevant to air pollutant transport, including prevailing wind direction.

The data was constrained to weekdays only and to the October-February months when NO_2 and $PM_{2.5}$ concentrations were highest (outside of wildfire season). $PM_{2.5}$ concentrations did not vary much across distances from freeways suggesting that RAMN was likely most sensitive to baseline or background $PM_{2.5}$ levels composed of both primary and secondary particles transported over longer distances than those to the nearest freeway. NO_2 concentrations were by far the highest within 0.5 miles from major freeways, and dropped beyond that distance.

While most NO_x from vehicles is emitted in the form of NO, secondary NO_2 is also rapidly formed through the titration of O_3 with NO, leading to elevated concentrations of NO_2 near major freeways.[82] The same process likely leads to RAMN detecting lower concentrations of O_3 within 0.5 miles from freeways and higher concentrations further away.
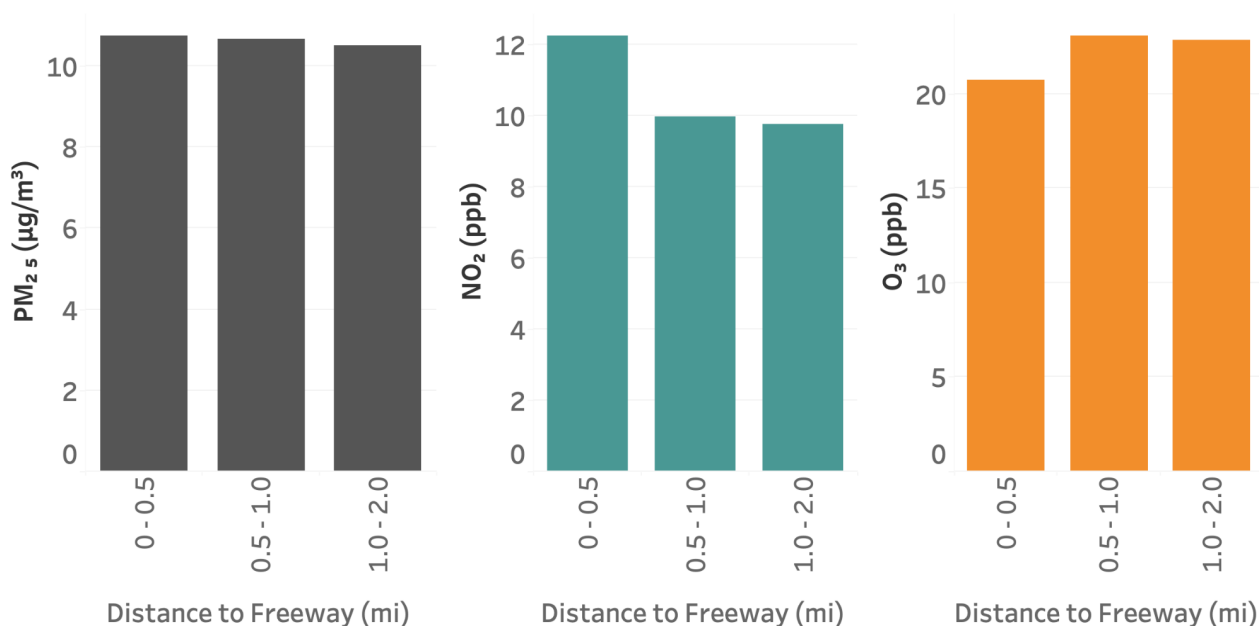
Figure 35. Average $PM_{2.5}$, NO_2, and O_3 concentrations measured at various proximities to the nearest major freeway (I-80, I-580, Richmond Parkway, Rumrill Boulevard).

[82] Yang, B., Zhang, K. M., Xu, W. D., Zhang, S., Batterman, S., Baldauf, R. W., ... & Wu, X. (2018). On-road chemical transformation as an important mechanism of NO2 formation. *Environmental science & technology*, *52*(8), 4574-4582. DOI: 10.1021/acs.est.7b05648

4.4 Black Carbon: Zeroing in on Summer, Winter and Wildfire Trends

Additional funding from CARB allowed us to add more specificity to the $PM_{2.5}$ data by deploying low-cost BC sensors at the 50 monitoring sites of the Richmond Air Monitoring Network. Sensors were deployed during three separate periods: (1) one wildfire smoke event; (2) one winter month; and (3) one late spring month. Below we discuss temporal and spatial BC trends observed across these three deployment periods.

4.4.1 Temporal Trends

The average BC concentration measured by all 50 sensors in winter 2021 was 0.52 µg m^{-3}, which was three times greater than the average of 0.17 µg m^{-3} measured in late spring (**Figure 36**). The difference between network-average $PM_{2.5}$ concentrations was much smaller—$PM_{2.5}$ concentrations were 18% higher in the late spring than they were in the winter. Dominated by the change in BC concentrations, the BC/$PM_{2.5}$ mass ratio decreased by 58% (from 0.09 to 0.04) between the winter and early spring period (not shown). The results presented below tend to focus on wintertime, when BC is highest.
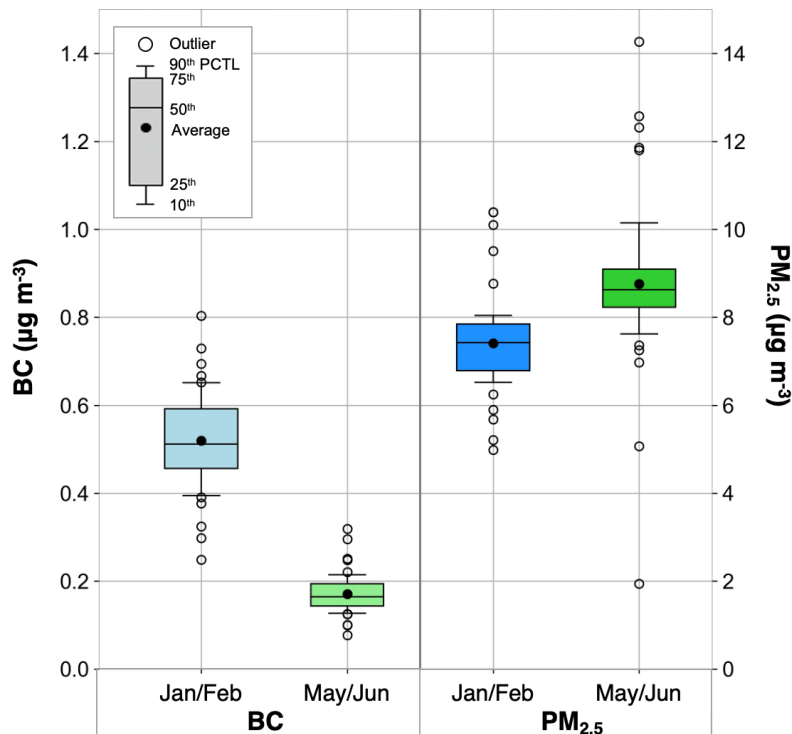
Figure 36. Boxplot distributions of site-average BC (left) and PM$_{2.5}$ (right) concentrations measured at the 50 monitoring locations in the winter (Jan/Feb) and late spring (May/Jun) of 2021. PCTL refers to percentile.

PSE

Diurnal trends in network average BC and PM$_{2.5}$ concentrations are presented in **Figure 37**. In addition to showing the distinction between concentrations in winter and late spring mentioned above, the plots in this figure also reveal a much more prominent variation in BC concentrations over the course of the day compared to PM$_{2.5}$, especially in the winter period. In the winter, BC concentrations were elevated in the morning and night, with peak concentrations that were seven times the lowest concentrations measured in the afternoon. Similar to the seasonal variation in BC/PM$_{2.5}$ ratio, the diurnal variation in this ratio is largely driven by changes in BC concentration and features a prominent early morning peak in both winter and late spring.
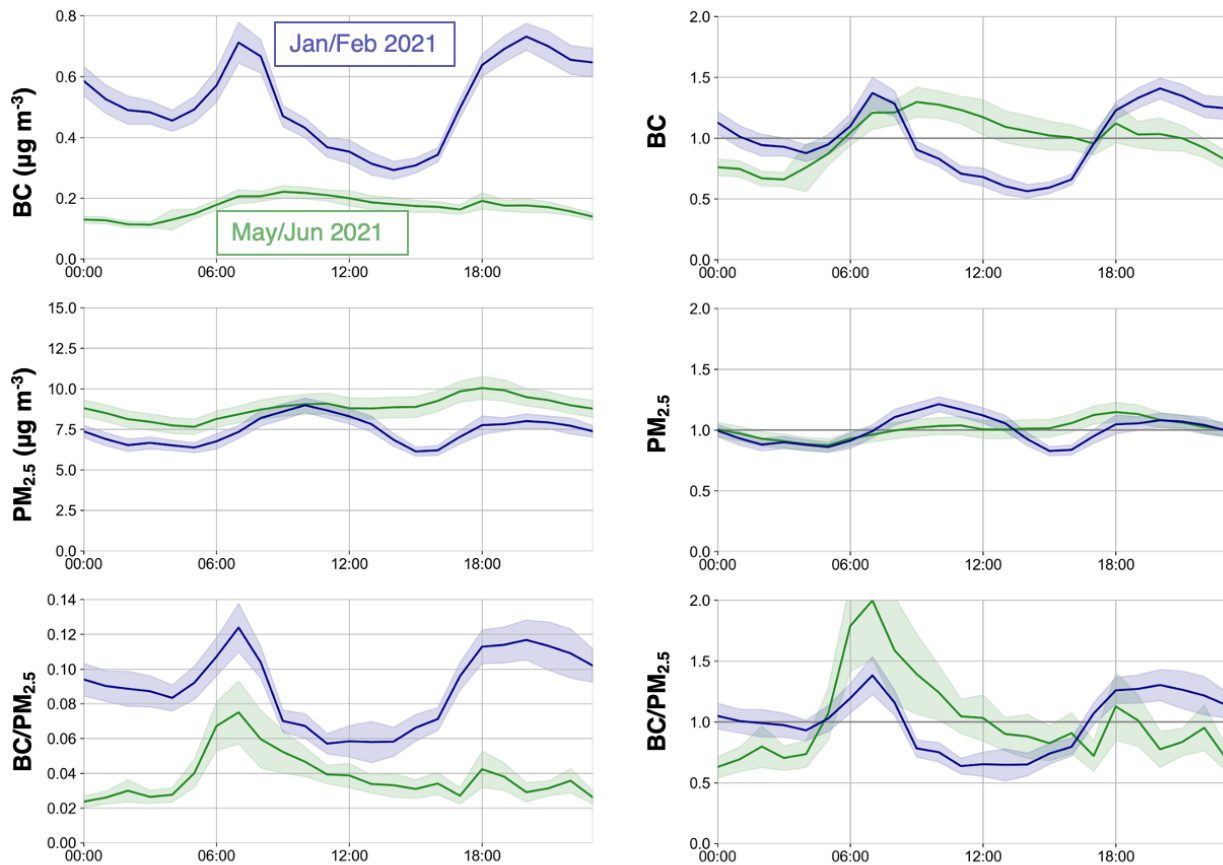
Figure 37. Diurnal trends of BC (top), PM$_{2.5}$ (middle), and BC/PM$_{2.5}$ ratio (bottom) measured in the winter (Jan/Feb, dark blue lines) and late spring (May/Jun, dark green lines). Plots on the left side panel show absolute concentrations and ratios. Plots on the right side panel show normalized trends, in which site-specific values were normalized by the network-average concentration or ratio in each season and for each pollutant. The solid line represents the average across all 50 sites and the shaded area represents the 95% confidence interval.

PSE

As shown in the plots on the right-hand side of **Figure 37**, where concentrations are normalized to the network average, winter BC concentrations range from 50% lower to 50% higher than the network-average concentration. $PM_{2.5}$ concentrations vary by only 20% of the network mean, and the peak in $PM_{2.5}$ occurs later in the morning than it does for BC. In the late spring, the diurnal variation of BC is not quite as strong as it is in the winter and the pattern is shifted, where the morning peak is considerably broader.

These seasonal and diurnal patterns of BC and $PM_{2.5}$ are similar to those measured elsewhere and generally governed by a combination of meteorology, local emissions and activity patterns, and atmospheric formation of $PM_{2.5}$.[83,84,85] The BC and PM trends shown above are affected by these factors, but the magnitude of the impact is greater for BC, a primary air pollutant, compared to $PM_{2.5}$, which is both a primary and secondary air pollutant. Lower wind speeds and lower atmospheric boundary layer heights in the winter inhibit the dispersion of pollutants and contribute to higher concentrations of BC.[86]

An example of this is shown by the wind contour plots colored by BC concentration in **Figure 38**. The wind data was obtained from a weather station ~65 meters away from the BC sensor at a school in San Pablo (site 40), which is between two designated truck routes. Wintertime wind speeds vary from ~0–5 km h^{-1}. In late spring, speeds are nearly twice as fast and infrequently less than 2 km h^{-1}. The highest BC concentrations typically occur with the slowest winds in the winter.

[83] Wyche, K. P.; Cordell, R. L.; Smith M, L.; Smallbone, K. L.; Lyons, P.; Hama, S. M. L.; Monks, P. S.; Staelens, J.; Hofman, J.; Stroobants, C.; et al. The Spatio-Temporal Evolution of Black Carbon in the North-West European 'Air Pollution Hotspot.' Atmos. Environ. 2020, 243 (May), 117874, DOI:10.1016/j.atmosenv.2020.117874.

[84] Kirchstetter, T. W.; Preble, C. V.; Hadley, O. L.; Bond, T. C.; Apte, J. S. Large Reductions in Urban Black Carbon Concentrations in the United States between 1965 and 2000. Atmos. Environ. 2017, 151, 17–23, DOI:10.1016/j.atmosenv.2016.11.001.

[85] Gantt, B.; Owen, R. C.; Watkins, N. Characterizing Nitrogen Oxides and Fine Particulate Matter near Major Highways in the United States Using the National Near-Road Monitoring Network. Environ. Sci. Technol. 2021, DOI:10.1021/acs.est.0c05851.

[86] Kirchstetter, T. W.; Preble, C. V.; Hadley, O. L.; Bond, T. C.; Apte, J. S. Large Reductions in Urban Black Carbon Concentrations in the United States between 1965 and 2000. Atmos. Environ. 2017, 151, 17–23, DOI:10.1016/j.atmosenv.2016.11.001.

PSE
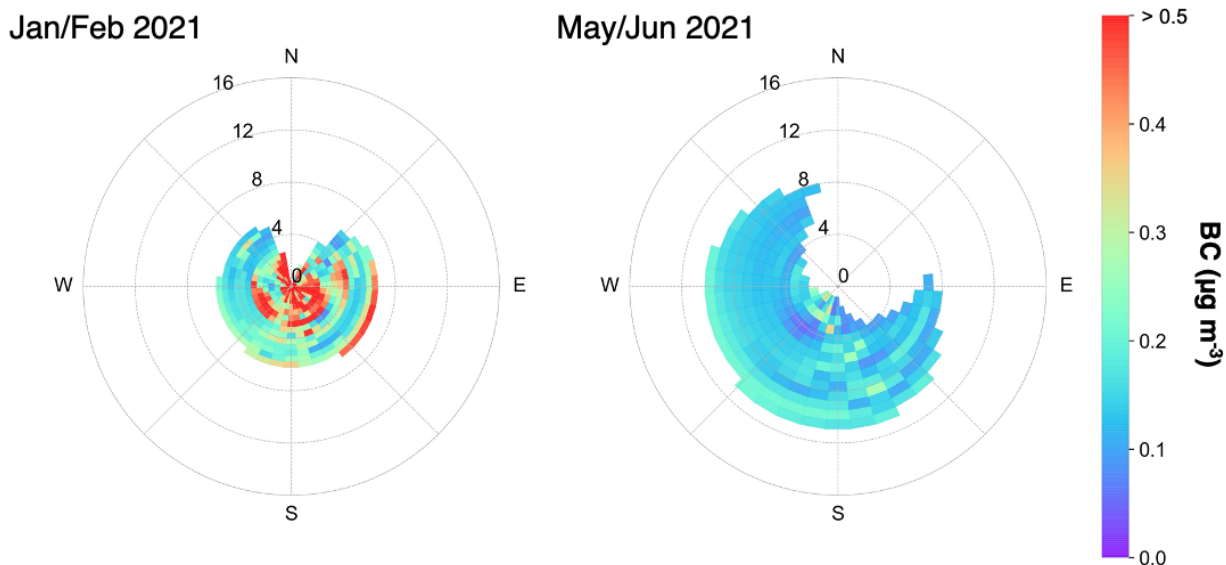
Figure 38. Wind contour plots showing the distribution of hourly wind speed (km h⁻¹) and direction colored by the concentration of BC during the winter (left) and late spring (right). The wind data was obtained from a weather station ~65 m away from the BC sensor at a school in San Pablo (site 40).

The wintertime early morning peak in BC concentrations coincides with the increase in on-road heavy-duty diesel truck activity.[87] Peak concentrations of NO_2, which is the product of rapid oxidation of diesel NO emissions and present in diesel truck exhaust, also occur at the same time. Together, these observations indicate that the morning BC peak can be attributed in large part to heavy-duty diesel truck emissions enhanced by a low atmospheric boundary layer in the morning, when emissions are mixed vertically through a smaller volume of the atmosphere than later in the day (**Figure 39**).[88]

The wintertime evening peak in BC concentration is as pronounced as its peak in the morning, whereas peaks in NO_2 and $PM_{2.5}$ are also evident but not as pronounced. The $BC/PM_{2.5}$ ratio also increases in wintertime evenings (**Figure 37**). Residential wood burning can contribute to elevated concentrations of both BC and $PM_{2.5}$ during wintertime evenings when the boundary layer is low. The concurrent rises in NO_2 concentration and the $BC/PM_{2.5}$ ratio suggest that diesel engine emissions are also a contributing factor.

---

[87] B.C. McDonald, Z.C. McBride, E.W. Martin, R.A. Harley, High-resolution mapping of motor vehicle carbon dioxide emissions. J. Geophys. Res. Atmos., 119 (2014), pp. 5283-5298, 10.1002/2013JD021219

[88] Kimbrough, S., Owen, R. C., Snyder, M., & Richmond-Bryant, J. (2017). NO to NO_2 conversion rate analysis and implications for dispersion model chemistry methods using Las Vegas, Nevada near-road field measurements. *Atmospheric Environment*, *165*, 23-34. DOI: 10.1016/j.atmosenv.2017.06.027

PSE

The weekly patterns of BC measured during this study are also shown in **Figure 39**. Historically in the Bay Area, BC concentrations have been much higher on weekdays than weekends because diesel truck activity followed the same pattern.[89] A similar trend in BC concentrations was observed in West Oakland as recently as 2017.[90] In contrast, in the current Richmond study, daily average BC concentrations were lowest midweek, which suggests that the weekly activity patterns of BC emission sources, including diesel trucks, are different than they have historically been in the Bay Area. Residential wood burning may also be a factor, assuming people tend to use their fireplaces more on weekends than weekdays. Truck counts and residential wood burning surveys, if available, would help in the interpretation of the weekly concentration trends.
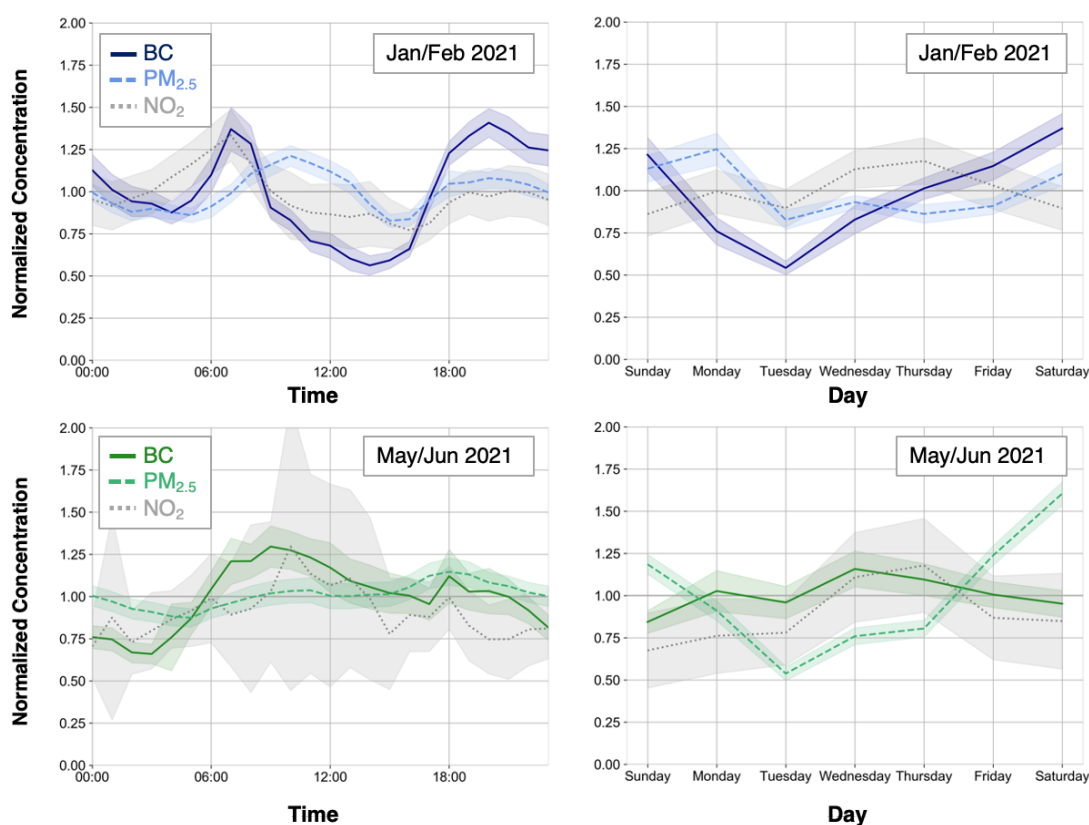
Figure 39. Diurnal (left) and weekly (right) patterns of normalized BC, PM$_{2.5}$, and NO$_2$ concentrations in the winter (top) and late spring (bottom). The lines indicate the network averages across all 50 sites and the shaded areas represent 95% confidence intervals.

[89] Kirchstetter, T. W.; Preble, C. V.; Hadley, O. L.; Bond, T. C.; Apte, J. S. Large Reductions in Urban Black Carbon Concentrations in the United States between 1965 and 2000. Atmos. Environ. 2017, 151, 17–23, DOI:10.1016/j.atmosenv.2016.11.001.

[90] Caubel, J. J.; Cados, T. E.; Preble, C. V.; Kirchstetter, T. W. A Distributed Network of 100 Black Carbon Sensors for 100 Days of Air Quality Monitoring in West Oakland, California. Environ. Sci. Technol. 2019, 53 (13), 7564–7573, DOI:10.1021/acs.est.9b00282.

PSE

4.4.2 Spatial Trends

The variation in BC concentrations across all 50 sites in winter and early spring are shown in **Figure 40** as normalized ratios of the site-average to the network-average in each season. The values indicated by the color scale show the degree to which site-average BC concentrations are greater than (red) or less than (blue) the network-average concentration. The sites that tend to experience higher levels of BC pollution are similar in winter and late spring and are clustered ~100–500 m from major roadways that border the community, such as the Richmond parkway (north/south) and I-580 (east/west). In addition, the major rail line runs along the south and west side of Richmond.
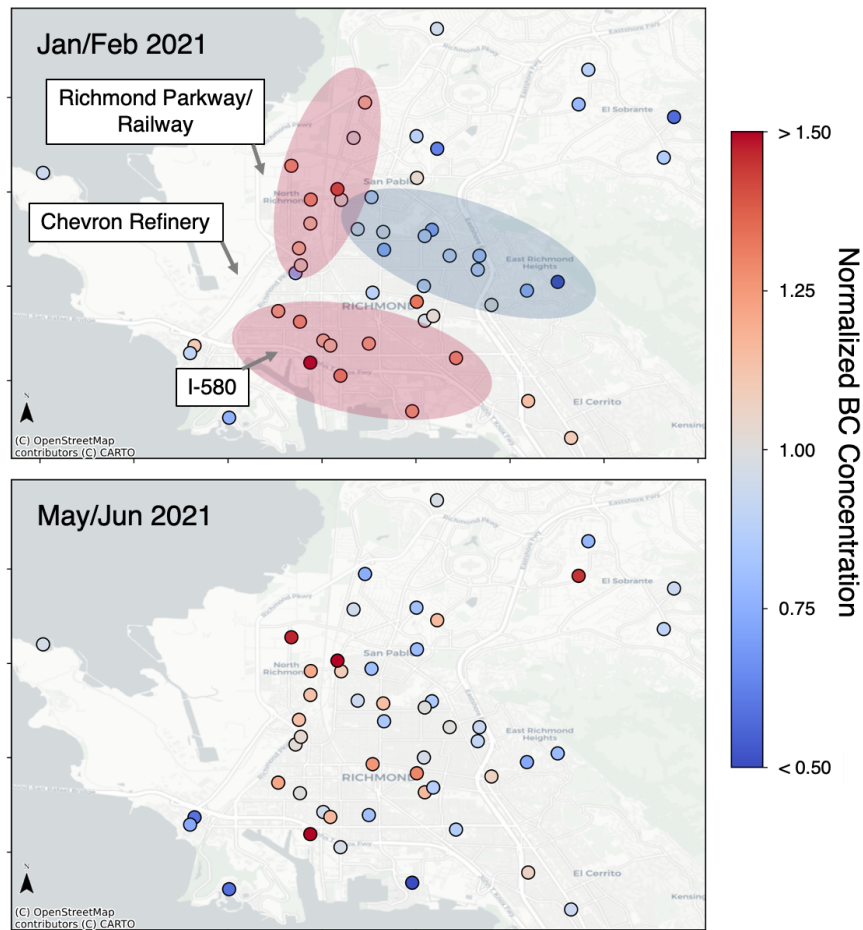
Figure 40. Site-average BC concentrations normalized to the network-average BC concentration in winter (top) and early spring (bottom). Those values > 1 indicate higher BC concentrations on average relative to the network average and are plotted in shades of red, while values < 1 are shown in shades of blue and indicate lower than average BC concentrations.

The monitoring sites fall into three land use categories—industrial, commercial, and residential—based on zoning by the City of Richmond and San Pablo. The highest levels of BC were measured in the areas zoned for industrial activity **(Figure 41**), which include sensors outside of three schools and one home. In the winter season when BC concentrations are highest in Richmond, the average BC concentration measured in areas zoned for industrial activity was 26% and 17% higher than in areas zoned as residential and commercial, respectively.
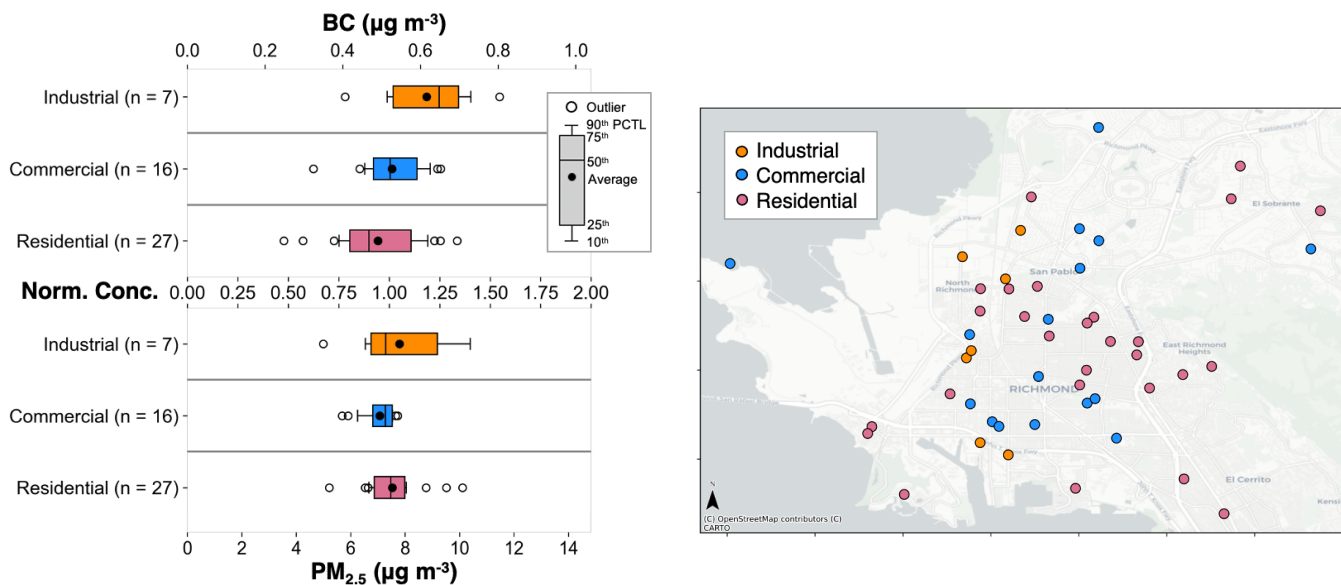
Figure 41. (Top) Boxplots of site-average BC and PM$_{2.5}$ concentrations measured in winter 2021 and categorized by land-use. Absolute concentration scales for BC and PM$_{2.5}$ are on the top and bottom axes, respectively, and the shared normalized concentration scale is shown in the middle. The number of locations per land-use category is noted in parenthesis. **(Bottom) Map of monitoring sites and their designated land use category: industrial, commercial, and residential.**

On average, BC concentrations at sites zoned for residential use were less than the entire network-average concentration, though concentrations varied at these residential sites from approximately half of the network average to as much as ~1.4 times the network average. The average concentration elevation at the industrial-zoned sites in the late spring was even larger (40% and 30% compared to residential and commercial sites, respectively), however the absolute differences in average BC concentrations in the late spring are smaller (not shown in **Figure 41**).

The relationships across land-use categories and the network-average were consistent for PM$_{2.5}$ in both the winter and late spring. PM$_{2.5}$ concentrations were less variable than BC: residential, commercial, and industrial sites had average PM$_{2.5}$ concentrations that varied by only ±5% of the network-average concentration. Commercial sites had the lowest PM$_{2.5}$ concentrations, on average 7–10% lower than residential and industrial sites.

The distributions of normalized BC and PM$_{2.5}$ concentrations are reported in **Figure 42**. These further illustrate the extent to which BC and PM$_{2.5}$ vary across the monitoring sites. In both seasons, approximately two-thirds of the sites experience PM$_{2.5}$ concentrations that are within ±10% of the network average, whereas only one-third of the sites have BC concentrations that are within 10% of the network average. This means that a majority of sites experienced comparable PM$_{2.5}$ concentrations, on average, while there was more spatial heterogeneity in BC concentrations across the community.
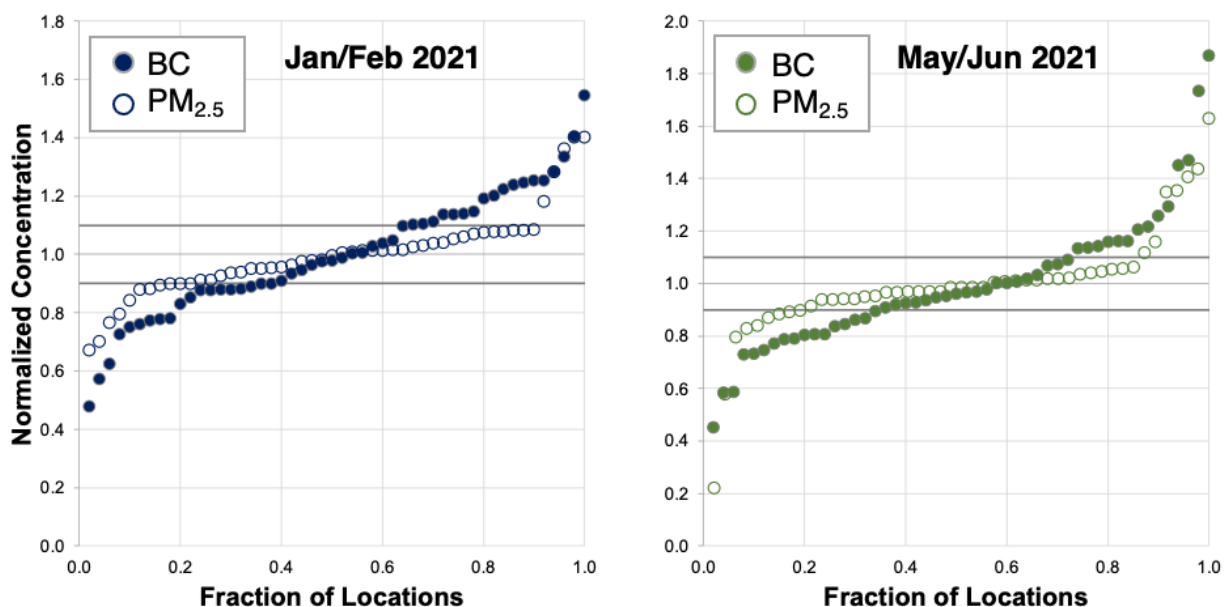
Figure 42. Ranked order distributions of normalized concentrations of BC (solid circles) and PM$_{2.5}$ (open circles) for each sampling period, where locations are ordered from lowest to highest concentration left-to-right on the x-axis. Gray horizontal lines mark 10% above and below the network average.

Figure 43 shows a ranked order of sites from most to least polluted with BC and PM$_{2.5}$. Five of the top ten sites most polluted with BC in winter are again among the top ten most polluted sites in late spring (4, 34, 21, 44, 9). In contrast, the other half of the top ten sites are not among the most polluted in late spring and one of them (10) is the site with the lowest average BC levels in late spring. Similarly, of the ten sites that have the lowest average BC levels in winter, half are again among the least polluted with BC in late spring (46, 2, 15, 17, 3)

while one (site 47) has the fourth highest BC concentration in late spring. Further, there is little commonality in the sites that experience the highest concentrations of BC and PM$_{2.5}$: only one of the sites with the highest wintertime average BC concentration (10) is among the sites in the top quintile for PM$_{2.5}$ in the winter, and the two most persistent wintertime BC hotspots (4 and 34) are in the cleanest quintile for PM$_{2.5}$.

Of the five sites that were consistent hotspots with elevated BC in both seasons, three are zoned for industrial activity (4, 34, 21). The other two (9 and 44) are adjacent to diesel sources. Site 9 is a home in North Richmond, approximately 250 m from a railway and less than 0.5 km from site 34. Similarly, site 44 is a home 200 m from a designated truck route, MacDonald Ave, in the North Richmond Heights neighborhood. All of the persistently clean sites are in residential zones within the North Richmond Heights, East Richmond Heights, and Point Richmond neighborhoods.

Figure 43. Site-average BC concentrations for winter (blue) and late spring (green), with sites ranked 1–50 from highest to lowest concentration on the x-axis from left to right. Error bars represent the 95% confidence interval for each site. The table below the plot notes the specific location numbers by season and pollutant. In the first row of this table, the 10 sites with the highest concentrations in winter (Jan/Feb) 2021 are shaded in red and the 10 cleanest locations are shaded in green. The shading for those 20 specific location numbers are repeated in the following rows for late spring (May/Jun) BC and winter PM$_{2.5}$.

4.4.3 Impact of Wildfire Smoke

During the August 2020 sampling campaign, air quality in Richmond was severely impacted by wildfire smoke that was transported to the Bay Area from other regions of California. Here we show how the wildfires affected concentrations and spatial patterns in BC and $PM_{2.5}$.

Figure 44 shows $PM_{2.5}$ concentrations measured with a beta attenuation monitor (BAM) at the Bay Area AQMD monitoring station in Richmond. Using the anomaly detection algorithm detailed previously, hours that were impacted by wildfire smoke were identified and are highlighted in blue in **Figure 44**. Average BAM $PM_{2.5}$ values during wildfire smoke impacted periods (36 µg m^{-3}) were more than three times higher than $PM_{2.5}$ concentrations when there was no smoke (11 µg m^{-3}).
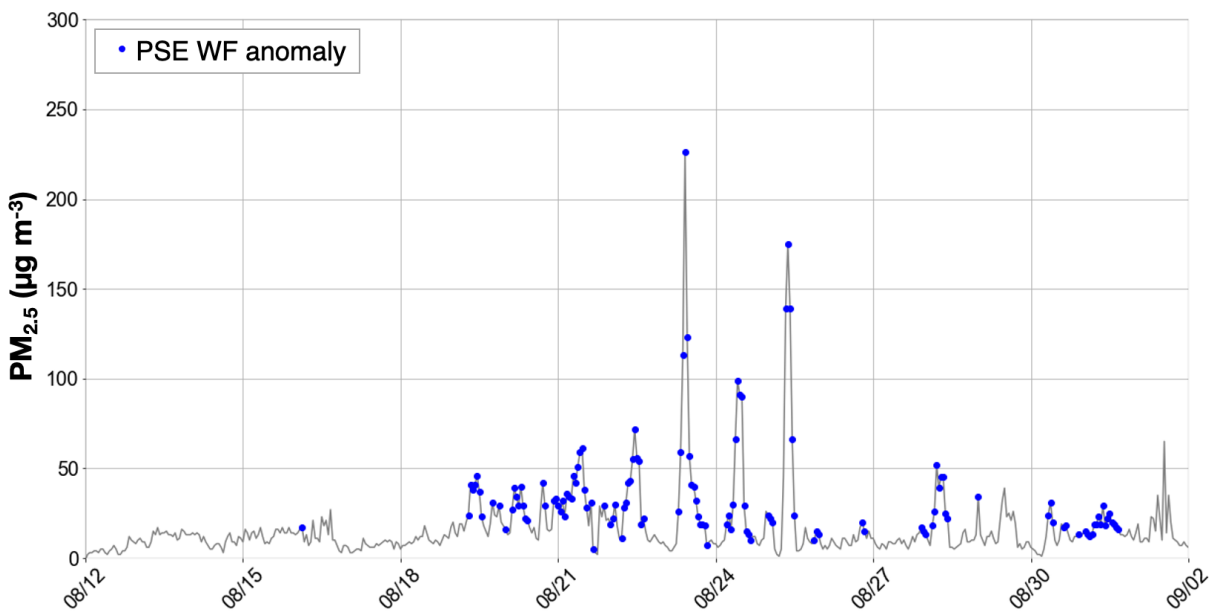
Figure 44. Hourly $PM_{2.5}$ mass concentrations measured at the Bay Area AQMD monitoring site in Richmond, California. Wildfire smoke-impacted periods are colored by blue dots.

As shown in **Figure 45**, BC and $PM_{2.5}$ concentrations were most elevated by wildfire smoke between 06:00 and 14:00. The average peak BC concentration during smoke-impacted days is ~4 times higher than baseline BC concentrations without smoke in August 2020. The average wildfire peak $PM_{2.5}$ was ~10 times higher than baseline $PM_{2.5}$ concentrations. The peak in BC and $PM_{2.5}$ concentrations decline rapidly in the afternoon and eventually reach evening concentrations similar to those observed on days without smoke. This diurnal pattern is likely due to the regional meteorology.
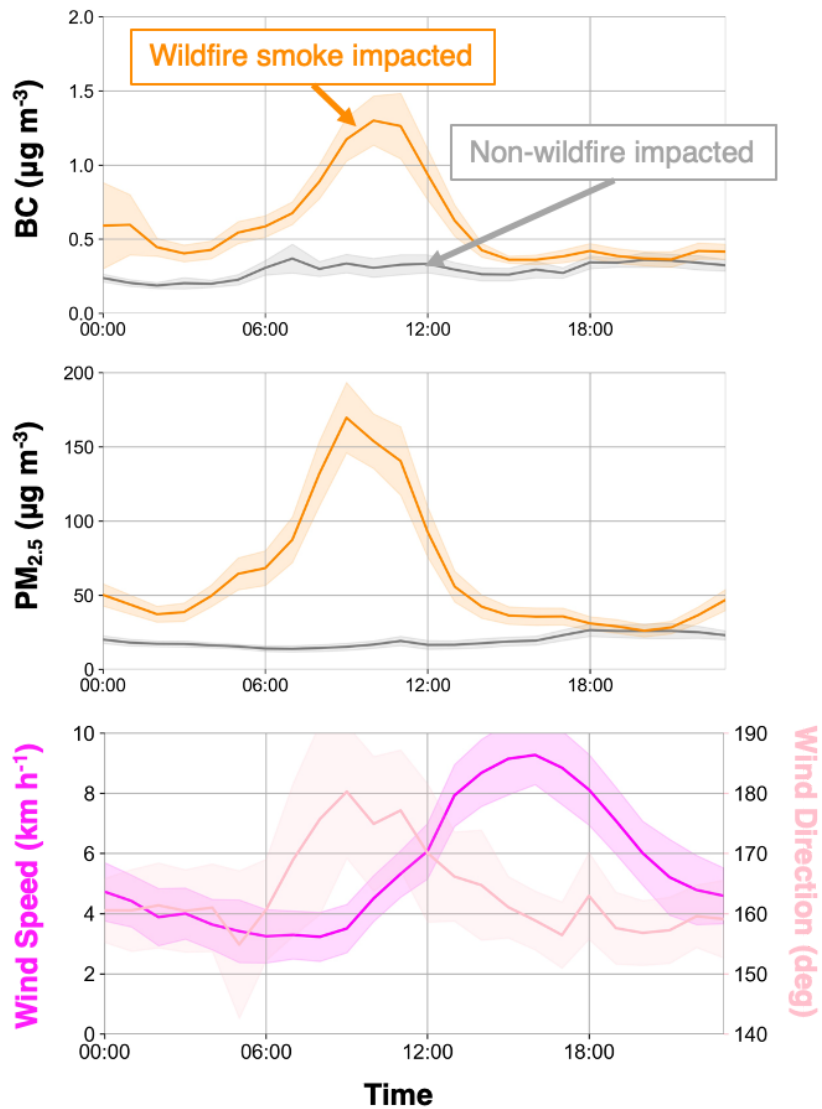
Figure 45. The diurnal pattern of BC (top) and PM$_{2.5}$ (middle) and during wildfire smoke (orange) and non-wildfire smoke (gray) impacted times. Also, the diurnal pattern (bottom) of wind speed (left axis, dark pink) and wind direction (right axis, light pink) during August 2020 as measured by a weather station near sampling locations 12 and 14 in East Richmond. The solid line represents the network average for pollutant concentrations or the site average for wind data and the shaded areas are the 95% confidence intervals.

4.4.4 Comparison to Regulatory Network

BC is not measured by the Bay Area AQMD regulatory site in San Pablo and therefore nearby regulatory sites are considered for comparison. In **Figure 46**, the average BC concentrations measured across RAMN in winter and late spring 2021 are compared to the eight monitors

PSE

operated by air quality management districts in Northern California. Two of these BC monitors are located immediately adjacent to major highways, designated as "near-highway" sites. The other six monitors are located within communities known to be heavily impacted by black carbon sources such as diesel engines or residential fireplaces, noted as "community" sites. Six of the eight monitors are in the Bay Area, including the two near-highway sites by I-880 and I-80. The Richmond network-average wintertime BC concentration measured in this study is lower than the mean concentrations measured by the six community monitors by approximately 20%. Notably, the Forest Knolls monitor is ~3 times greater, due to residential wood burning that is common in that community. In the summertime, when BC levels are lower everywhere due to increased pollutant dispersion (and no wintertime residential wood burning in Forest Knolls), the levels of BC in Richmond are similar to those measured in four of the six other cities.
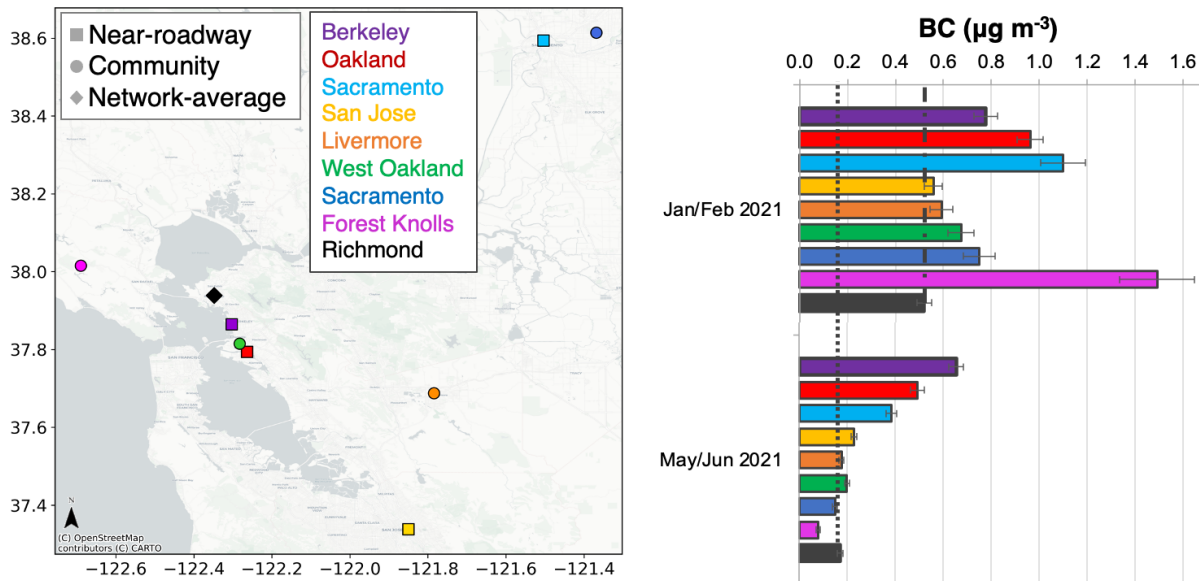
Figure 46. (Left) Map of the eight AQMD monitoring sites where BC is measured. This includes two that are immediately adjacent to major highways (squares) and six community sites (circles). The center of the RAMN network of BC monitors is denoted with a black diamond. **(Right) Average BC concentrations measured at these sites during the winter (Jan/Feb) and late spring (May/Jun) of 2021.** The RAMN-average winter and spring BC concentrations are also shown as dashed and dotted lines, respectively.

PSE

4.5 Refinery Flares, Plumes, and PM Hotspots

Short-term emissions from key stationary sources of $PM_{2.5}$ in Richmond-San Pablo were not easy to pinpoint with our sensor network due to the limited information available for industrial operational activities. However, some limited data related to refinery flaring events were available through the Bay Area AQMD. Below we discuss refinery flares and PM hotspots observed by our sensor network network.

4.5.1 Refinery Flares

Refineries in the Bay Area are required to submit monthly flare volume reports[91] and related causal analyses[92] subject to the requirements set out in Bay Area AQMD Regulation 12, Rule 11.[93] We examined Bay Area AQMD reports on emissions from flaring events at the Chevron refinery alongside $PM_{2.5}$ data collected by RAMN. The Bay Area AQMD provides daily data on vent gas flow (in standard cubic feet) and emissions of methane (CH_4), sulfur dioxide (SO_2), and non-methane hydrocarbons (NMHC) from each of the facility's eight stacks reported in pounds per day.[94] SO_2 is a known precursor to secondary $PM_{2.5}$ and NMHCs are precursors for both secondary $PM_{2.5}$ and O_3 formation. We evaluated flaring events in relation to both hourly $PM_{2.5}$ spikes measured by RAMN and during $PM_{2.5}$ plumes picked up by individual RAMN sensors as revealed by our more granular 10-min data.

---

[91] Bay Area AQMD. (2022). Refinery Flare Monitoring.
[92] Bay Area AQMD. (2022). Flare Causal Reports.
[93] Bay Area AQMD. (2021). Regulation 12 Rule 11: Flare Monitoring at Petroleum Refineries - 2021 Amendment (Current).
[94] Bay Area AQMD. (2022). Refinery Flare Monitoring.

PSE
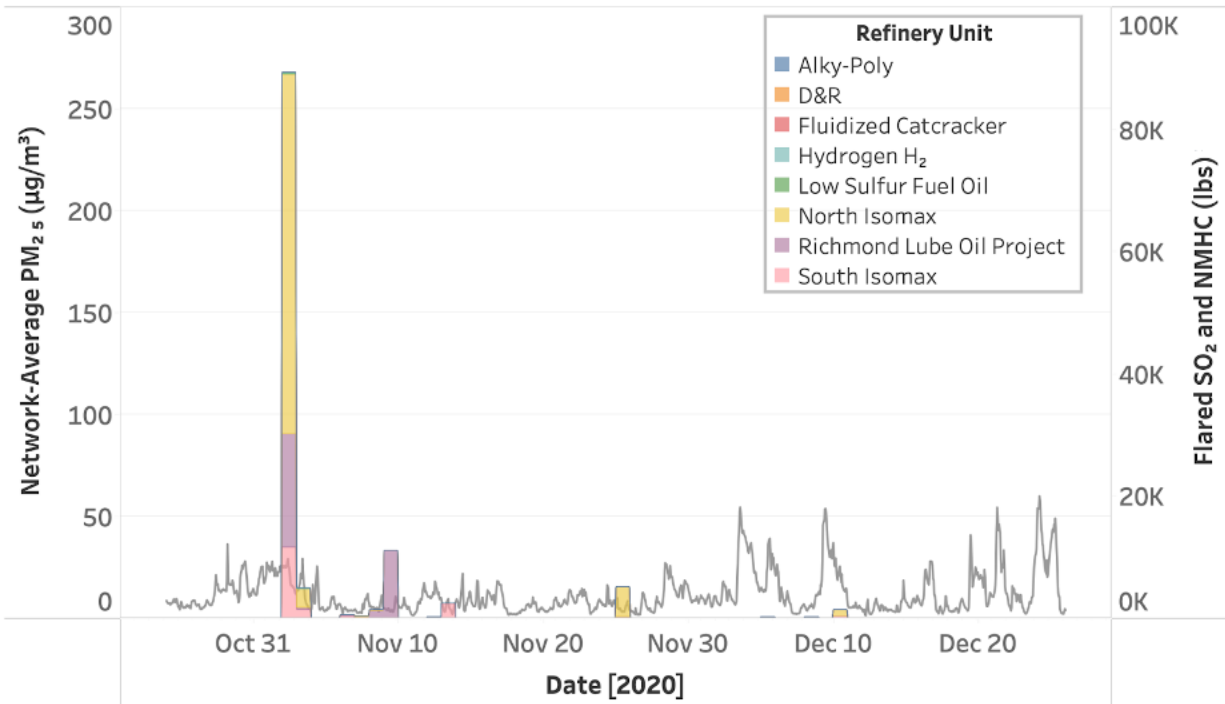
Figure 47. Network-average hourly PM$_{2.5}$ (µg/m^3) (solid black line) and reported Richmond Chevron refinery flare emissions of SO$_2$ and NMHCs (lbs). Data are shown for a two-month period between October 25-December 25, 2020.

Flaring events of various volumes and durations were reported during the RAMN study period. The large majority of these events did not coincide with spikes in the hourly PM$_{2.5}$ measured by RAMN. In fact, larger PM$_{2.5}$ spikes were often observed on days when no flares were reported (outside of wildfire season). The most significant flaring event reported during the study period occurred on November 2-3, 2020 (**Figure 47**). The emissions associated with this event exceeded 80,000 lbs of SO$_2$ in addition to nearly 10,000 lbs of NMHCs that were emitted from several of the refinery processing units.

Figure 48 (top) shows a heat map of 10-min averaged PM$_{2.5}$ concentrations reported by individual sensors in RAMN during the three days surrounding this large flare event (November 2-4, 2020). The event was reported to have started around 1 pm on November 2, 2020 and to have continued until approximately 6 am on November 3, 2020. We note that our sensor network detected high levels of PM$_{2.5}$ in excess of 50 µg/m^3 in the early morning of November 2, 2020 prior to the reported start of the event. A plume moving through the network was also detected starting around 5 am on November 2, 2020 and continuing until around 12 pm on November 3, 2020, with PM$_{2.5}$ concentrations exceeding 50 µg/m^3 at several

PSE

RAMN locations (**Figure 48, top)**. The prevailing wind direction during the time was from the south-southwest (**Figure 48, bottom**).
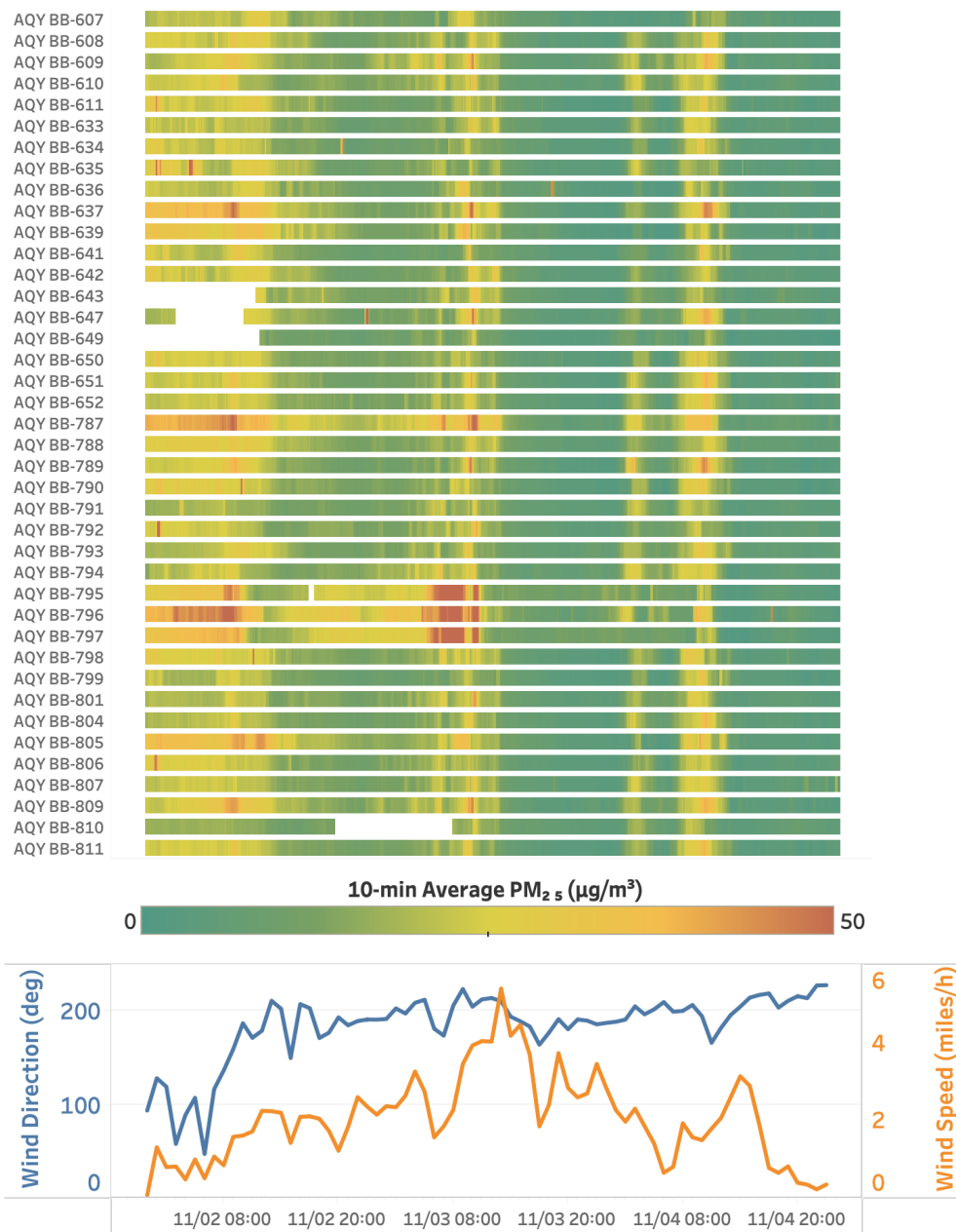
Figure 48. PM$_{2.5}$ and wind data for the days surrounding a refinery flare event that occurred on November 2-3, 2020. 10-min averaged PM$_{2.5}$ data reported by individual RAMN sensors (top). Average hourly wind direction and wind speed (bottom). Data are for the time period starting at 12:00 am on November 2, 2020 and ending at 11:59 pm on November 4, 2020.

Figure 49 shows the movement and spatial extent of this plume and the locations that were likely most impacted by it. The potentially impacted areas were located in the north-eastern parts of the Richmond-San Pablo area (top-right corner of each map) and downwind from the industrial areas to the southwest where the flaring occurred (bottom-left corner of each map).
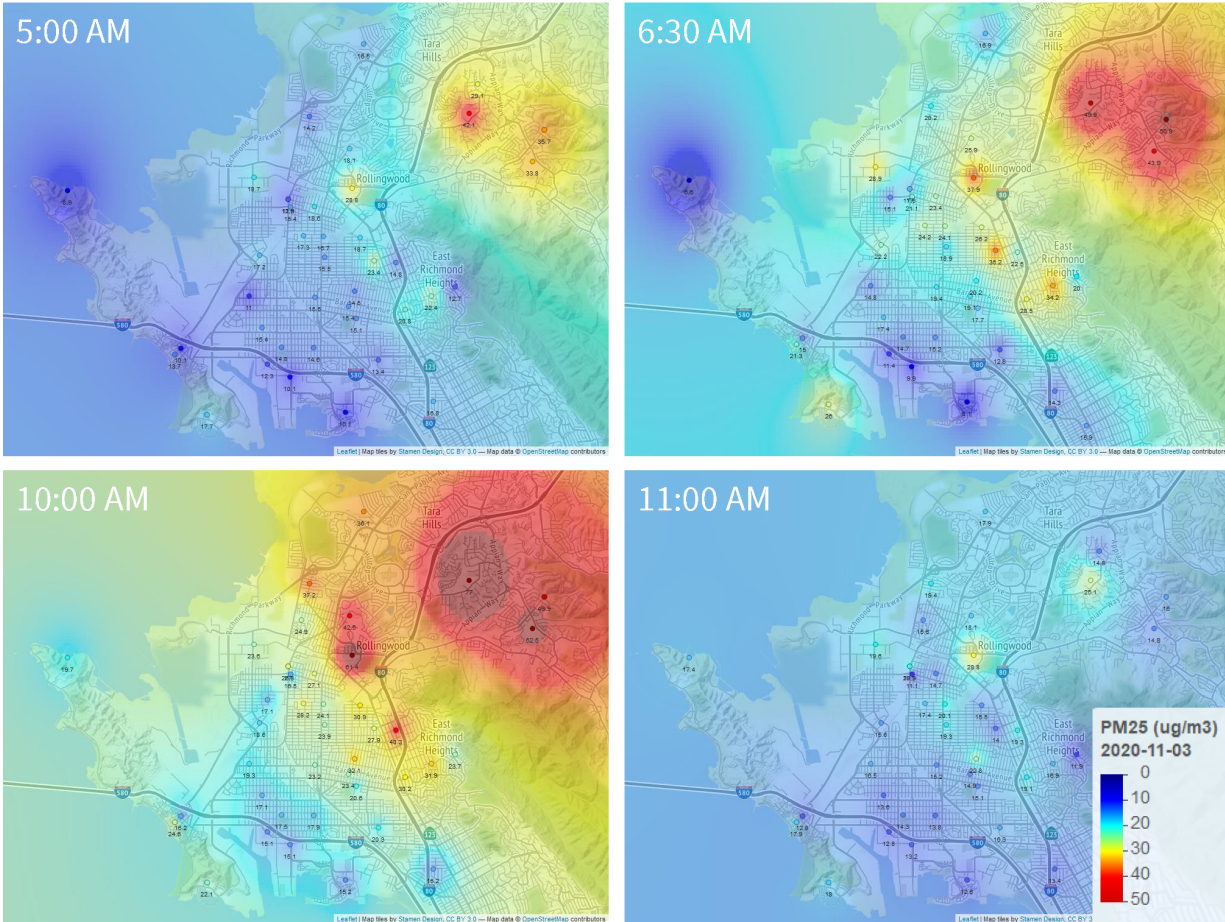
Figure 49. Heat maps showing PM$_{2.5}$ concentrations across RAMN sites at four different times of the day on November 3, 2020 during a reported refinery flare event. The maps were created using inverse distance weighted interpolation.

Flares at the Chevron refinery normally emit quite high through refinery smokestacks. Thus, the higher PM$_{2.5}$ concentrations measured by RAMN to the north-east, i.e. further downwind, may be due to the fact that it can take time for the flare emissions to reach ground level or that those areas are located at a slightly higher altitude up in the hills.

We also note that another PM$_{2.5}$ plume passed through the area on the morning of November 4th, which is also visible in **Figure 48 (top)**. Videos of each of these plumes (not shown here)

PSE

were created to visualize the speed at which plumes moved through the area and identify the locations that appeared to be most impacted.

4.5.2 PM Hotspots

Finally, we also looked at the spatial distribution of acute $PM_{2.5}$ exposure events, such as the number of days exceeding the NAAQS $PM_{2.5}$ 24-hour standard of 35 µg/m^3 or the number of hours by RAMN-site that exceeded hourly $PM_{2.5}$ concentrations of 50 µg/m^3. These maps are shown in **Figure 50 (left)** and **Figure 50 (right)** respectively.

Number of Daily-Average $PM_{2.5}$ Measurements > 35 µg/m^3
0 — 24

Number of Hourly $PM_{2.5}$ Measurements > 50 µg/m^3
0 — 400
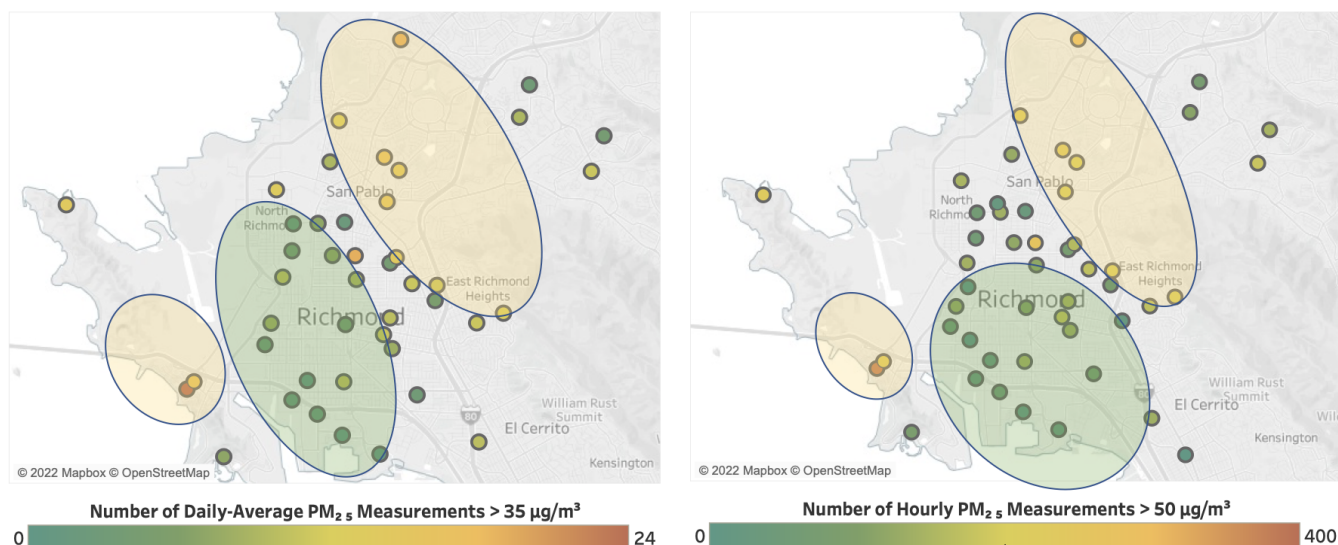
Figure 50. Maps of RAMN monitors and number of acute exposure events. Left: Sites colored by the number of $PM_{2.5}$ daily-average concentrations exceeding the NAAQS 24-hour standard of 35 µg/m^3. Right: Sites colored by number of $PM_{2.5}$ hourly concentrations exceeding 50 µg/m^3.

4.6 Measurements in Context: Comparison to CalEnviroScreen 4.0 (CES)

CES is the environmental justice screening tool developed by the California Office of Environmental Health and Hazard Assessment (OEHHA) to identify communities that are disproportionately impacted by environmental pollutants and socioeconomic stressors.[95] CES integrates health, environmental burden, and socioeconomic data to develop a cumulative score and assign a percentile rank for each census tract in relation to all other census tracts in the state. California uses CES to identify disadvantaged communities, defined as the census tracts that score in the top 25 percent statewide on the cumulative CES score—these are the 25 percent of California communities burdened the most by a combination of health,

---

[95] OEHHA. (2021, February). Draft CalEnviroScreen 4.0.

PSE

environmental and socioeconomic factors. CES percentiles for the cumulative CES scores and Population Characteristics in Richmond-San Pablo are shown in **Figure 1** of this report**,** and CES percentiles for air pollutant and health outcome indicators are shown in **Figure 2** above.

In the absence of hyperlocal air quality data, air pollution indicators in CES are calculated using a variety of techniques, including spatial interpolation of air monitoring data available through the sparse regional network of regulatory sites, satellite observations, emission inventories, and modeling.[96] As such, these estimates may be too coarse to enable accurate understanding of exposure to air pollutants within small local communities and to properly identify the areas most impacted by air pollution. Hyperlocal air quality data collected by RAMN can help shed light around these issues and test the validity of these concerns.

CES uses three air pollution exposure indicators in its cumulative impact methodology: O_3 concentrations, $PM_{2.5}$ concentrations, and estimated diesel PM emissions. **Figure 51** compares average summer O_3 concentrations by census tract as measured by RAMN (May-Oct) with O_3 concentrations by census tract estimated (modeled) in CES.
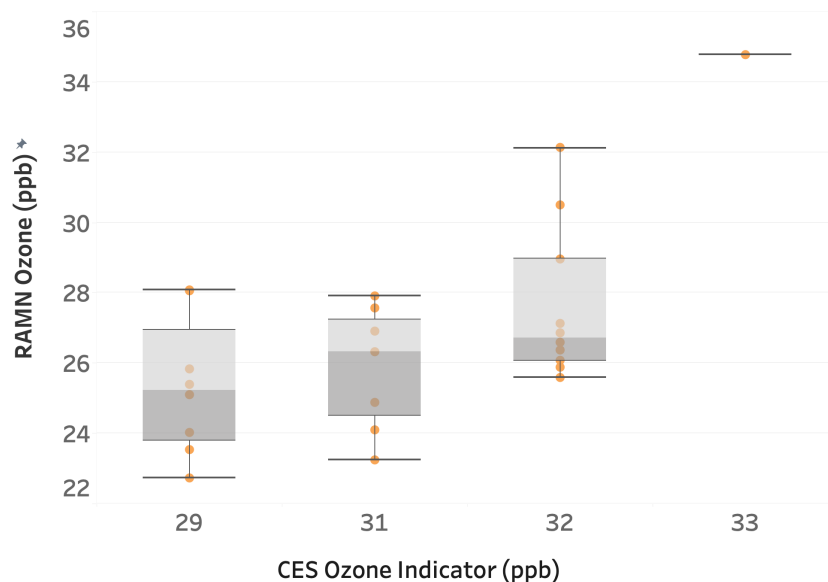
Figure 51. Boxplot of average O_3 concentrations by census tract measured by RAMN vs CES O_3 estimates by census tract.

The low granularity of sparse regulatory data means that the CES O_3 indicator tends to assign relatively uniform O_3 concentrations across census tracts in California (see also **Figure 2)**. In **Figure 51**, all census tracts in Richmond-San Pablo (except one) are grouped into only three

---

[96] August, L.; Komal Bangia, ·; Plummer, L.; Prasad, S.; Ranjbar, K.; Slocombe, A.; Wieland, W.; Cogliano, V.; Faust, J.; Hirsch, A.; et al. (2021). CalEnviroScreen 4.0.

O_3 concentration bins, each of them assigned an integer value (in ppb). In contrast, RAMN provides significantly more granular data as actual ground-level O_3 concentrations were measured by our network in each of the census tracts. In addition, the spread in the average O_3 concentrations measured by RAMN is significantly broader than the CES estimates, ranging between 23-35 ppb, compared to 29-33 ppb in CES. Despite these differences and the lower spatial resolution of the CES O_3 indicator, the two datasets are moderately well correlated (pearson correlation coefficient r = 0.52; R^2 = 0.27; p < 0.01), suggesting that the CES O_3 indicator does a fairly decent job in identifying impacted communities.

The same is not true for the CES $PM_{2.5}$ indicator. **Figure 52** shows a scatter plot of CES-estimated average $PM_{2.5}$ concentrations compared to RAMN measurements. Each point on the scatter plot represents the mean annual $PM_{2.5}$ concentration in a census tract within the study area. We note that the spread in the CES data is extremely small—all $PM_{2.5}$ concentrations fall within a narrow band of 0.3 $\mu g/m^3$ (8.9 - 9.2 $\mu g/m^3$). In contrast, the spread in $PM_{2.5}$ concentrations measured by RAMN across all census tracts within the study area is an order of magnitude larger (10.7 - 14.4 $\mu g/m^3$). In addition, we note a slight negative slope apparent in the scatterplot data, indicative of a negative correlation. All this suggests that the CES $PM_{2.5}$ indicator does a particularly poor job in identifying communities impacted by fine particulate air pollution and may incorrectly attribute higher $PM_{2.5}$ concentrations to communities in the Richmond-San Pablo area that are less impacted, and vice versa.
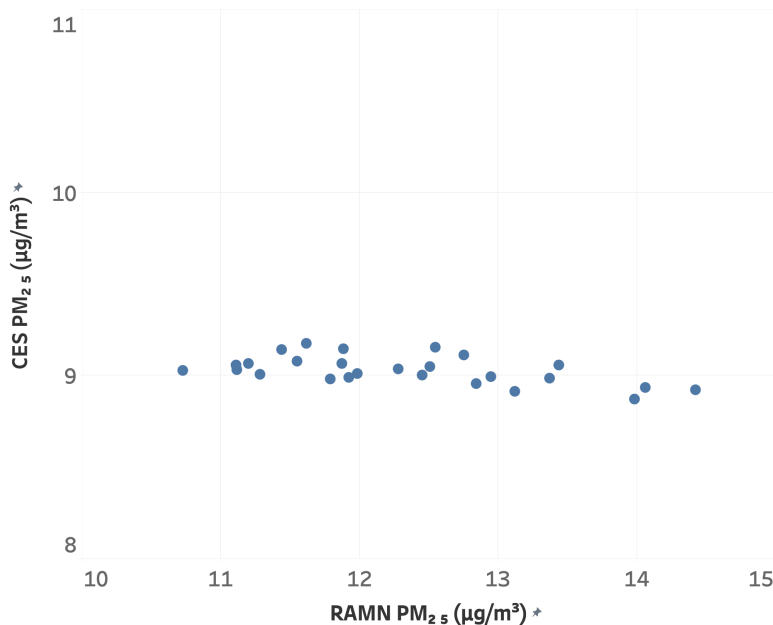
Figure 52. Scatter plot of average $PM_{2.5}$ concentrations by census tract measured by RAMN vs CES estimates. Each dot represents a single census tract in the Richmond-San Pablo area.

PSE

BC concentrations measured during this study are overlaid in **Figure 53** on a map of CES census tract estimates of diesel particulate matter (DPM, tons yr^{-1}) emissions from point, area, on-road mobile, and ocean-going vessels.[97] Lower BC concentrations measured in the northeast and southwestern areas of our study domain largely overlap with lower CES emission estimates, and elevated BC concentrations overlap with the highest CES emission estimates southwest of the domain center. However, some monitoring locations with relatively high average BC concentrations are within census tracts with low CES emission estimates, and vice versa.

Whereas the CES emission estimates serve as indicators of pollution levels averaged over entire census tracts, a distributed network of air pollution sensors, like RAMN, is able to resolve concentration differences within individual census tracts. Thus, data from air pollution sensor networks could be used in combination with CES estimates to better understand the hyperlocal environmental burdens experienced by California's most impacted communities.
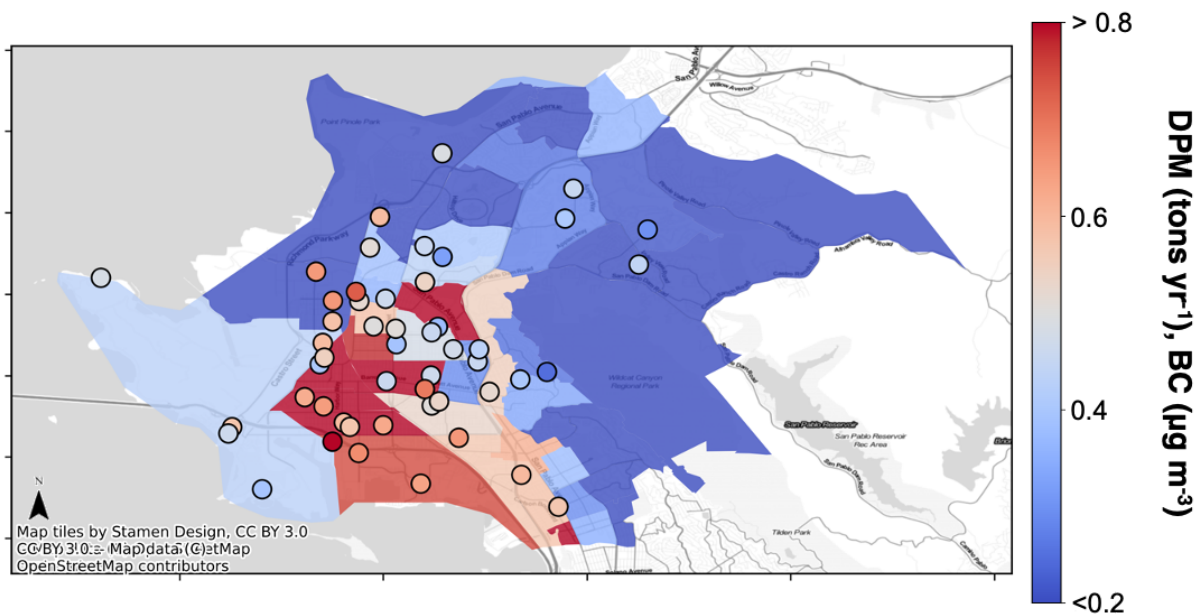
Figure 53. Winter 2021 site-average BC concentrations (μg m^{-3}) measured in this study (colored circles) overlaid onto a map of CES census tract DPM emissions (tons yr^{-1}). CES estimates are based on inventories and models of on- and off-road emissions in 2016.[98]

---

[97] August, L.; Komal Bangia, ·; Plummer, L.; Prasad, S.; Ranjbar, K.; Slocombe, A.; Wieland, W.; Cogliano, V.; Faust, J.; Hirsch, A.; et al. (2021). CalEnviroScreen 4.0.
[98] Ibid.

PSE

Below we highlight key findings from the Richmond Air Monitoring Network and recommendations for air pollution mitigation and future research.

5.1 Key Findings

5.1.1 Traffic Influence on Local Air Quality

Our findings point to traffic as an important source of $PM_{2.5}$, NO_x and BC emissions in the Richmond-San Pablo region. Our traffic emission estimates (see the 'On-Road Mobile Sources' section above) indicate that while passenger vehicles make up the majority of annual vehicle miles traveled, heavy-duty trucks contribute a disproportionate amount of on-road $PM_{2.5}$, PM_{10}, and NO_x emissions. RAMN measurements revealed that:

- Concentrations of $PM_{2.5}$ and NO_2 were generally elevated near freeways, during commuter hours, and at locations and times that can be associated with industrial truck traffic.

- Areas near the two major freeways (I-80 to the east and I-580 to the south) experienced higher ambient concentrations of $PM_{2.5}$ and NO_2. Similarly, industrial areas near the Richmond Parkway to the west and I-580 to the south experienced persistently high ambient concentrations of BC, especially in the morning/evening commute hours.

- Further supporting a connection to traffic, RAMN observed that NO_2 concentrations were highest within a half-mile of major freeways, and dropped significantly beyond that distance. Elevated levels of $PM_{2.5}$ and NO_2 were observed near freeways around the time of the morning and evening commute.

The wintertime early morning peak in BC concentrations is most likely due to a peak in heavy-duty diesel truck activity, enhanced by a low atmospheric boundary layer and lower wind speeds during the winter months. Peak concentrations of NO_2, which is primarily formed as the product of rapid oxidation of diesel NO emissions present in diesel truck exhaust, also occur at the same time, further supporting this association. BC concentrations were up to 50 percent higher in neighborhoods near I-580 (Marina Bay, Coronado/Santa Fe, Richmond Annex) and in neighborhoods near the Richmond Parkway and the more industrial areas to the west (Iron Triangle/Atchison Village and North Richmond).

PSE

Residential wood burning, a source not fully examined in this report due to limited data availability, may also be an important contributing factor here, particularly for the higher BC and $PM_{2.5}$ concentrations observed during winter months.

5.1.2 Spatial Variability in Air Pollution

RAMN's spatially granular data enabled us to observe spatial patterns in air pollution that revealed significant variability of $PM_{2.5}$, BC, NO_2 (and even O_3) across neighborhoods and land use categories in Richmond-San Pablo. $PM_{2.5}$, BC and NO_2 exhibited higher spatial variability than the secondary pollutant O_3, which speaks to the influence of local sources of $PM_{2.5}$, BC, and NO_2 emissions, like traffic and industry, as well as the role of meteorological conditions (like prevailing wind patterns). In particular, we found that:

- Average neighborhood $PM_{2.5}$ levels were highest in neighborhoods in the south (Point Richmond, Richmond Annex), and in the north (Hilltop, May Valley), where average $PM_{2.5}$ concentrations were roughly 20 percent higher compared to the average concentrations measured by the Bay Area AQMD regulatory site in San Pablo.

- Outside of wildfire season, RAMN-measured $PM_{2.5}$ concentrations tracked higher than average AQMD concentrations during the late fall and early winter (November - December). Several neighborhoods in central and northern Richmond had average $PM_{2.5}$ concentrations up to 50% higher than the AQMD average during these months.

While some of the seasonal differences between RAMN and AQMD measurements may be due to systematic differences in in sensor technology, monitoring methods, or calibration procedures or potentially attributable to seasonal changes in $PM_{2.5}$ composition that can influence the sensitivity of our low-cost PM sensors to $PM_{2.5}$, RAMN-measured differences across neighborhoods point to ground-level spatial variations in average $PM_{2.5}$ concentrations that should still persist if differences between RAMN and AQMD were indeed systematic.The spatiotemporal trends of BC in the Richmond-San Pablo community were found to be even more variable than those of $PM_{2.5}$.

- The sites that tended to experience the highest levels of BC pollution were clustered ~100–500 m from the major roadways that border the community to the south and west—the Richmond parkway and I-580.

- These sites were also closest to major industrial areas located to the south and west of the community, as well as the major rail line that runs along the west and south side of Richmond.

PSE

The more uniform $PM_{2.5}$ concentrations compared to BC indicate that $PM_{2.5}$ measurements alone do not capture the heterogeneity of local pollution sources within a community. This highlights the importance of measuring primary air pollutants such as BC—an indicator of diesel engine activity—along with other more source-specific primary pollutants (e.g., speciated PM and specific VOCs) in spatially distributed community monitoring networks like RAMN. Greater variations in local concentrations of primary pollutants, such as BC, point more directly to block-by-block differences and hot spots in air pollution that a community can mitigate through emission reduction plans, compared to more regional air pollutants like $PM_{2.5}$ and O_3.

Many neighborhoods had NO_2 averages that exceeded the AQMD reference monitor averages on both hourly and monthly time scales. In particular:

- Average NO_2 concentrations were roughly 30 percent higher in two southern neighborhoods close to I-580 (Point Richmond and Marina Bay) compared to the AQMD reference monitor.

- Concentrations were around 10 percent higher in several other neighborhoods close to the I-80 and I-580 freeways (Hilltop, East Richmond Heights, Park Plaza/Laurel Park, and Coronado/Santa Fe).

Residential and commercial zones were generally more impacted by $PM_{2.5}$ and NO_2, while O_3 concentrations remained fairly consistent across land use categories. People living in areas zoned for industrial activity seem to experience higher BC pollution levels than those in residential and commercial zones.

While BC, $PM_{2.5}$ and NO_2 exhibited significantly more spatial variability than the more regional air pollutant O_3, RAMN still found spatial variability in O_3 concentrations across neighborhoods and site locations:

- Average O_3 concentrations were highest in northern neighborhoods (Hilltop, North Richmond, Point San Pablo, San Pablo, and North Richmond), located further away and downwind of major freeways and industrial zones.

- O_3 concentrations were lowest in the southern neighborhoods (Point Richmond, Marina Bay, Richmond Annex/Parkview, Park Plaza/Laurel Park, Coronado/Santa Fe, and Iron Triangle/Atchison Village).

PSE

5.1.3 Public Health and Regulatory Context

We interpreted data collected by RAMN by comparing absolute concentrations to both regional averages from AQMD and to national ambient air quality standards. When comparing absolute air pollutant concentrations by neighborhood to federal standards, we note that:

- Average $PM_{2.5}$ concentrations measured by RAMN generally hovered around or exceeded the federal NAAQS 3-year annual mean $PM_{2.5}$ standard of 12 μg/m^3 in many Richmond-San Pablo neighborhoods.

- RAMN-wide $PM_{2.5}$ concentrations over the 27-month-long study period averaged 12.6 μg/m^3 (95% CI 12.4-12.8).

Again, we should note that specific data completeness and data quality requirements for NAAQS are not necessarily met by our sensor network, including that data are averaged over a three-year period. Additionally, air quality data evaluated for NAAQS may exclude exceptional events that meet certain criteria, such as some wildfire smoke episodes.

RAMN observed substantially lower average NO_2 and O_3 concentrations compared to NAAQS standards. However, it is important to note that any exposure to air pollutants may adversely impact health and adverse health effects have been observed at levels below health-based standards.

5.1.4 Air Quality Impact of Wildfire Smoke

Average $PM_{2.5}$ concentrations during wildfire-smoke-impacted periods were up to ten times higher than $PM_{2.5}$ concentrations when there was no smoke. While NAAQS may exclude some exceptional events such as wildfires, we note that the entire study area experienced average $PM_{2.5}$ concentrations during wildfire season that were almost three times as high as the 12 μg/m^3 annual standard. During specific wildfire events, the study area also experienced average daily $PM_{2.5}$ concentrations up to five times higher than the NAAQS 24 hour limit of 35 μg/m^3, indicative of acute exposure events. BC, a short-lived climate-forcing agent and a key component of wood smoke, was also significantly elevated during wildfire events, with average peak BC concentrations roughly four times higher during smoke-impacted days than baseline conditions.

5.1.5 Air Pollution and CalEnviroScreen (CES)

In the broader context of cumulative burdens, many factors—including but not limited to air pollution—contribute to the health outcomes experienced by a community. Communities with elevated health risk factors, including higher prevalence of underlying health conditions,

lack of access to healthcare, socioeconomic burdens, and poor housing conditions, face much greater risk from exposure to air pollution. In the absence of hyperlocal air quality data, CES uses regional air quality data and emissions estimates to model average concentrations for certain air pollutants by census tract. These averages are then integrated with environmental burden and socioeconomic data to identify environmental justice communities. By expanding neighborhood-level air monitoring, RAMN was able to provide more detailed data that could be used to inform and refine exposure assessments for $PM_{2.5}$, NO_2, O_3, and BC concentrations.

When comparing RAMN data to CES, we found that average air pollutant concentrations of $PM_{2.5}$, NO_2, and O_3 were generally higher in neighborhoods not designated as disadvantaged communities by CES. This finding underscores the importance of examining air pollution within the broader context of cumulative demographic and environmental burdens. Additional investigations on the influence of other air pollutants not measured by RAMN, such as air toxics and VOCs in particular, and the impacts of cumulative environmental, health, and socioeconomic burdens are needed to more comprehensively investigate the high prevalence of poor health outcomes experienced by the Richmond-San Pablo community.

The CES O_3 indicator generally aligned well spatially with RAMN data in identifying communities disproportionately exposed to this pollutant. However, O_3 is a regional pollutant with less variability across space as compared to NO_2 and $PM_{2.5}$. Spatial patterns of BC concentrations generally aligned well with the CES diesel particulate matter (DPM) indicator, which notably is based upon reported stationary and mobile source emissions of DPM rather than ambient air quality monitoring, as is the basis for the other air pollutant indicator of interest ($PM_{2.5}$, NO_2, O_3). This finding requires further examination and may be linked to several limitations of CES, both in the underlying data and methods used for developing the CES $PM_{2.5}$ indicator, as well as the more limited duration of our study resulting in non-overlapping time periods used for our comparison.

PSE

5.2 Mitigation Strategies and Recommendations

RAMN sheds light on the hyperlocal variations of $PM_{2.5}$, NO_2, O_3, and BC concentrations throughout the Richmond-San Pablo community. RAMN data point to commuter traffic and industrial diesel-truck activities as key sources of local air pollution, suggesting that heavy-duty vehicle electrification and other emissions reductions from traffic should be prioritized. This can be achieved through:

- Requiring or providing incentives for small and large businesses to electrify truck fleets.

- Retiring old medium- and heavy-duty diesel trucks.

- Rerouting trucks away from areas experiencing cumulative environmental burdens.

- Restricting industrial development that brings new heavy traffic into dense, urban areas and environmental justice communities.

Community groups would also benefit from tree planting and other urban greening efforts along traffic corridors to protect sensitive groups from vehicular air pollution.[99]

In addition, coordinated efforts by local, regional, and state governments should focus on expanding electrified public transit in the area to reduce overall vehicle travel while also improving transit options for households with limited mobility. These efforts should include ongoing engagement of local communities and community-based organizations. Access to electric vehicle (EV) charging infrastructure, particularly in apartment buildings and multifamily housing residences, should be expanded to encourage EV adoption. Addressing the impacts of wildfire smoke locally (beyond forest-level interventions) may require investments in local resilience hubs and community centers where community members can find protected spaces with access to filtered air.

Current and future air monitoring efforts by the Bay Area AQMD should urgently focus on increasing community access to data on other key air pollutants not captured by RAMN. Many health-damaging air pollutants are difficult to measure with current low-cost air sensor technology. However, some of them are actively being measured by the Bay Area AQMD as part of the Richmond-San Pablo Community Air Monitoring Plan (CAMP).[100] Some of these air pollutants include toxic air contaminants emitted from key stationary sources of air pollution in the community, which may be more correlated with health outcomes data for the study

---

[99] USDA. (2017). [Trees Give Roads a Breath of Fresh Air](#).
[100] BAAQMD. (2022). [Air Toxics Monitoring Study](#).

PSE

area than the air pollutants measured by RAMN. These data collection efforts should be expanded and used to inform targeted actions that can help reduce exposure in the community and improve health outcomes.

In addition, the Chevron Richmond refinery community air monitoring system measures several toxic air contaminants, including ammonia, BTEX (benzene, toluene, ethylbenzene, and xylene), and BC at three locations in the community—Point Richmond, Atchison Village, and North Richmond.[101] Measurements from these sites are available to the community in real time. However, historical data from these three community air monitors are yet to be made publicly available.[102] We strongly recommend that these data are released to the public so that they can be evaluated in the context of community health outcomes and used to inform future actions and monitoring activities.

Additional information on key stationary sources of air pollution in the community should also be made publicly available and used to inform future actions, monitoring activities, and evaluation of existing data, including data collected by RAMN. These additional data should include, but are not limited to:

- More detailed temporal emissions data (e.g., by hour of day and day of week) for specific industrial activities in the area, including operational schedules of various refinery units, precise timing and duration of flaring events, fluid catalytic cracking unit (FCCU) historic hours of operation, and bulk carrier (tanker) loading and unloading schedules.

- Routes and schedules for industry-associated heavy-duty trucking activities.

- Recent residential wood burning surveys, if available, to allow for further interpretation of anomalies in hourly, daily, and seasonal BC and $PM_{2.5}$ concentration trends.

Finally, while CES air pollutant indicators (developed using sparse regional air monitoring and emissions data) can provide decent estimates of air pollution concentrations at the census tract level, we have shown that a distributed network of air sensors like RAMN can provide much more accurate information and measure ground-level concentration differences within individual census tracts. Data from RAMN and other low-cost air quality sensor networks in California can therefore be used in combination with CES estimates to better understand

---

[101] Chevron Richmond refinery fenceline monitoring system. (2022). About.
[102] Chevron Richmond refinery fenceline monitoring system. (2022). Resources.

PSE

hyperlocal exposure to air pollution and its role in exacerbating environmental burdens within the most impacted communities in the state.

PSE

AB 617	Assembly Bill 617
ABCD	Aerosol Black Carbon Detector
APEN	Asian Pacific Environmental Network
AQMD	Bay Area Air Quality Management District
AQ-SPEC	Air Quality Performance Evaluation Center
AQMD	Air Quality Management District (as in Bay Area AQMD)
BAM	beta attenuation monitor
BC	Black carbo
BTEX	benzene, toluene, ethylbenzene, xylenes
CARB	California Air Resources Board
CES	CalEnviroScreen 4.0
CH_4	methane
CI	confidence interval
DPM	diesel particulate matter
FEM	federal equivalent method
FRM	federal reference method
H_2S	hydrogen sulfide
HPMS	Highway Performance Monitoring System
LBNL	Lawrence Berkeley National Laboratory
m	meter
m^3	cubic meter
MAE	mean absolute error

MLD	Monitoring and Laboratory Division, California Air Resources Board
MOMA	mean variance moment matching
mph	miles per hour
NAAQS	National Ambient Air Quality Standards
NMHC	non-methane hydrocarbons
NO	nitrogen monoxide
NO_2	nitrogen dioxide
NO_X	nitrogen oxides
O_3	ozone
OEHHA	Office of Environmental Health Hazard Assessment
PCTL	percentile
PM	particulate matter
$PM_{2.5}$	particulate matter less than or equal to 2.5 microns in diameter
PM_{10}	particulate matter less than or equal to 10 microns in diameter
ppb	part per billion
ppm	part per million
PSE	PSE Healthy Energy
RAMN	Richmond Air Monitoring Network
RH	relative humidity
RMSE	room-mean-square error
ROG	reactive organic gases
SCAQMD	South Coast Air Quality Management District
SO_2	sulfur dioxide
µg	microgram

PSE

U.S. EPA   United States Environmental Protection Agency

VMT   vehicle miles traveled

VOC   volatile organic compounds

WCCUSD   West Contra Costa Unified School District

QA/QC   quality assurance and quality control

Mobile Source Emissions Methodology

Estimates for mobile source emissions were calculated on an annual level using 2017 vehicle miles traveled data from the Highway Performance Monitoring System (HPMS) and 2017 vehicle emissions from CARB's Emissions Factor (EMFAC) tool. The HPMS dataset provides street-level annual average daily traffic (AADT) and street segment length in miles for major roadways in California, from which the vehicle miles traveled (VMT) each roadway was calculated. The EMFAC tool provides emissions (in tons per year) and VMT for every vehicle subclass across various geographic scales for California, including at the county level. These two datasets were merged to provide an estimate of $PM_{2.5}$ and NO_x emissions by road segment for each major vehicle class (passenger cars, buses, light trucks, medium trucks, and heavy duty diesel trucks). Medium trucks were defined as Class 4-6 trucks, while heavy trucks were classified as Class 7-8 trucks. These vehicle classes do not account for every type of vehicle driven in Contra Costa County—EMFAC accounts for additional vehicle classes such as motorcycles, motor homes, construction equipment, etc. However, the five aforementioned vehicle classes account for greater than 99% of the county's roadway VMT.

EMFAC provides vehicle emissions information for several pollutants, including $PM_{2.5}$, PM_{10}, NO_x, SO_x, CO, and more. Emissions are provided from engine exhaust as well as from brake and tire wear (in the case of particulate matter emissions). The dataset also provides multiple vehicle subclasses within each vehicle class (e.g., 10+ subclasses of heavy duty diesel truck). Emissions factors were calculated by summing VMT and emissions across all subclasses for each vehicle class (cars, light trucks, medium trucks, heavy trucks, and buses), then dividing the total emissions estimate for each class (in tons/year) by the total class VMT estimate (in miles/year) to generate an emissions factor in units of tons/mile. VMT proportions for each of the five main vehicle classes was also calculated to generate estimates for street-level VMT (from HPMS) by vehicle class. The HPMS VMT, derived by multiplying Annual Average Daily Traffic (AADT) by road segment length (in miles), was then multiplied by 365 days to approximate annual VMT for the street segment. This street-level VMT by vehicle class was then multiplied by the emissions factor for each vehicle class to output an estimate for $PM_{2.5}$ and NO_x emissions (in tons/year) by vehicle class for each major street segment, narrowed to the Richmond area.

Aeroqual AQY Data Processing and Quality Assurance

Each AQY device transmits data directly to the Aeroqual Cloud, a platform provided by the monitor manufacturer. Although devices are equipped with SIM cards to facilitate continuous cellular network connectivity and ongoing data sharing with the cloud, SIM card failure, power loss (e.g., unplugging), and other similar issues can lead to data gaps. When a device comes back online, if prior data are stored on the internal SD card, they are sent to the cloud. To maximize data completeness, we built a downloader script that requests data from Aeroqual Cloud on a one-minute basis, first looking for any missing data in the last eight weeks and beginning the data request with the first missing one-minute timestamp. This file was then averaged into 10-minute and 60-minute intervals. This averaging was only conducted if data were at least 75 percent complete for a given averaging period, otherwise, the data for this time were discarded. The downloader script was run weekly but data were also inspected more frequently directly on the Aeroqual Cloud.

Due to different meteorological conditions in Richmond-San Pablo compared to Sacramento, and issues with ongoing sensor drift, the initial field calibration parameters obtained in Sacramento did not transfer well. Ongoing calibration was needed for all pollutants being monitored—though especially for NO_2, which displayed severe drift towards lower values throughout the deployment period and especially during the transfer period from Sacramento to the study area. This sensitivity to different environmental conditions is a well-knows challenge with these sensors.[103] We contracted with Aeroqual, Inc. to receive monthly calibration parameters using their patent-pending mean variance moment matching (MOMA) approach detailed in the literature.[104,105] Briefly, this method assigns each sensor to a proxy site (such as the San Pablo AQMD reference monitor) where air pollution concentrations are well known and follow a similar probability distribution to the sensor site, and uses the mean and variance of both the AQY unit and the proxy site over a certain period of time to adjust the sensor sensitivity to the target analyte and its zero point (i.e., calculate the *gain* and *offset* for each sensor—**Equations A1** and A**2**).

---

[103] Farquhar, A. K., Henshaw, G. S., & Williams, D. E. (2021). Understanding and correcting unwanted influences on the signal from electrochemical gas sensors. *ACS sensors*, *6*(3), 1295-1304. https://doi.org/10.1021/acssensors.0c02589

[104] Miskell, G., Alberti, K., Feenstra, B., Henshaw, G. S., Papapostolou, V., Patel, H., Polidori, A., Salmond, J. A., Weissert, L., & Williams, D. E. (2019). Reliable data from low cost ozone sensors in a hierarchical network. *Atmospheric Environment*, *214*, 116870. https://doi.org/10.1016/j.atmosenv.2019.116870

[105] Weissert, L., Miles, E., Miskell, G., Alberti, K., Feenstra, B., Henshaw, G. S., Papapostolou, V., Patel, H., Polidori, A., Salmond, J. A., & Williams, D. E. (2020). Hierarchical network design for nitrogen dioxide measurement in urban environments. *Atmospheric Environment*, *228*, 117428. https://doi.org/10.1016/j.atmosenv.2020.117428

$$\text{gain} = \sqrt{\frac{\text{var}\langle PM_{2.5\,ref}\rangle}{\text{var}\langle PM_{2.5\,AQY}\rangle}}$$

Equation A1

$$\text{offset} = \overline{PM_{2.5\,ref}} - \text{gain} * \overline{PM_{2.5\,AQY}}$$

Equation A2

For $PM_{2.5}$, the proxy site was the nearest regulatory air monitor, which was the San Pablo - Rumrill monitoring station for all but two monitors—those were closer to and calibrated against the Berkeley Aquatic Park regulatory monitor. For O_3 and NO_2, each AQY was assigned to the nearby regulatory monitor with the most similar land use.[106] Possible monitors included San Pablo, Vallejo, San Leandro, San Ramon, and Berkeley Aquatic Park.

Although calibration parameters (gain and offset) were provided each month by Aeroqual using one-week of proxy data, a continuous drift detection framework developed by Aeroqual has also been published in the scientific literature based on a three-day rolling probability distribution that signals when recalibration is needed and uses 30-days of data for recalibration.[43,44] To test the effectiveness of the more simplified, monthly MOMA framework, we re-created the drift detection framework described in the literature for O_3 and NO_2 and compared our results to those of the monthly calibration provided by Aeroqual. Additionally, we tested the effectiveness of $PM_{2.5}$ calibration using re-calibration periods of various lengths and using raw and relative humidity-corrected data. Our analysis indicated that the continuous recalibration method provides slightly better results than the once-monthly calibration from Aeroqual using one-week of data. The simpler monthly MOMA method that Aeroqual provided, however, still performed very comparably to the more sophisticated and more computationally-intensive approach, and also avoided the risk of potentially overcorrecting the data. We therefore used the calibration parameters generated by Aeroqual through the simplified MOMA process for our analyses.

Aeroqual applies a proprietary relative humidity (RH) correction to all $PM_{2.5}$ data uploaded to the cloud. This correction generally improves data quality, and MOMA calibration with relative humidity-corrected data performs better than with completely raw data. One notable exception was during acutely high $PM_{2.5}$ events, such as during ground-level wildfire smoke in the summer and fall. During these events, measured $PM_{2.5}$ concentrations exhibited a curious

---

[106] Weissert, L., Miles, E., Miskell, G., Alberti, K., Feenstra, B., Henshaw, G. S., Papapostolou, V., Patel, H., Polidori, A., Salmond, J. A., & Williams, D. E. (2020). Hierarchical network design for nitrogen dioxide measurement in urban environments. *Atmospheric Environment*, *228*, 117428. https://doi.org/10.1016/j.atmosenv.2020.117428

PSE

bifurcation due to Aeroqual's RH correction algorithm, with fine particle pollution being underestimated when relative humidity is high and overestimated when it is low (**Figure A1, top**). This led to sometimes severe overestimation or underestimation of $PM_{2.5}$ concentrations during certain times of the day. To correct for this effect, we applied an RH-dependent "reverse" growth factor to effectively remove Aeroqual's internal RH correction during unusually high $PM_{2.5}$ events and added an additional wildfire gain correction factor (**Figure A1, bottom**). These wildfire corrections were the same across all $PM_{2.5}$ sensors and across all wildfire events and were added on top of the MOMA correction.
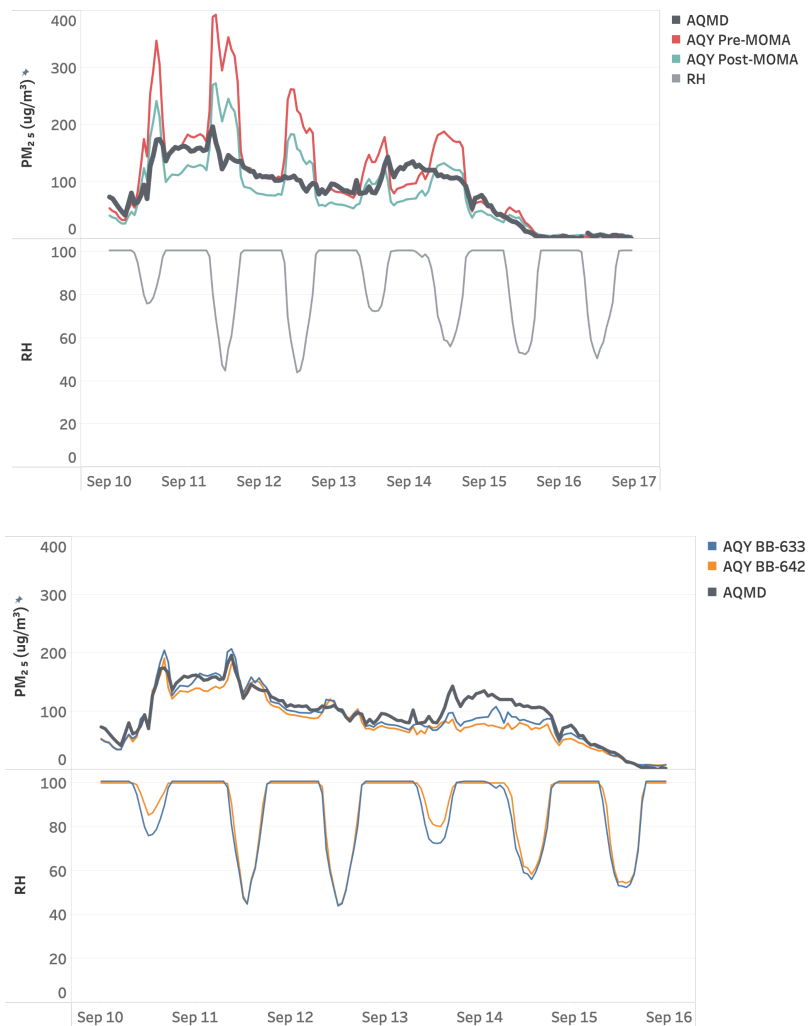
Figure A1. Hourly $PM_{2.5}$ concentrations measured by the AQMD reference beta attenuation monitor (BAM) and two Aeroqual AQYs collocated at the San Pablo AQMD regulatory site during a major wildfire smoke event ("Orange Skies" in the Bay Area, Sept. 10-15, 2020). Top: AQY BB-642 pre- and post- MOMA calibration compared with BAM; AQY RH measurements are shown below. **Bottom:** AQYs after applying the "reverse growth

PSE

factor" RH and wildfire correction; AQY RH measurements are shown below. The RH data suggests that the RH sensors may be over-reading and flatlining at high RH.

To apply the wildfire corrections, we also had to identify ground-level wildfire smoke events on an hourly basis. We used the AnomalyDetection R package[107] to detect high $PM_{2.5}$ events for each AQY unit throughout its deployment. Briefly, this package uses a Seasonal Hybrid Extreme Studentized Deviate (S-H-ESD) test to detect long- and short-term anomalies based on the data's seasonal and recent trend components. After identifying such anomalies for each AQY, we calculated the percent identifying an anomaly for any given timestamp. If over 50 percent of deployed AQYs detected an anomaly, we deemed the event a "network anomaly" and applied the relative humidity-dependent reverse growth factor correction to the entire network. Network anomalies during the months of July, August, September, and October and after known wildfire events were labeled as wildfires for the purposes of filtering out ground level smoke events during subsequent analyses.

Following calibration and RH growth factor/wildfire corrections, data quality issues like periodic negative values or abnormally high measurements due to sensor failures sometimes remained. Filtering out these data while leaving real spikes in air pollution intact is a balancing act which requires a combination of automated processes and manual data evaluation. For the automated portion, we removed data that met any of the conditions described in **Table A1**. After this process, we visually examined the data for remaining abnormalities by comparing spikes in each monitor to other nearby monitors. This and all of the above procedures were performed on 10- and 60-minute data to produce the final datasets used in our analyses.

Table A1. Data Removal Flags.

Condition	O_3	NO_2	$PM_{2.5}$
Sensitivity (long-term)	AQY >= Network Median + 3*Interquartile Range for 24 hours +		
Sensitivity (short-term)	AQY >= 300 ppb	AQY >= 200 ppb	AQY >= 800 µg/m3
Sensor flatline	AQY == 0.0 for 24 hours or longer		
Negative value	AQY < 0		

[107] *AnomalyDetection R package*. (2022). [R]. Twitter. https://github.com/twitter/AnomalyDetection (Original work published 2014)

PSE

ABCD Data Quality Assurance and Control

The BC concentration data was adjusted to compensate for a well-known filter loading artifact using **Equation 3**.[108] BC and BC_0 are the adjusted and unadjusted BC concentrations, respectively. ATN is the reported attenuation of light by the filter, and a is the correction parameter that adjusts BC_0 so that concentrations are independent of filter loading. The value of the compensation parameter, $a = 0.64$, was derived from prior measurements of ambient urban air in nearby West Oakland and was used during all periods except those impacted by wildfire smoke, when a correction of $a = 0.55$ was used.[109] The wildfire smoke parameter value ($a = 0.55$) was derived from previous work and new field and laboratory measurements made during periods of heavy wildfire smoke.[110] During QA/QC, the dataset was also scrubbed of BC concentrations measured when attenuation levels were excessive ($ATN > 100$). Hourly BC concentrations were calculated from minutely average data if 95% of the seconds in the minute and 95% of the minutes in an hour remained.

$$BC = \frac{BC_0}{a \cdot exp\left(\frac{-ATN}{100}\right) + (1-a)}$$
Equation A3

[108] Jimenez, J.; Claiborn, C.; Larson, T.; Gould, T.; Kirchstetter, T. W.; Gundel, L. Loading Effect Correction for Real-Time Aethalometer Measurements of Fresh Diesel Soot. J. Air Waste Manag. Assoc. 2007, 57 (7), 868–873, DOI:10.3155/1047-3289.57.7.868.

[109] Caubel, J. J.; Cados, T. E.; Preble, C. V.; Kirchstetter, T. W. A Distributed Network of 100 Black Carbon Sensors for 100 Days of Air Quality Monitoring in West Oakland, California. Environ. Sci. Technol. 2019, 53 (13), 7564–7573, DOI:10.1021/acs.est.9b00282.

[110] Caubel, J. J.; Cados, T. E.; Kirchstetter, T. W. A New Black Carbon Sensor for Dense Air Quality Monitoring Networks. Sensors (Switzerland) 2018, 18 (3), 1–18, DOI:10.3390/s18030738.